AD-A009 894

ELECTROMAGNETIC DIRECTION FINDING TECHNIQUES

G. A. Thiele

Ohio State University

Prepared for:

Naval Regional Procurement Office

March 1975

UNCLASSIFIED

SECURITY CLASSIFICATION OF THIS PAGE (When Data Entered)

REPORT DOCUMENTATION PAGE

1. REPORT NUMBER	2. GOVT ACCESSION NO. 3. RECIPIENT'S CATALOG NUMBER
4. TITLE (and Subtitle) ELECTROMAGNETIC DIRECTION FINDING TECHNIQUES	5. TYPE OF REPORT & PERIOD COVERED Final Report 6. PERFORMING ORG. REPORT NUMBER ESL 3735-3
7. AUTHOR(s) G. A. Thiele	8. CONTRACT OR GRANT NUMBER(s) Contract N00140-74-C-6017
9. PERFORMING ORGANIZATION NAME AND ADDRESS The Ohio State University ElectroScience Laboratory, Department of Electrical Engineering, Columbus, Ohio 43212	10. PROGRAM ELEMENT, PROJECT, TASK AREA & WORK UNIT NUMBERS Project N66604-3-000279 Task D.O. -51
11. CONTROLLING OFFICE NAME AND ADDRESS Naval Regional Procurement Office, Philadelphia Newport Division, Bldg. No. 11, Naval Base Newport, Rhode Island 028 0	12. REPORT DATE March 1975 13. NUMBER OF PAGES 74
14. MONITORING AGENCY NAME & ADDRESS (if different from Controlling Office)	15. SECURITY CLASS (of this report) Unclassified 15a. DECLASSIFICATION DOWNGRADING SCHEDULE

16. DISTRIBUTION STATEMENT (of this Report)

17. DISTRIBUTION STATEMENT (of the abstract entered in Block 20, if different from Report)

18. SUPPLEMENTARY NOTES

19. KEY WORDS (Continue on reverse side if necessary and identify by block number)

Antennas
Direction Finding
Geometrical theory of diffraction

20. ABSTRACT (Continue on reverse side if necessary and identify by block number)

This final report summarizes research and development addressed to the problem of electromagnetic direction finding in the UHF frequency range. Both theoretical and experimental investigations are described under three topical headings. These include the analysis of slot antennas on a conducting cylinder, the hardware development of a T-bar fed slot antenna, and the computer aided design of a lossy wire (distributively loaded) circular array. The report concludes with recommendations for future investigations and hardware development.

DD FORM 1473 EDITION OF 1 NOV 65 IS OBSOLETE

UNCLASSIFIED

SECURITY CLASSIFICATION OF THIS PAGE (When Data Entered)

NOTICES

When Government drawings, specifications, or other data are used for any purpose other than in connection with a definitely related Government procurement operation, the United States Government thereby incurs no responsibility nor any obligation whatsoever, and the fact that the Government may have formulated, furnished, or in any way supplied the said drawings, specifications, or other data, is not to be regarded by implication or otherwise as in any manner licensing the holder or any other person or corporation, or conveying any rights or permission to manufacture, use, or sell any patented invention that may in any way be related thereto.

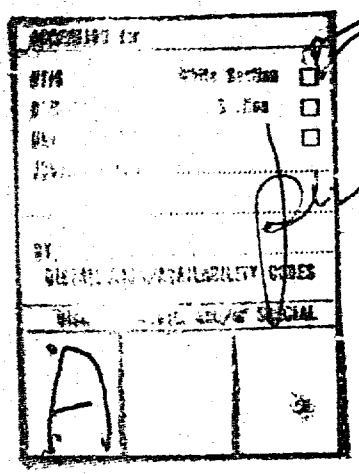

Letter on file

REPRODUCTION QUALITY NOTICE

This document is the best quality available. The copy furnished to DTIC contained pages that may have the following quality problems:

- Pages smaller or larger than normal.
- Pages with background color or light colored printing.
- Pages with small type or poor printing; and or
- Pages with continuous tone material or color photographs.

Due to various output media available these conditions may or may not cause poor legibility in the microfiche or hardcopy output you receive.

☐ If this block is checked, the copy furnished to DTIC contained pages with color printing, that when reproduced in Black and White, may change detail of the original copy.

CONTENTS

I. INTRODUCTION

During the course of the research and development effort undertaken on Contract N000140-74-C-6017, several different investigations, both experimental and theoretical, have been addressed to the general problem of direction finding (DF) from an antenna system configured on a cylinder. Over the frequency range of interest, the cylinder diameter varies from one-sixth wavelength to 25 wavelengths. The lower portion of this frequency range is the more difficult portion to attain DF information, especially if one used only amplitude comparison techniques. Therefore, the emphasis in this final report is in that portion of the frequency range where the cylinder diameter varies from one-sixth wavelength to approximately 6 wavelengths. Both orthogonal polarizations are considered.

The general problem of arriving at a DF antenna system can be divided into two main aspects. The first aspect concerns itself with how many elements are needed for a specified accuracy and how they should be oriented on the cylinder. Section II answers these questions for all but the very lowest frequencies while Sections IV and V dwell mostly upon the lowest frequencies.

The second aspect of the problem is concerned with the physical realization of the necessary antenna elements for use on the cylindrical configuration. This forms the subject of Section III and part of Section IV. Section III describes an experimental effort to develop a T-bar fed slot antenna for use on a cylinder. Section IV describes a computer study which resulted in the design of a lossy wire array for possible use at the lower frequencies.

Section V discusses some of the problems and limitations inherent at the lower frequencies whereas Section VI summarizes the results of the first five sections. While some conclusions are drawn in Section VI, some questions remain unanswered and await the results of work to be done on a following program.

II. GTD ANALYSIS OF A CYLINDRICAL SLOT ARRAY

This section deals with the analysis of a conformal antenna array which consists of rectangular slots in a perfectly-conducting circular cylinder. In the present study, one is interested in ascertaining the complex voltages received at each of the slot antenna terminals when an electromagnetic plane wave is incident on the array. The object of this study is to determine the feasibility of employing such a slot array for the purposes of direction finding; the feasibility of the array is to be determined from a knowledge of the variations in voltages received at the slot antenna terminals as a function of the direction (in azimuth) of the incoming signal.

In this initial study, the DF antenna array is modelled by an infinitely long perfectly-conducting circular cylinder perforated with three or four identical, thin, small rectangular slots which are placed uniformly along the circumference of the cylinder. Since the cylinder is assumed to be infinitely long, and only a single array is considered, the present study neglects the effects of truncation arising from the finiteness of the actual cylinder, and it also neglects the presence of any other vertically stacked arrays (for the different frequency bands). The effects of the former may be neglected if one assumes that the cylinder is sufficiently long in comparison with the slot dimensions such that the interactions between the slots and the ends of the cylinder is not significant. Also, it must be assumed that the arrays for the different frequency bands are stacked sufficiently far apart on the cylinder so that the effects of their interaction (coupling) are negligible.

The geometrical configuration of the conformal array under study is illustrated in Fig. 2-1. The array is illuminated by an arbitrarily polarized plane electromagnetic wave which is incident from an arbitrary direction in azimuth and elevation; however, in the present DF application, the elevation angle of the incoming wave will generally be within 30° of the horizon. The elevation angle, θ and the azimuthal angle, ϕ associated with the direction of the incident wave are indicated in Fig. 1; the inclination of the slot axis with respect to the z-direction, which is denoted by the angle θ_0, is also indicated in the same figure.

The array configuration of Fig. 2-1 is analyzed via a short circuit admittance matrix formulation which is presented in Reference 2; in this formulation, the voltages received at the array slot terminals* are expressed in terms of the slot mutual admittances, and

*Each of the slots is assumed to be connected to waveguides such that the end walls of the waveguides form the circular cylindrical surface of the array; the slot terminals at the reference plane within each waveguide is then taken to be the dominant mode a half wavelength (for the sake of definiteness) from the slot aperture.

the short circuit currents induced in the slots by the incident electromagnetic plane wave. The induced short circuit currents and the mutual admittances are calculated by the Geometrical Theory of Diffraction (GTD).

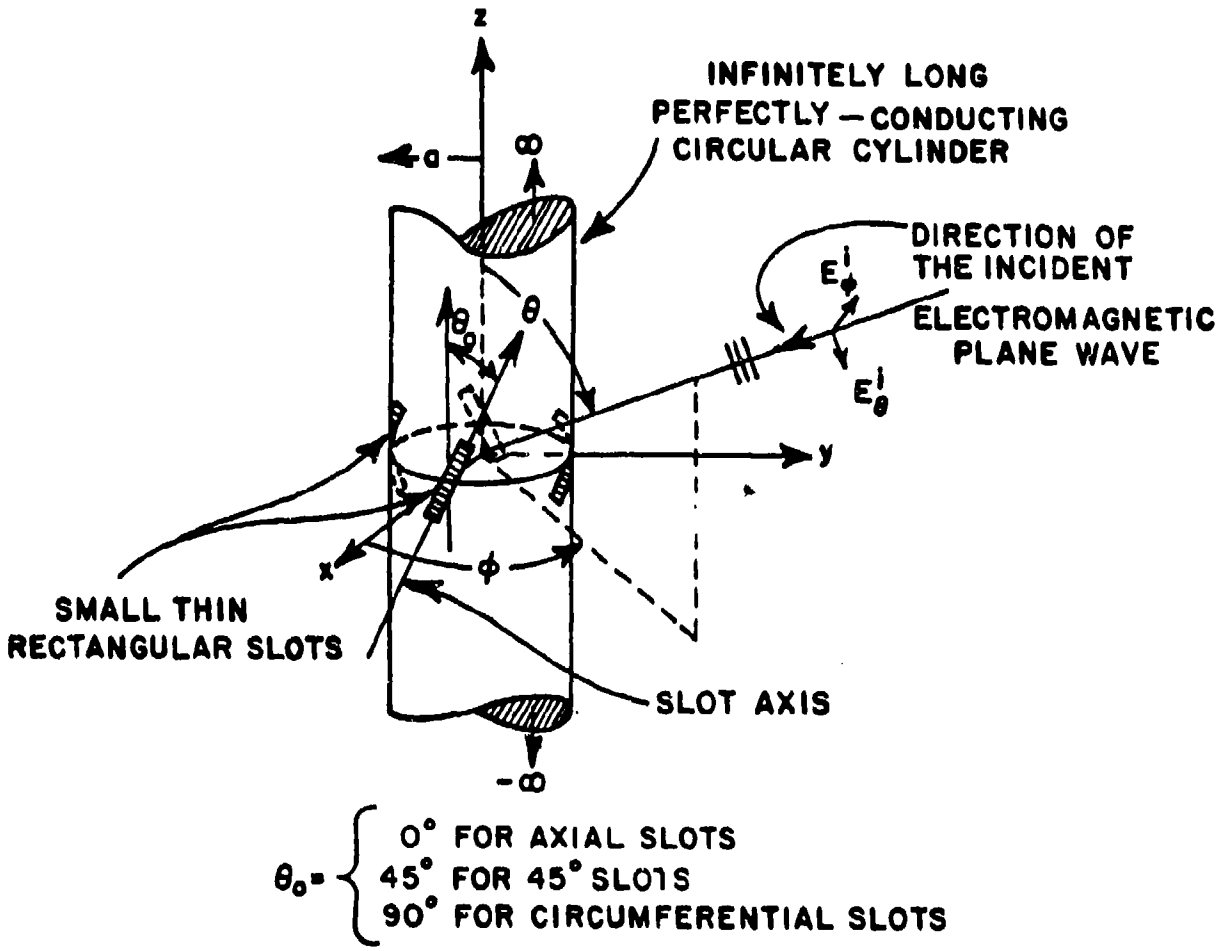

Fig. 2-1. An array of rectangular slots in a perfectly conducting circular cylinder.

Some of the numerical results based on the analysis of Reference 2 are presented in the following paragraphs for the voltages received by the slot array in a circular cylinder as a function of the azimuthal angle, ϕ, of the incoming wave. The cylinder size is varied from ka=3 to ka=48; here k and "a" refer to the free space wave number and the radius of the cylinder, respectively. Although the GTD solution employed here is valid for kasinθ_0>>1, it is expected to yield accurate

results for circular cylinders as small as ka=3 (and $\theta \geq 30°$); this estimate of accuracy is based on previous experience with related problems analyzed by the GTD.

Three different slot array configurations are considered; these are the axial slot array, the circumferential slot array, and the inclined (θ_0=45° in Fig. 2-1) slot array, respectively. Referring to Fig. 1, it is seen that the electric field associated with the incident electromagnetic plane wave may be decomposed into it's $\hat{\theta}$ and $\hat{\phi}$ directed components which are denoted by E^i_θ and E^i_ϕ, respectively. The axial slot array is receptive only to E^i_ϕ (this fact may be verified via reciprocity, since an axial slot in a cylindrical surface radiates only a $\hat{\phi}$ directed electric field); on the other hand, the circumferential and 45° slot arrays are receptive to both E^i_ϕ and E^i_θ (except for $\theta = \pm \pi/2$ when the circumferential slot in a cylinder is receptive only to the E^i_θ component). Consequently, the circumferential or the 45° slot arrays are to be preferred for certain applications. From the numerical results obtained, it appears that a three or four element slot array on a circular cylinder can be effectively employed for DF purposes.

The voltages $V_j (j = 1,2,3 \cdots N)$ received at the j^{th} slot when the array (of Fig. 2-1) is illuminated by an electromagnetic plane wave are found in terms of I^{sc} and Y_{jp}, the short-circuit current and N-port admittance matrix respectively (see Fig. 2). In the present applications, N is either three or four. One notes that there is a directional ambiguity present in the N=2 case; consequently this case is not very useful for direction finding applications. The polarization angle* δ, and the elevation (θ) and azimuthal (ϕ) angles, respectively, specify the polarization and angle of arrival of the incident plane wave. The amplitude of the incident plane wave is taken to be unity. Three types of slot arrays are considered, namely, the axial, circumferential, and the inclined (45°) slot arrays. The values of ka selected in the calculations in [2] are ka = 3,6,12, and 48, respectively. The slots are assumed to be open circuited.

Representative plots of the magnitude of the induced short circuit current, I^{sc}_p are shown in Figs. 2-3 to 2-7 for ka = 12 as a function of the azimuthal variation ϕ of the incoming plane waves. Different elevation angles (θ), slot orientation angles (θ_0) and polarization are considered. The variation of I^{sc}_p is directly proportional to the voltage induced in the p^{th} slot in the absence of all the other slots. Figures 2-3 to 2-7 are essentially self-explanatory. However, several things should be pointed out. First, the circumferential slot will respond to a phi-polarized signal if the direction of arrival is not normal to the cylinder axis (i.e., $\theta \neq \pi/2$). This is illustrated in Fig. 2-5. The effect is even more pronounced at lower frequencies. Secondly, the 45° slot which,

*$\delta=\pi/2$ corresponds to E^i_ϕ, whereas $\delta=0$ corresponds to E^i_θ.

of course, responds to both polarizations exhibits a strong asymmetry for the phi-polarization when $\theta \neq \pi/2$. This effect is demonstrated in Fig. 2-7a.

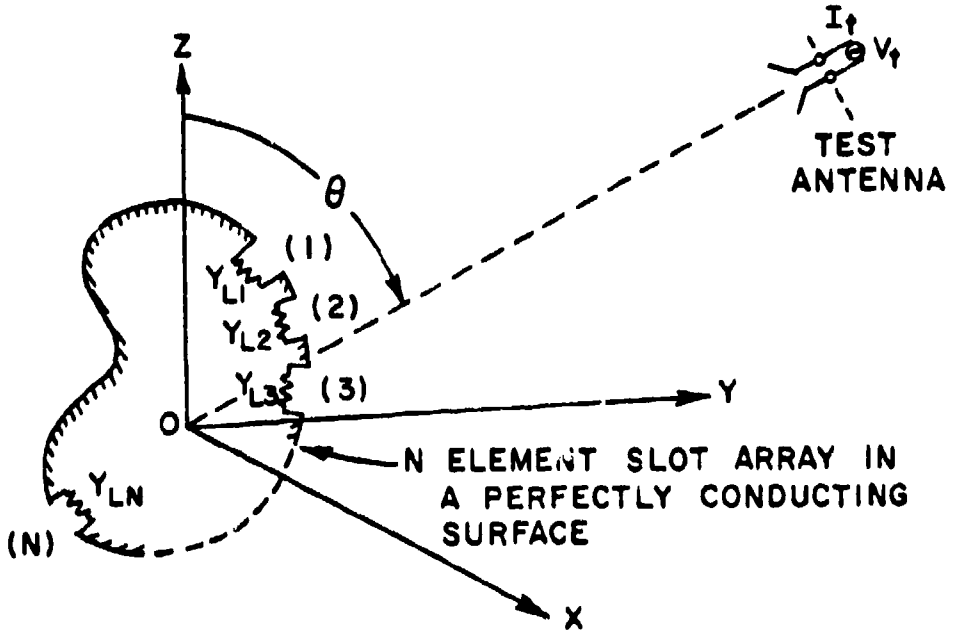

Fig. 2-2. An N-element passive slot array illuminated by a test antenna.

Figure 2-8 indicates the voltages received by an axial slot array as a function of ϕ, for given θ, and slot dimensions. The received voltage scale is labeled VNORM and ϕ is labeled PHI (ϕ is plotted in degrees). Only the range $0° \leq \phi \leq 180°$ is considered as the received voltages at the different slots interchange roles so that their behavior in the range $180° \leq \phi < 360°$ may be readily extrapolated from the plots for $0° \leq \phi \leq 180°$. Since the axial slots are receptive to only a $\hat{\phi}$-directed incident electric field (E_ϕ^i), the axial slot array is receptive to only a linearly polarized incident plane wave. In general, the voltage variations (at any given port) increase with increase in frequency (i.e., with increase in cylinder size or ka). These variations are smooth except for angles of arrival (ϕ) which are in the deep shadow region of the slots where the corresponding received voltages indicate a ripple (fluctuation) which is more pronounced at the higher frequencies.

The voltage plot (for N = 3 case) indicates voltage amplitude crossovers at ϕ = 0°, 60°, 120° and 180°; these crossovers provide useful information for direction finding. It is seen from the plot in Fig. 2-8, that there are in general at least two ports at which the voltages differ by 6-8 dB, for any ϕ.

Figures 2-9a and 2-9b indicate the voltages received by a circumferential slot array; these plots are labeled similar to those in Fig. 2-8. When θ = 90°, (i.e., along the horizon) the circumferential slot array receives only a θ-directed incident electric field. However, for $\theta \neq 90°$, the circumferential slots are receptive to both, θ and ϕ directed incident electric fields. Thus, the circumferential slot array is receptive to elliptically polarized incident plane waves for $\theta \neq 90°$ as seen in Figs. 2-9a and 2-9b.

The 45° slots have the characteristics of both the axial, and circumferential slots, respectively. The 45° slots would thus be receptive to elliptically polarized incident plane waves even for θ = 90° (along the horizon) as shown in Figs. 2-10a and 2-10b, except when the 45° slots are in the deep shadow region of the field incident on the configuration where the slots are receptive to almost linearly polarized incident plane waves. The received voltage patterns for the 45° slot array in general exhibit smoother variations than those for the circumferential slot array. The voltage variations of course increase with increase in frequency (or ka) for axial, circumferential and 45° slot arrays as may be predicted from GTD considerations. Additional results for axial, circumferential and 45° slots may be found in Reference 2.

From the numerical results above, it is seen that the variations in the voltages received at the array ports (as a function of the angle of arrival of an incoming signal) are such that they could be used for the purposes of direction finding. However, the practical effectiveness of such a DF configuration would be limited by the dynamic range of the receiver, the sensitivity of the receiver over the dynamic range, and the effects of the environment surrounding the DF configuration. If an amplitude comparison DF scheme is employed, with a three element array (N=3), then certainly the minimum azimuthal resolution can be estimated on the basis of the maximum and minimum differences in the received voltage amplitudes at any two of the three antenna ports. These maximum and minimum amplitude differences occur periodically (in ϕ) for different azimuthal (ϕ) angles. Additional information on the DF resolution may be obtained from a knowledge of the order or sequence in which the received voltages at the N ports are increasing or decreasing in each of the four azimuthal quadrants; the plots in Reference 2 provide the necessary details. The four slot array, of course, provides additional DF information over the three slot array case; consequently, a four slot array could improve DF resolution. In general, one would

expect the DF resolution to improve with increase in frequency of the incoming wave primarily due to the larger variations in the received voltages at higher frequencies.

Since the phase variations of the received voltages at the various ports are a function of the azimuthal direction of the incoming signal, and since these phase variations are not as rapid at the lower frequencies as they are at the higher frequencies, one could use the phase information along with the amplitude information for the received voltages for a higher azimuthal resolution at the lower frequencies, if desired. One also could use two different three element slot arrays for a given frequency band in which the slots are interlaced in an echelon fashion, e.g., the three slots in the first array are separated 120° apart in the same plane, whereas the three slots of the other array are configured similarly except they are in a plane which is vertically displaced from the plane containing the first three slots; furthermore, the slots in the lower plane are shifted by 60° in azimuth with respect to the slots in the upper plane, or vice versa. The two arrays could also employ different slot types. This configuration if used to DF independently with each of the two slot arrays (corresponding to the lower and the upper plane locations, respectively) would provide additional look angles and hence more DF information on the incoming wave. The echelon arraying of the slots would avoid crowding the six elements in one plane along the circumference of the cylinder.

In conclusion, the relative merits of the axial, circumferential and 45° slot arrays in cylinders for the purposes of direction finding may be evaluated from the results and discussions in parts A, B and C of Section III of Reference 2. It is noted from Section III that the 45° slot arrays have the characteristics of both the axial and the circumferential slot arrays; furthermore, the 45° slot arrays yield slightly smoother variations in the received voltages as a function of the azimuth of the incoming wave than the circumferential slot arrays. For $\theta < 90°$ (i.e., above the horizon), the voltages received by a 45° slot array exhibit asymmetries (i.e., the values for $0° < \phi < 180°$ are different from the values for $180° < \phi < 360°$) which are the same for each slot. One may be able to employ this property of the 45° slot array to advantage for direction finding.

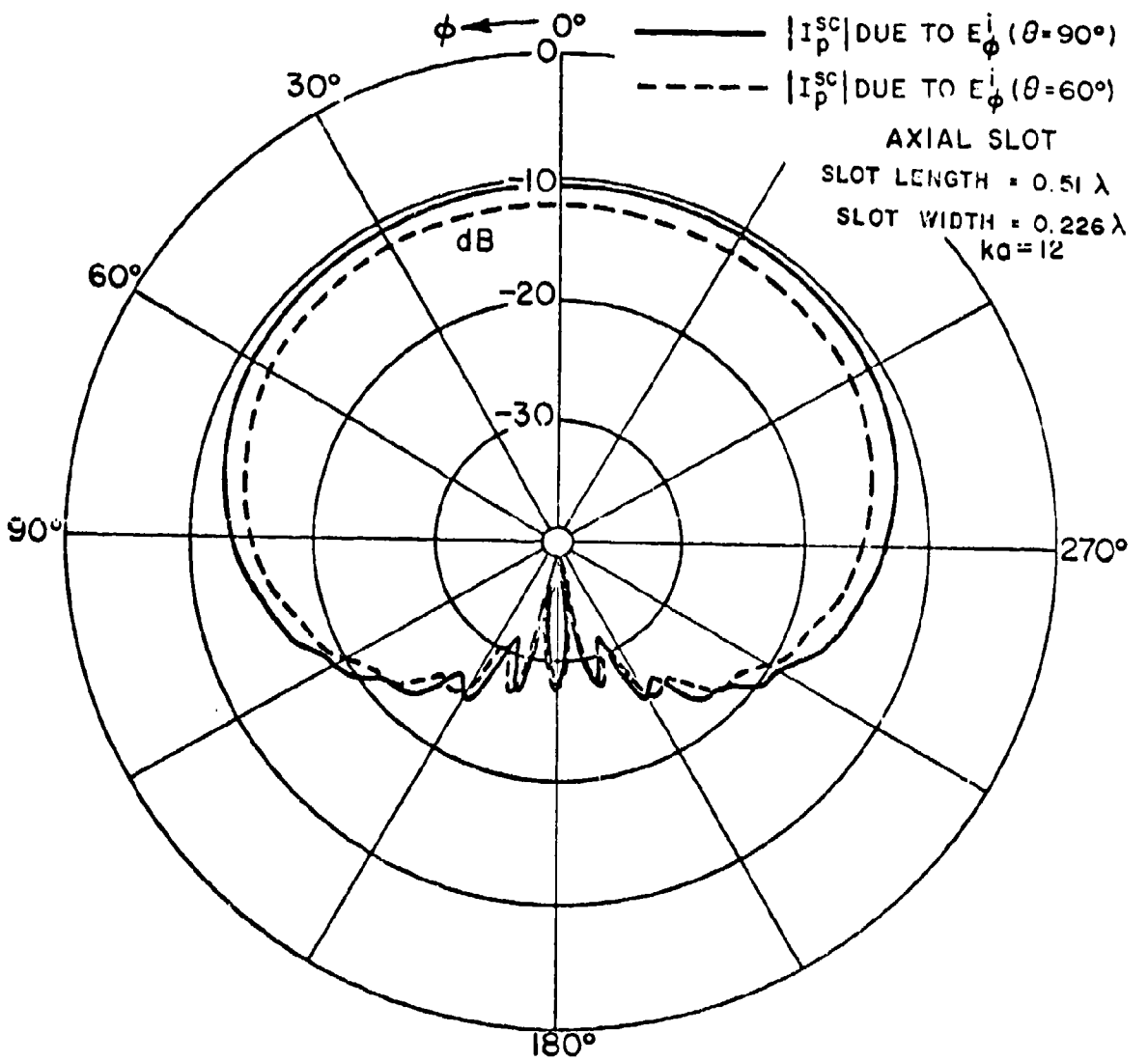

Fig. 2-3a. $|I_p^{sc}|$ vs ϕ for an axial slot.

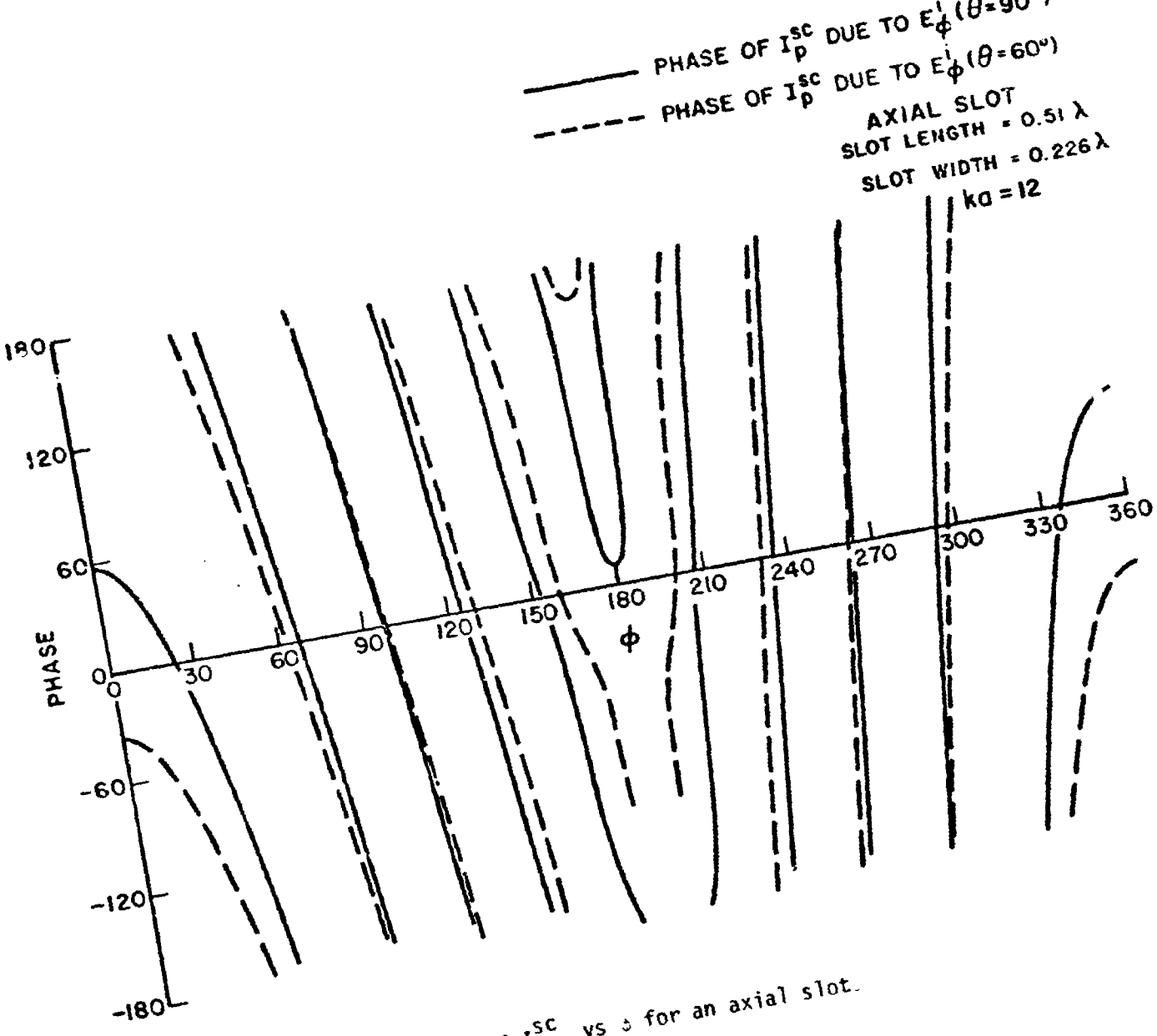

Fig. 2-3b. Phase of I_p^{sc} vs ϕ for an axial slot.

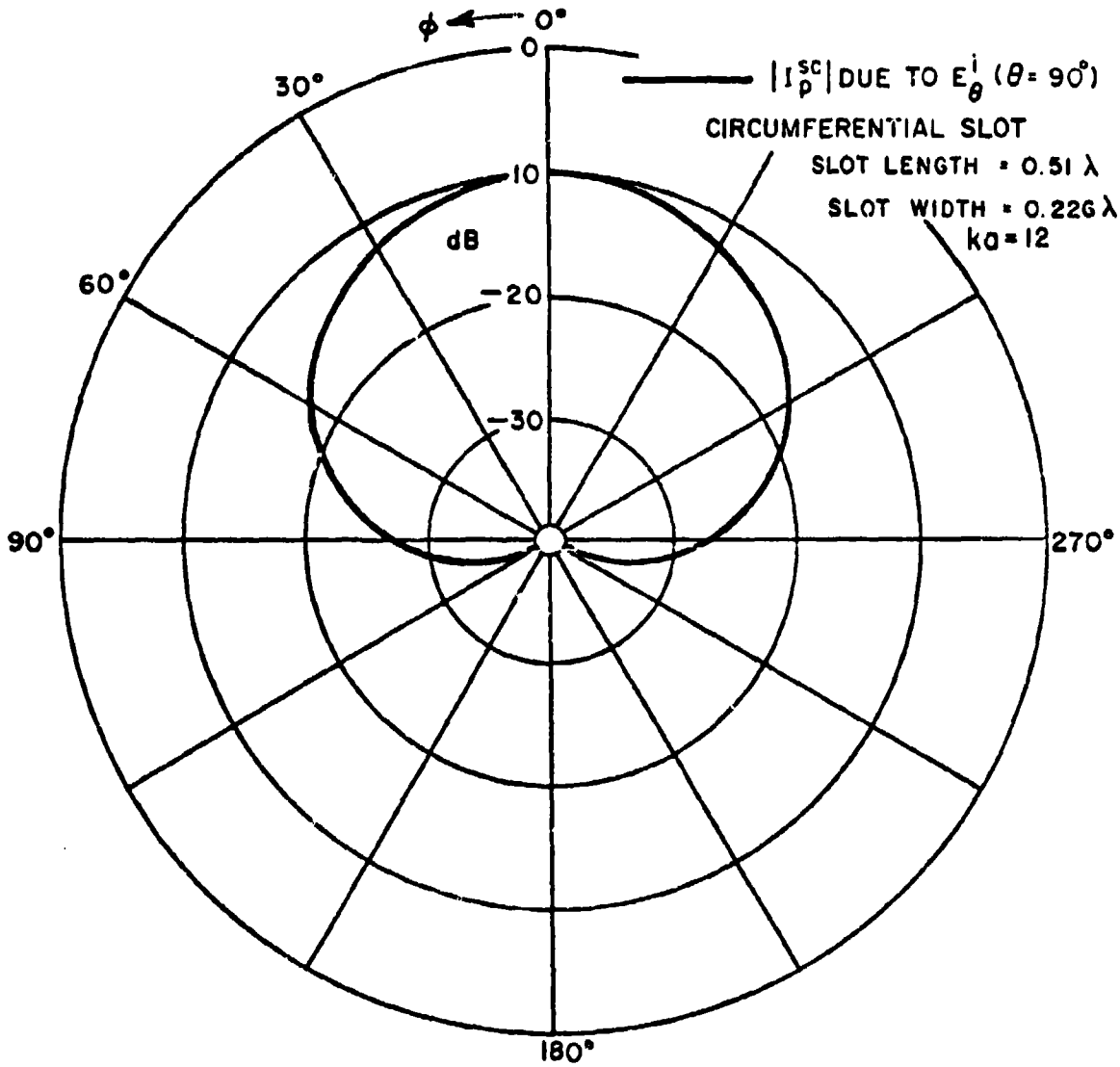

Fig. 2-4a. $|I_p^{sc}|$ vs ϕ for a circumferential slot. (Note: $I_p^{sc} = 0$ due to E_ϕ^i at $\theta = 90°$ for a circumferential slot.)

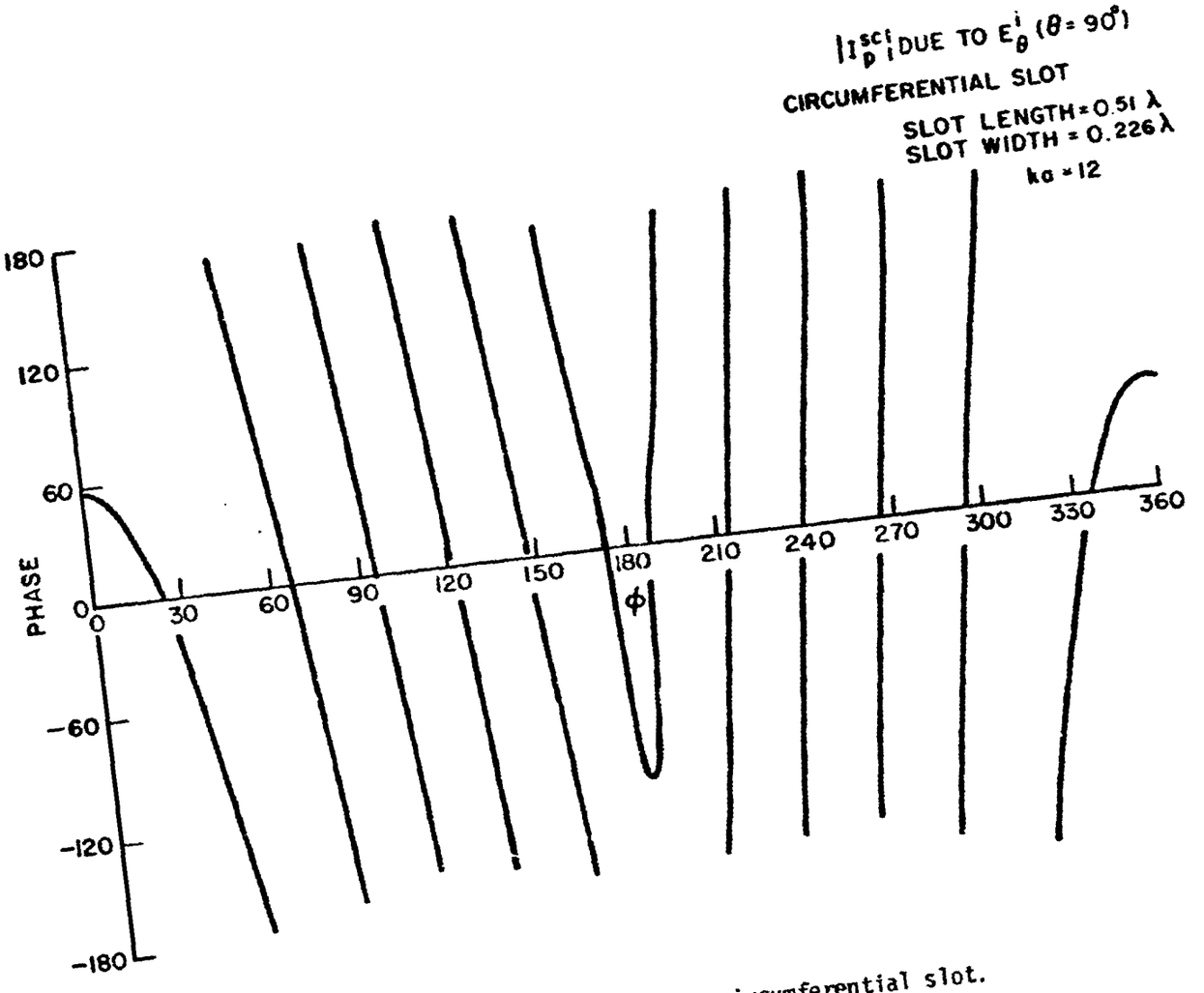

Fig. 2-4b. Phase of I_p^{sc} vs ϕ for a circumferential slot.

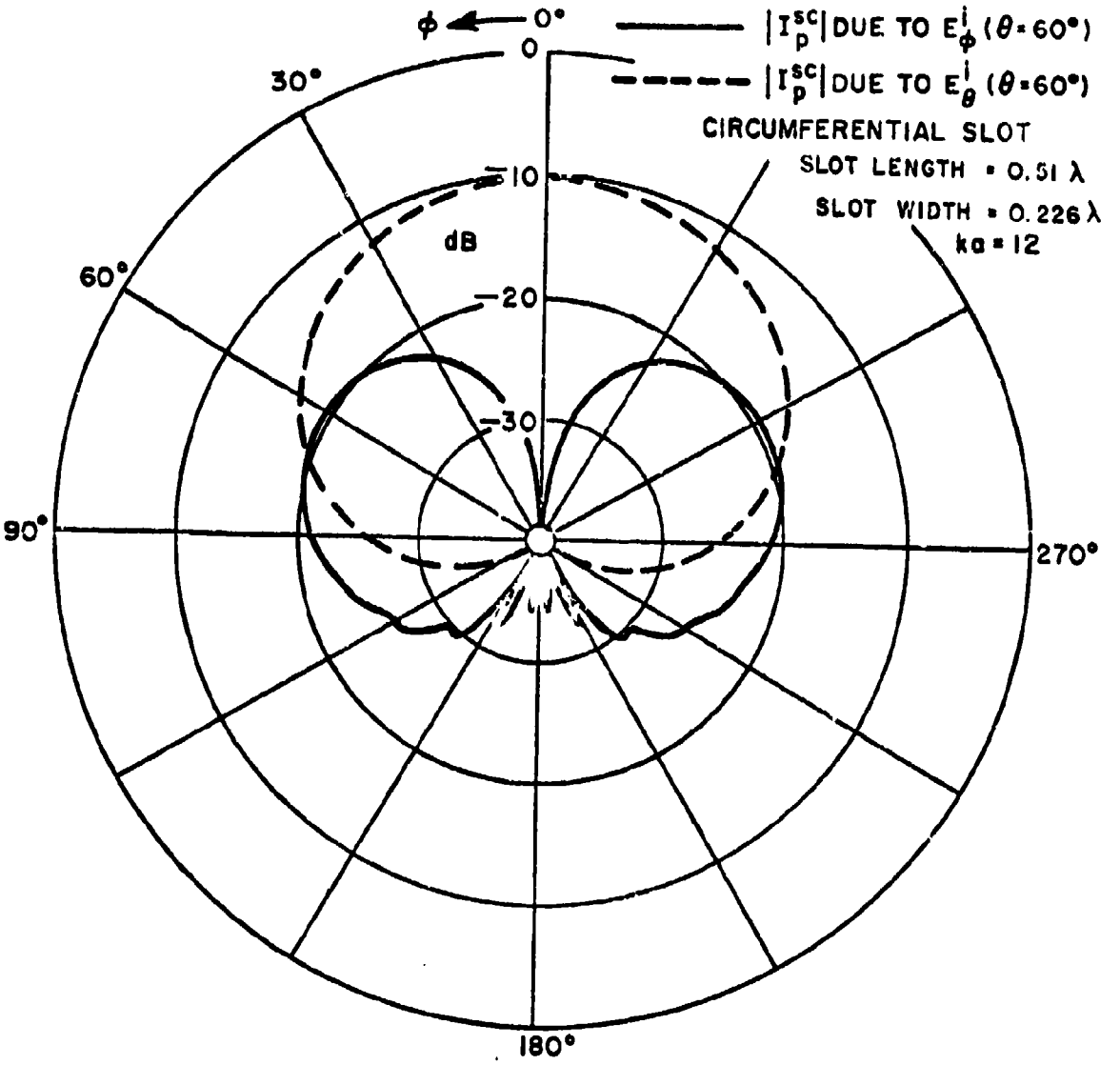

Fig. 2-5a. $|I_p^{sc}|$ vs ϕ for a circumferential slot.

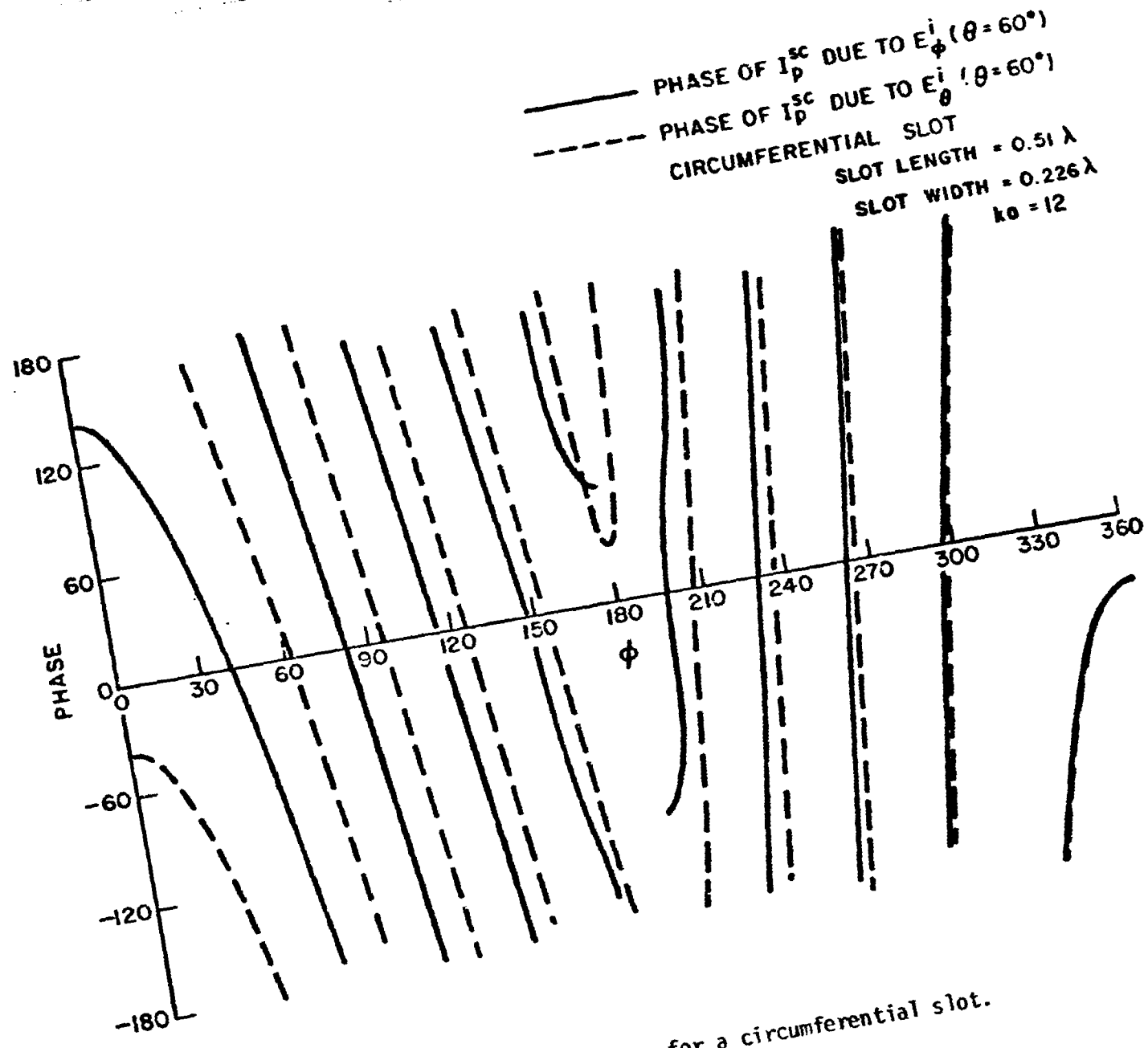

Fig. 2-5b. Phase of I_p^{sc} vs : for a circumferential slot.

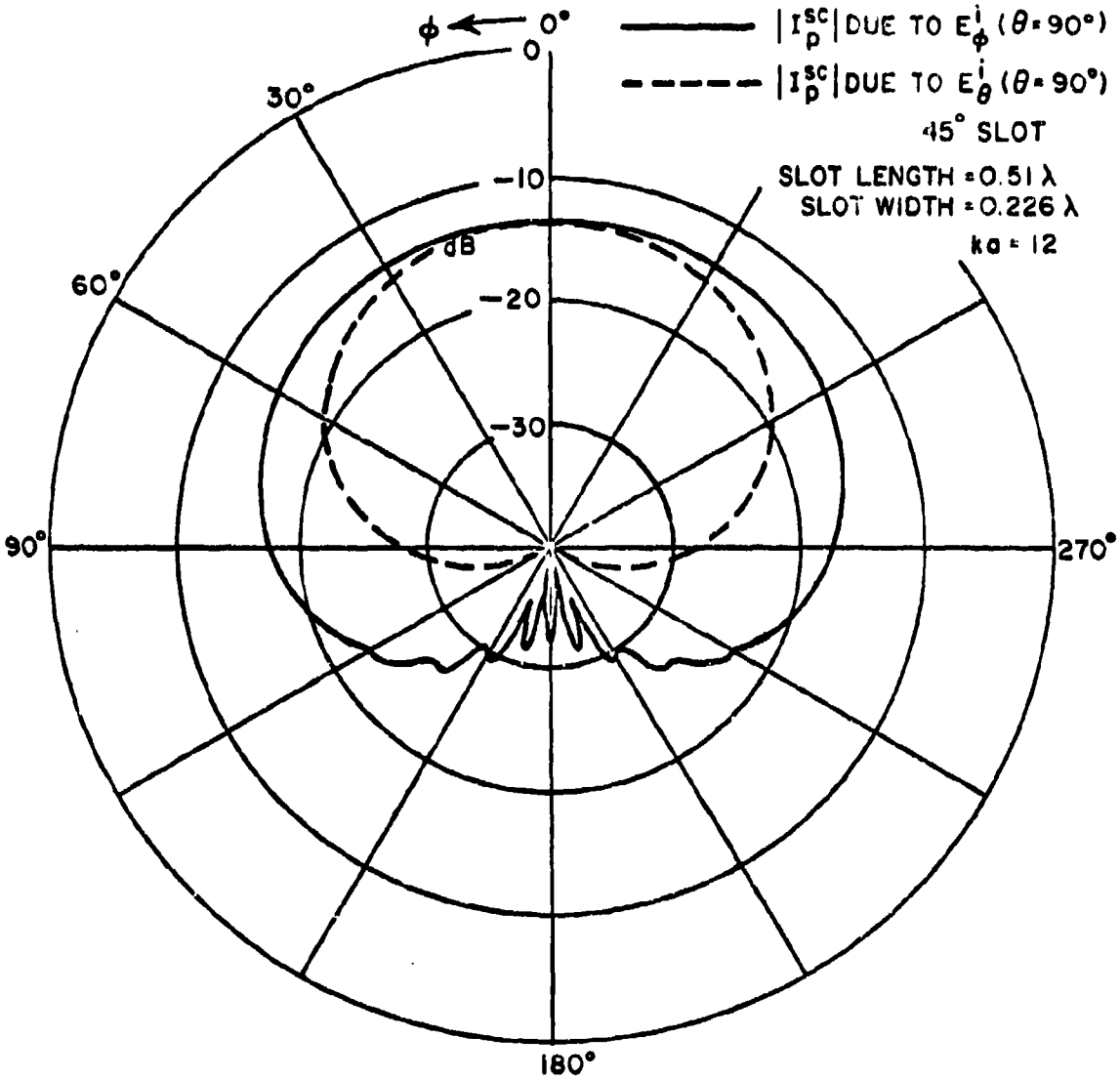

Fig. 2-6a. $|I_p^{sc}|$ vs ϕ for a 45° slot.

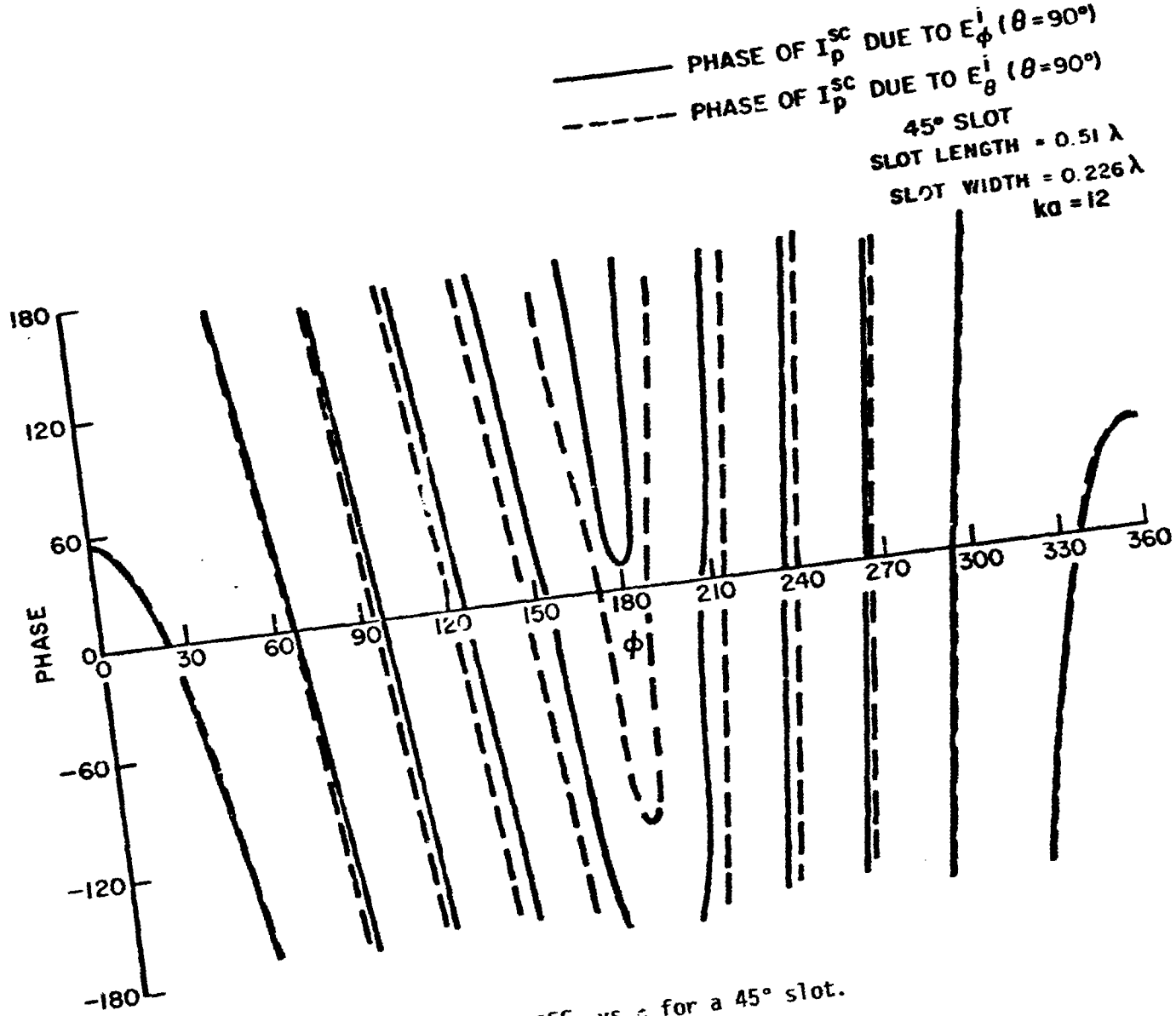

Fig. 2-6b. Phase of I_p^{sc} vs ϕ for a 45° slot.

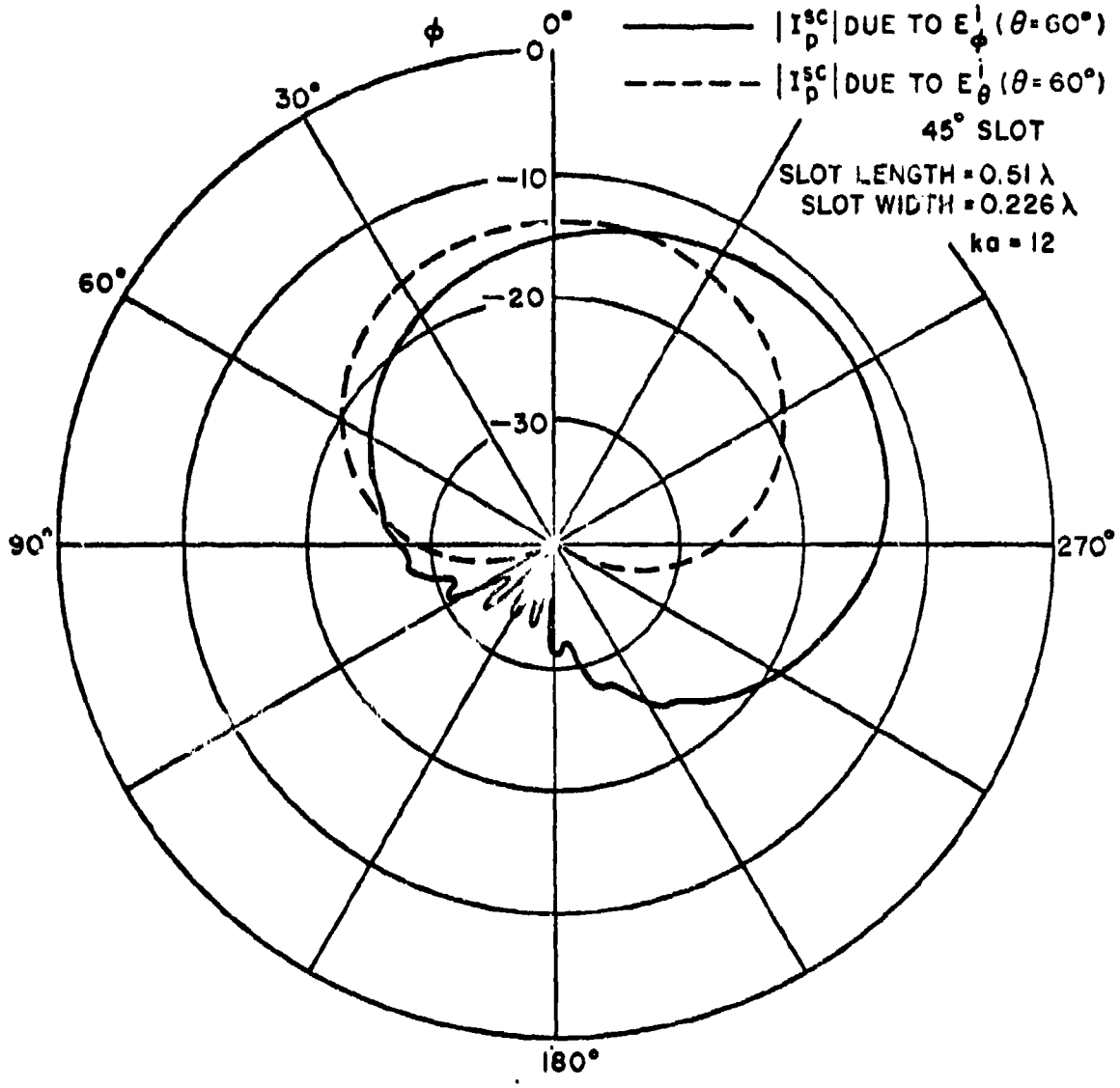

Fig. 2-7a. $|I_p^{sc}|$ vs ϕ for a 45° slot.

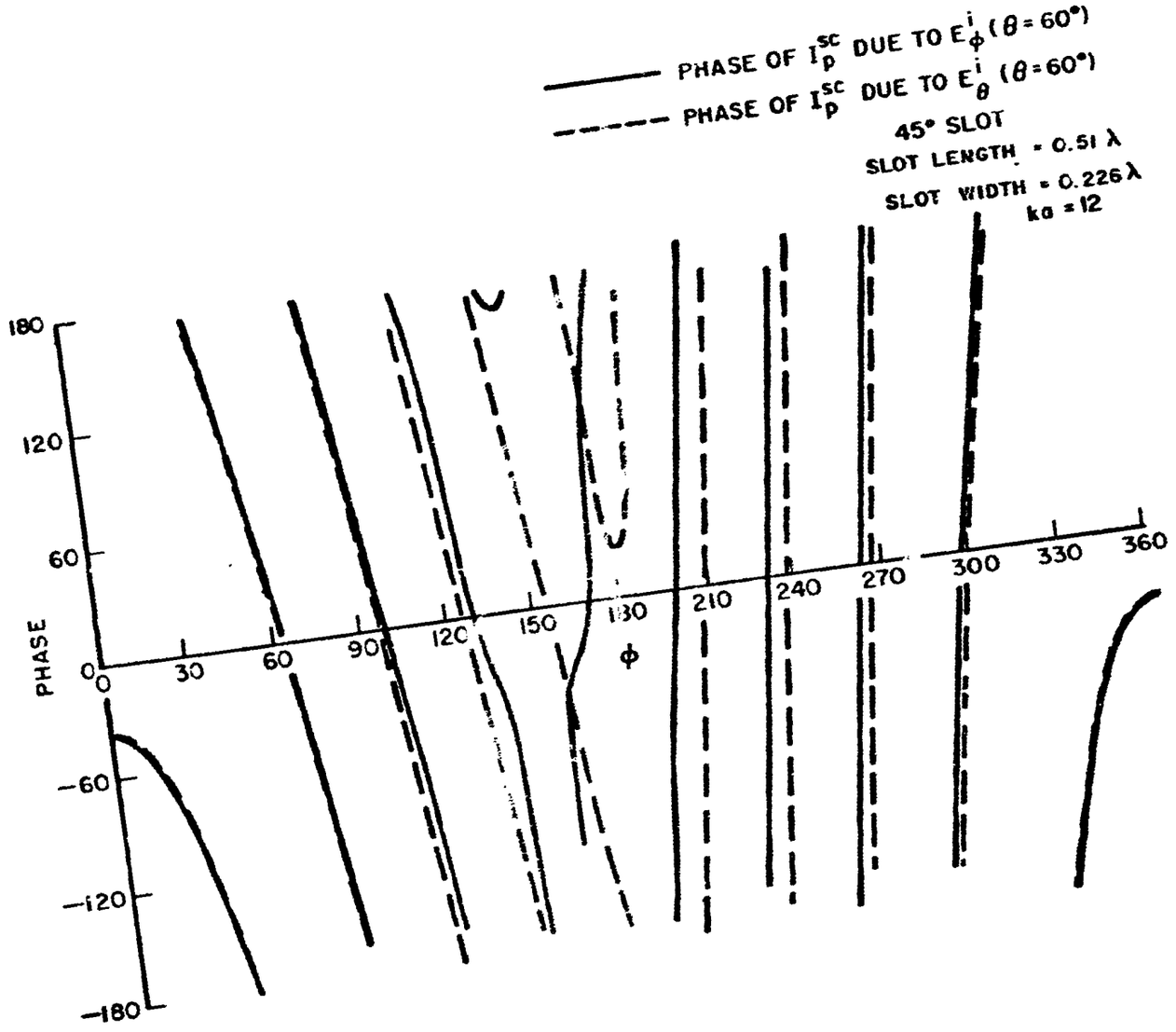

Fig. 2-7b. Phase of I_p^{sc} vs ϕ for a 45° slot.

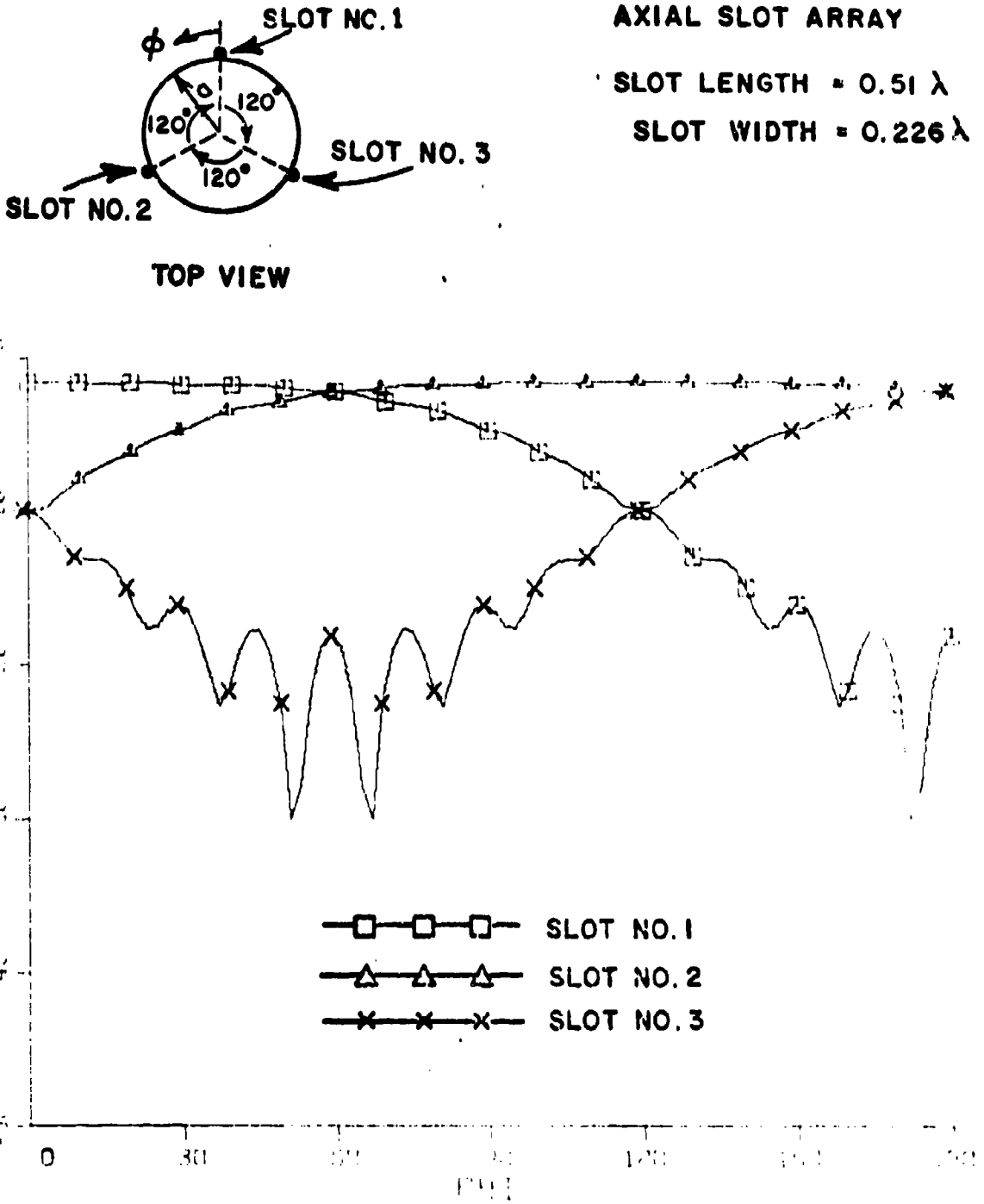

Fig. 2-8. Magnitude (in dB) of voltages received at the array ports due to an $E^1_\phi(\delta=\pi/2)$ on a cylinder of ka=12 for θ=75°.

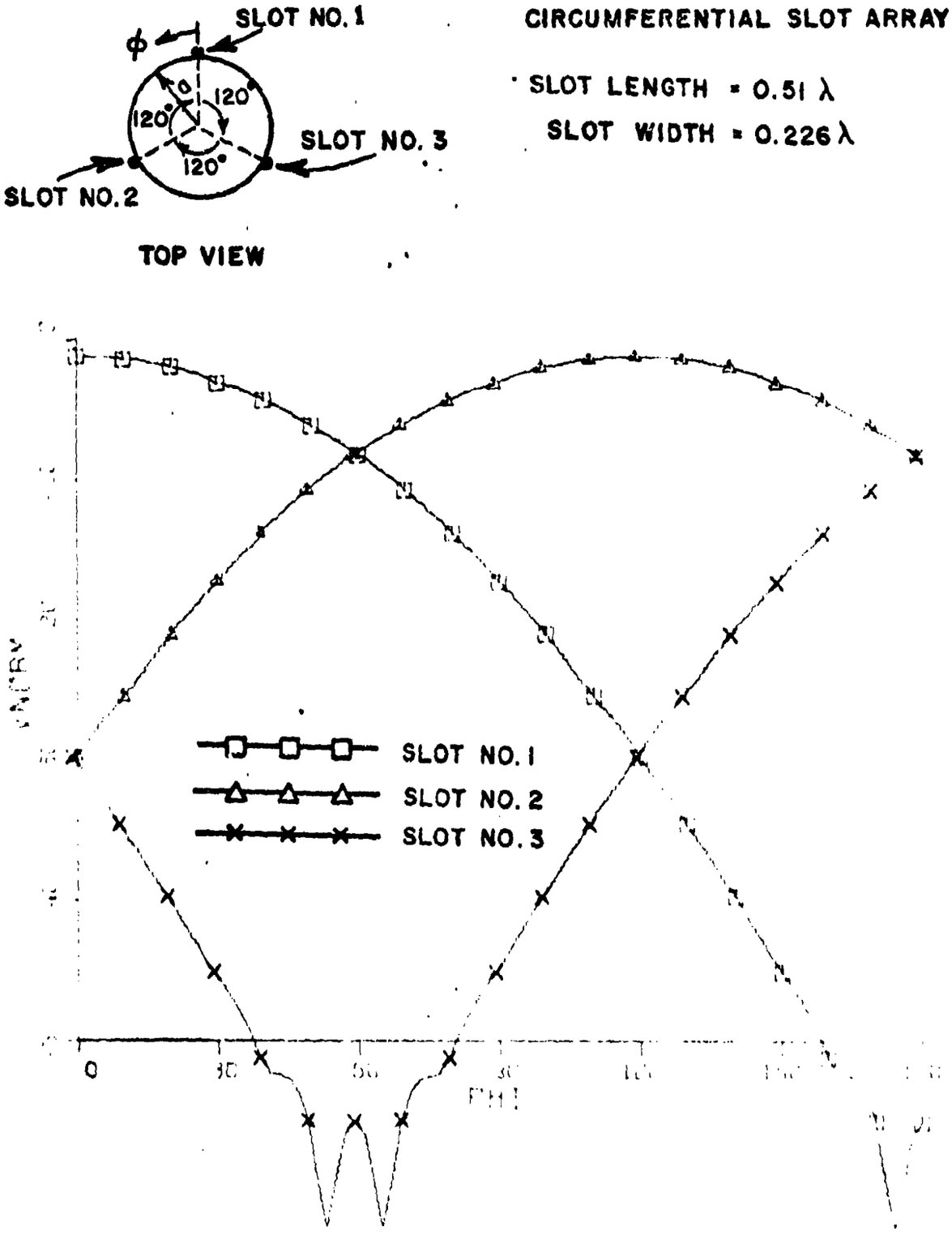

Fig. 2-9a. Magnitude (in dB) of voltages received at the array ports due to an $E_\phi^i(\phi=0)$ on a cylinder of ka=12 for $\theta=75°$.

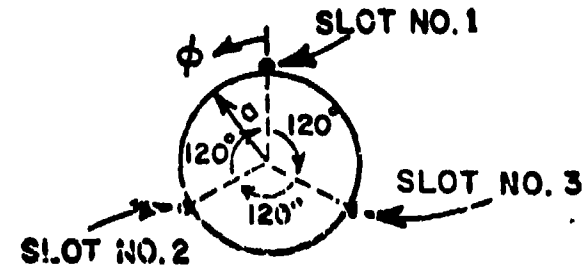

TOP VIEW

CIRCUMFERENTIAL SLOT ARRAY

SLOT LENGTH = 0.51 λ

SLOT WIDTH = 0.226 λ

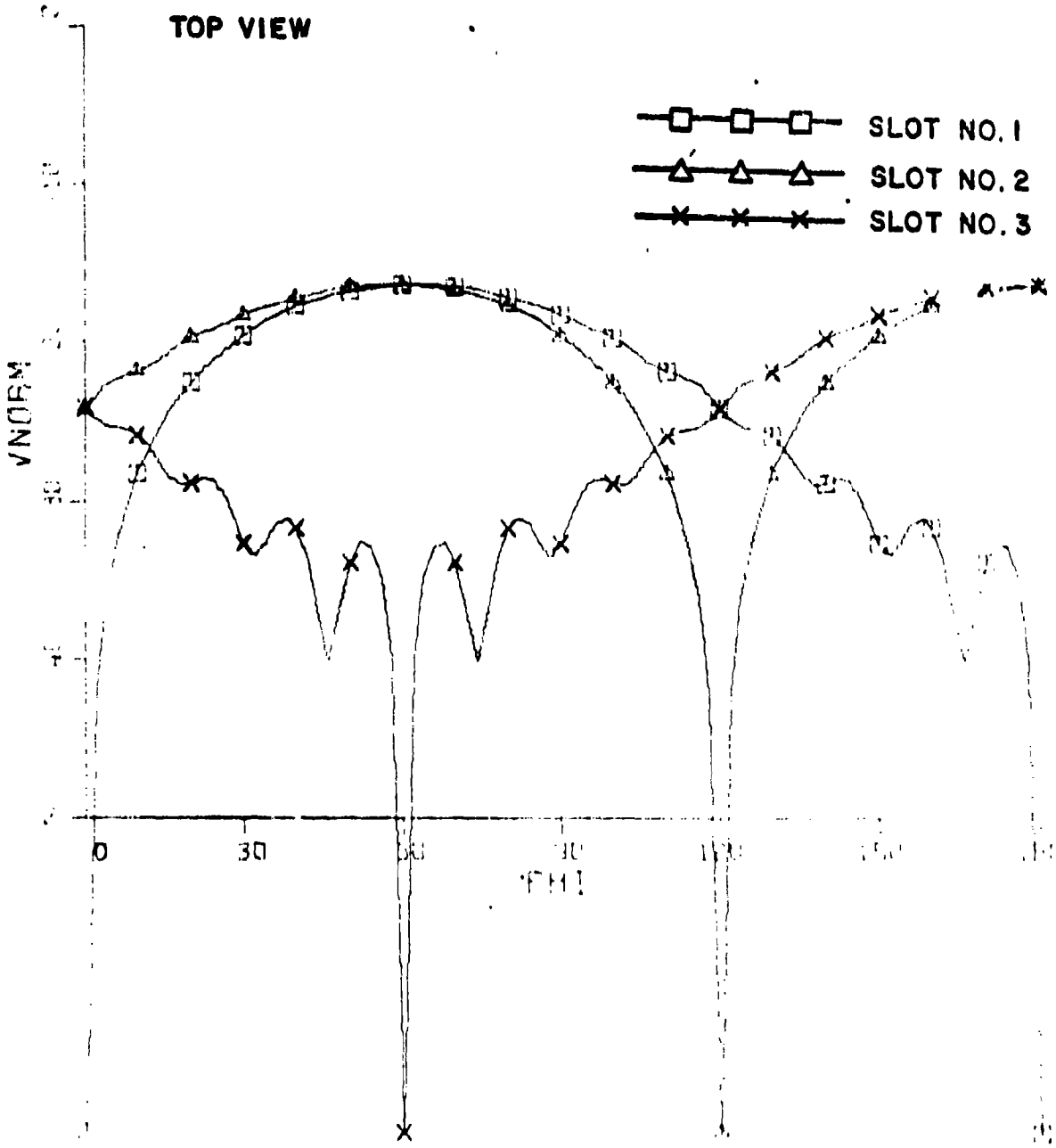

Fig. 2-9b. Magnitude (in dB) of voltages received at the array ports due to an $E_\phi^i(\alpha=\pi/2)$ on a cylinder of ka=12 for n=75.

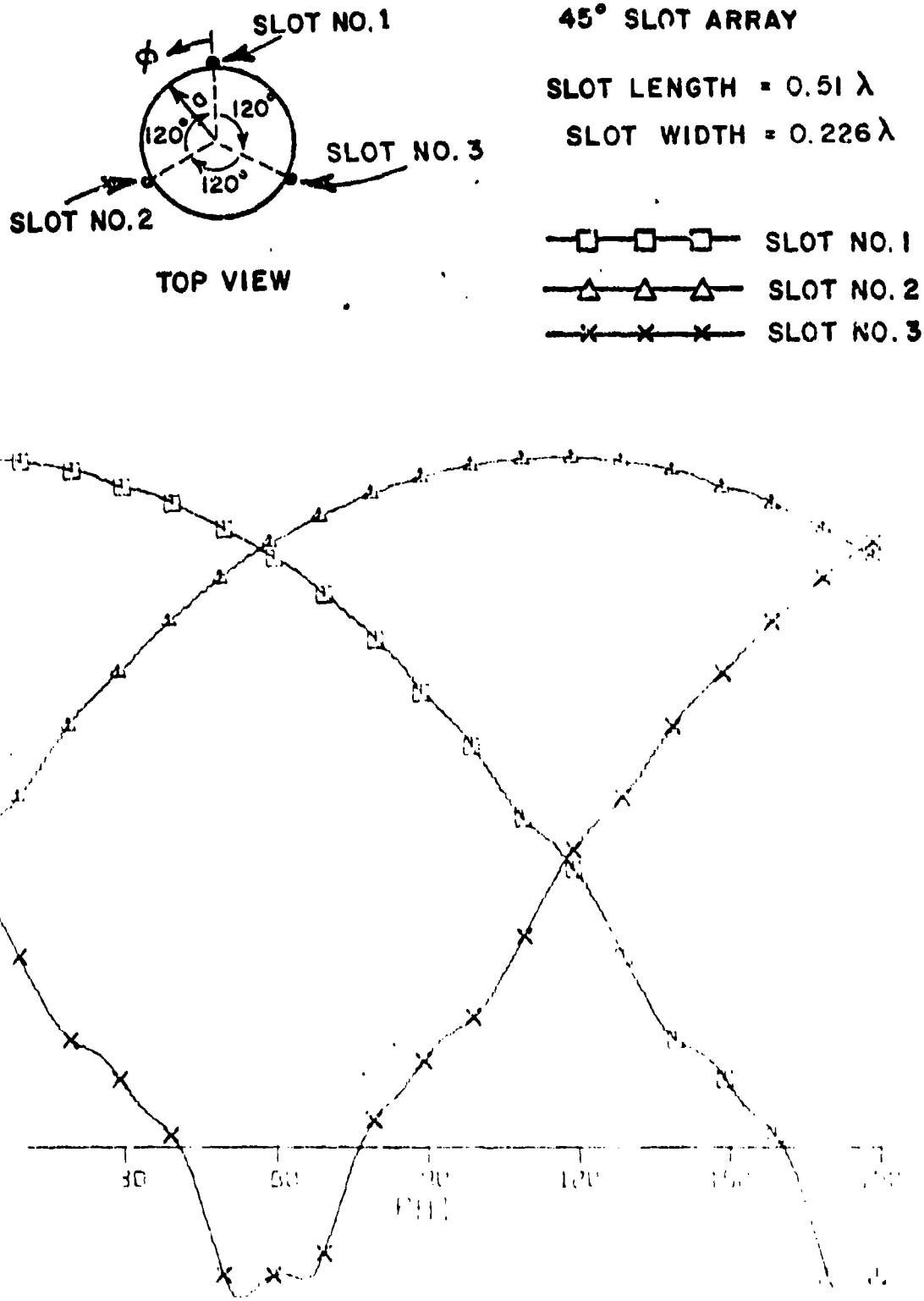

Fig. 2-10a. Magnitude (in dB) of the voltages received at the array ports due to an $E_\theta^1(\delta=0)$ on a cylinder of ka=12 for θ=75°.

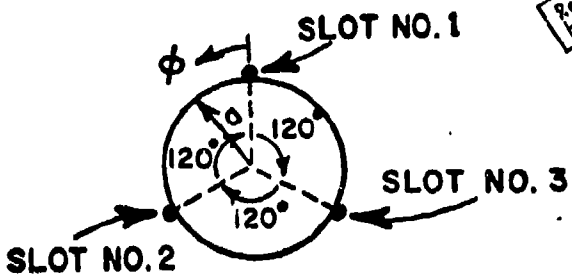

TOP VIEW

45° SLOT ARRAY

SLOT LENGTH = 0.51 λ

SLOT WIDTH = 0.226 λ

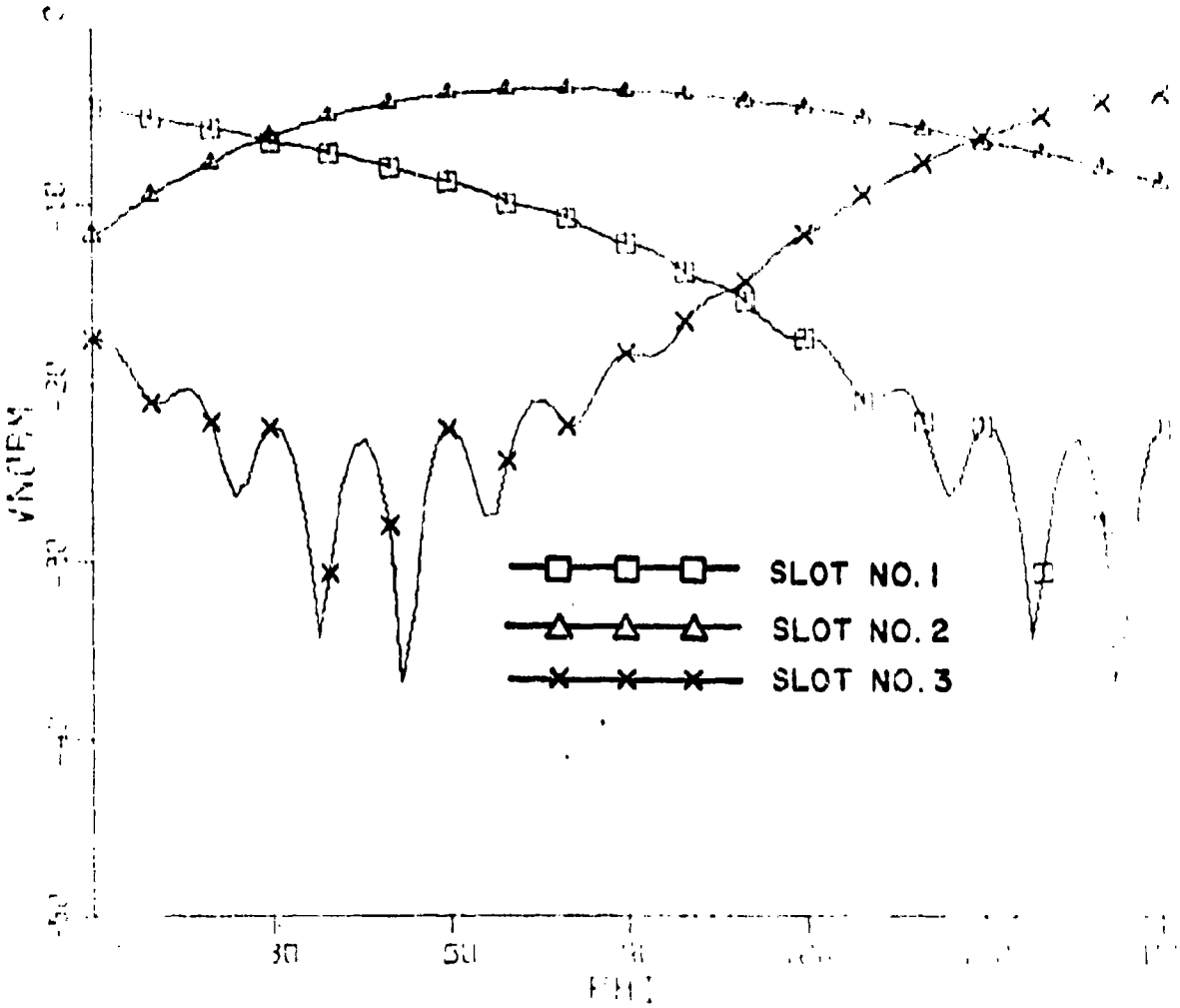

Fig. 2-10b. Magnitude (in dB) of the voltages received at the array ports due to an $E_\phi^i(\alpha=\pi/2)$ on a cylinder of ka=12 for θ=75°.

III. EXPERIMENTAL DEVELOPMENT OF A T-BAR SLOT ANTENNA

One possible antenna element for use in a direction finding array on a cylindrical surface is a slot antenna. Most slot antennas require a quarter wavelength from the backwall to the aperture plane which, for the cylindrical application here, is a prohibitively large distance. However, it has been found during the course of this investigation that a T-bar fed slot antenna can be designed over a large (i.e., 4:1) frequency range such that the distance from the backwall to the aperture is considerably less than a quarter wavelength over most of the bandwidth. The final configuration of the T-bar antenna is shown in Fig. 3-1.

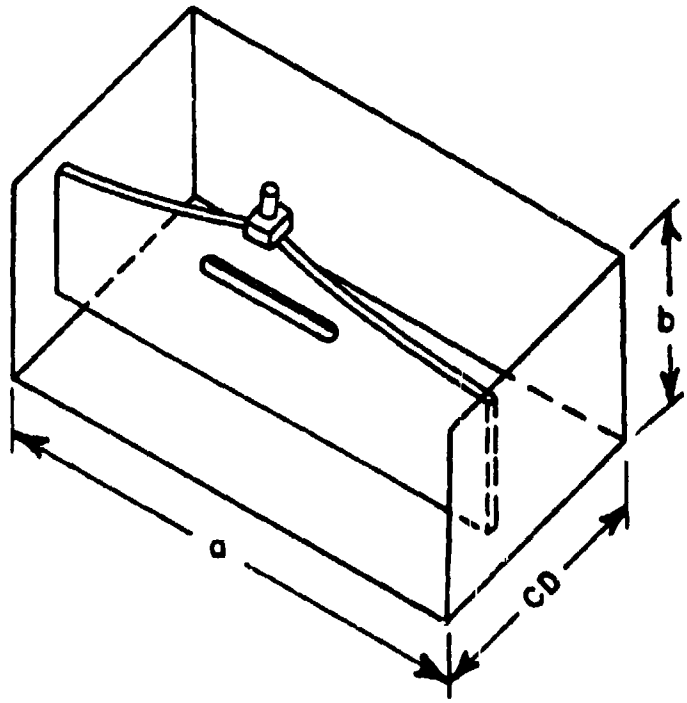

Fig. 3-1. A cavity backed T-bar fed, planar, slot antenna with top of cavity removed for viewing purposes.

Some of the highlights of the experimentation that led to this development are described below and in [3] for both the planar and cylindrical cases.

A. Planar T-Bar Slot Antenna

In a previous study of T-bar fed slot antennas, E.H. Newman of The Ohio State University concluded that T-bars of thin rectangular cross sections exhibited essentially the same input impedance as T-bars of circular cross section and that the T-bar geometry is one of the important parameters in determining bandwidth. Thus, the first antenna parameter optimized over the desired four to one bandwidth during this investigation was the T-bar geometry.

Newman, in his study, considered bandwidth as that frequency range where the VSWR of the antenna remains below 2.0. However, other important performance parameters such as efficiency, gain, and radiation patterns (not necessarily independent of each other) may also be expressed in terms of bandwidth. Investigating each of the performance parameters over a four to one frequency range with the design of an optimum T-bar slot antenna as the final goal would indeed be a lengthy process when one considers all possible combinations of the T-bar antenna variables such as cavity depth, T-bar depth, cavity tuning and dielectric loading. Therefore, an experimental system which would sample each of the performance parameters simultaneously as the antenna parameters were varied and would quickly describe the interrelationship of the antenna parameters was needed. A swept frequency insertion loss measurement provided such information. A block diagram of this experimental procedure is shown in Fig. 3-2. Measuring the forward or reverse transmission coefficient (S_{12} or S_{21}) at the scattering parameters device, the ratio of power received to power transmitted is obtained. It is apparent that measurements over a swept frequency range contain information about the radiation pattern in a narrow region broadside to the antenna and also the gain of the antenna which in turn is related to efficiency, directivity, and antenna mismatch. Substituting a reference antenna of comparable bandwidth for the test antenna, the insertion loss measurement provides a method to quickly check the cummulative effect of these important performance parameters while investigating different combinations of the antenna variables. The S-parameter device used in these experimental investigations will also measure the return loss at the antenna port which gives the VSWR of the antenna.

Using the insertion loss and VSWR measurement system, the T-bar geometry was varied in a successful attempt to optimize the T-bar as described in the following paragraphs.

One method to expand the bandwidth of a waveguide is the application of a single or double ridge. The ridge expands the bandwidth of a waveguide by decreasing the lower-cutoff frequency and increasing the cutoff frequency of the higher order modes.

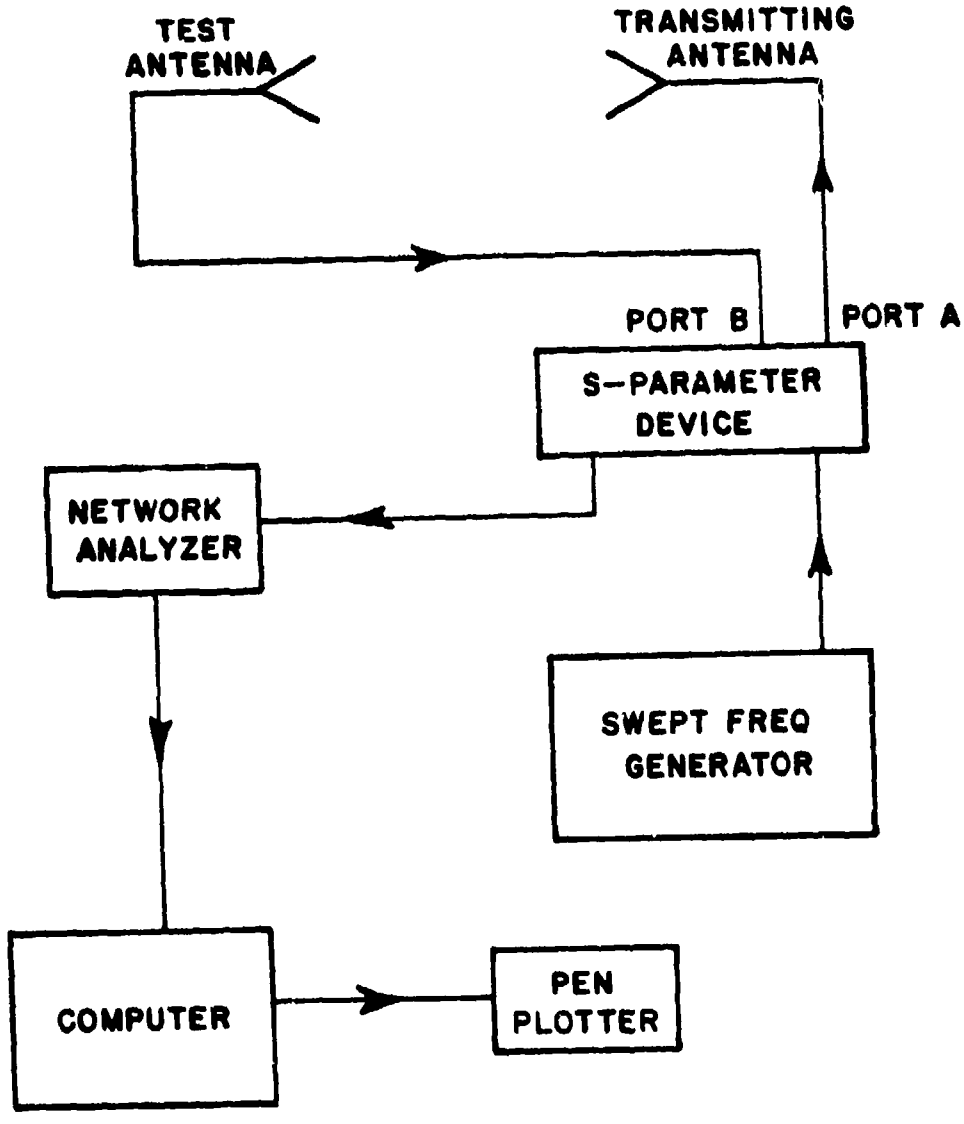

Fig. 3-2. A block diagram of the experimental procedure used to measure the insertion loss between two antennas.

The T-bar antenna (whose cavity exhibits waveguide characteristics) was altered as shown (Fig. 3-3) and a ridge of dimensions 4.88 x 5.08 cm, was installed corresponding to a bandwidth of 2.74 for a waveguide of similar dimensions. Experimental investigations of the ridged T-bar antenna showed an improvement in insertion loss performance over the nonridged case. However, attempts to improve performance still further with different T-bar geometries and ridge sizes, showed that the best results were ultimately obtained when (1) the ridge was removed, (2) the notch in the T-bar was terminated resulting in rectangular slot in the T-bar, and (3) the peaked feed point of the T-bar replaced with a gradual slope as shown in Fig. 3-4.

This investigation also showed an eight to twelve dB increase in insertion loss which occurred at approximately 1500 MHz, thus limiting the bandwidth performance. Resorting to another waveguide matching technique, tuning stubs of various sizes were positioned about in the cavity while measuring the insertion loss. The spike at 1500 MHz can be effectively reduced using this procedure without any loss elsewhere in the bandwidth if the stubs are located on the bottom of the cavity in the vicinity of the T-bar and are shorter than the distance between the T-bar and cavity bottom. The best performance was achieved when the tuning stubs were located $\pm$10 cm from the center of the aperture which corresponds to a spacing of one wavelength at the troublesome frequency of 1500 MHz.

Following the discovery of the slot within the T-bar as a useful tuning aid, the next investigation was to determine what effect the length, width, shape of such a slot, and its position in the T-bar has on the overall performance of the antenna. Investigation of the slot length initiated with a small circular hole in the center of the region where the slot was previously located in the T-bar. This hole was then lengthened symmetrically in incremental steps recording the insertion loss after each increase. The best performance was achieved when the slot length was 7.5 cm which corresponds to 0.5 wavelength at the highest frequency of the desired bandwidth (7.5 cm), and decreases when the length is increased above 7.5 cm. The slot only affects the bandwidth above 1500 MHz and the insertion loss shows greatest improvement (10 dB above the no slot case) at 2000 MHz. The slot configuration is depicted in Fig. 3-1.

After establishing the length of the slot within the T-bar, the next investigation was to determine the effects of the width of such a slot. Following the same procedure as before, the width of a 7.5 cm slot was increased incrementally with no substantial changes in previous performance.

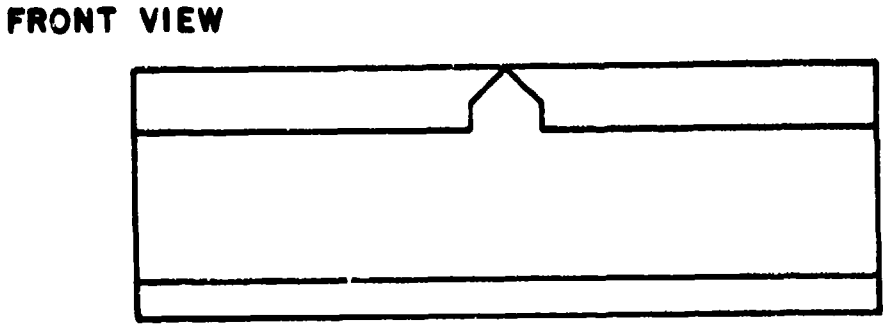

Fig. 3-3. a) Front view of the original planar T-bar slot antenna.

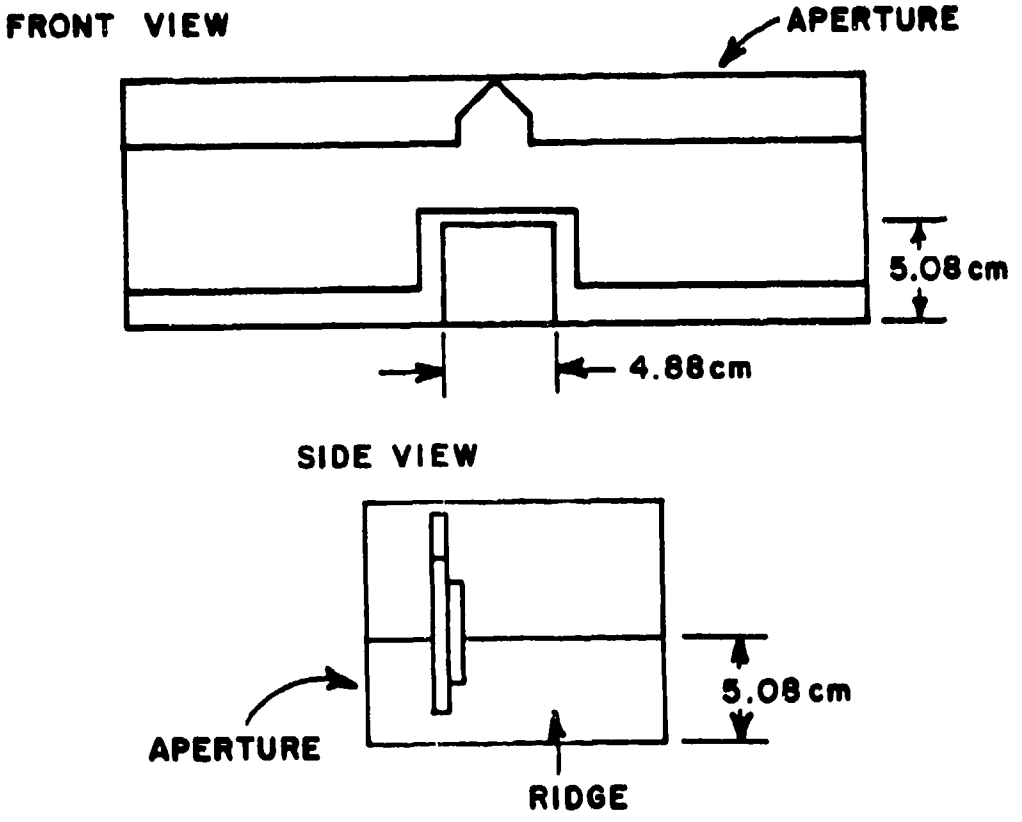

Fig. 3-3. b) The planar T-bar slot antenna with single ridge.

The position of the slot was investigated by constructing T-bars with the slot incrementally moved from 1 cm above the bottom of the T-bar up to 5.0 cm. The insertion loss performance improved in each case up to a distance of 4.0 cm. Above 4.0 cm the insertion loss remained essentially the same. This T-bar with slot length 7.5 cm, slot width 0.8 cm, and distance from slot to T-bar bottom 4.0 cm is hereafter termed T-bar D. This is the T-bar that is shown in Fig. 3-4.

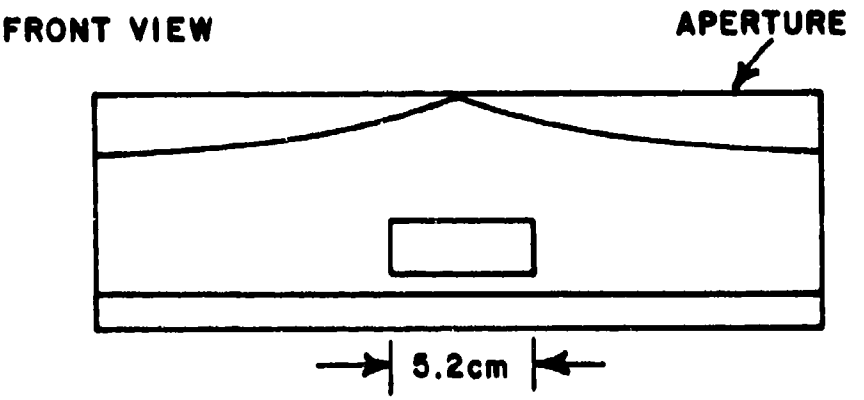

Fig. 3-4. The front view of the planar T-bar slot antenna showing the slotted T-bar which resulted from the ridge investigation.

The remaining questions about the T-bar geometry regard the shape of such a slot and the actual shape and size of the T-bar. After an experimental study of the triangular, square, and rectangular shapes, it was concluded that the original narrow rectangular slot with rounded corners was optimal. Various feed angles and T-bar widths were also investigated but did not give comparable performance to T-bar D.

The next measurements were made to determine the effects of cavity depth on bandwidth performance. The best VSWR-impedance bandwidth should occur when the distance from the T-bar probe feed to the back wall of the cavity is a quarter wavelength at mid-frequency. Therefore, it is desirable to determine what tradeoffs exist between bandwidth and cavity depth in terms of insertion loss and VSWR. Using T-bar D, the air filled T-bar fed slot was investigated while varying cavity depth from 2.25 inches to 1.25 inches in 0.125 inch steps. The experimental results showed that from 500 to 1500 MHz the insertion loss increases as cavity depth is decreased. However, above 1500 MHz it decreases. The limit of the insertion

loss decrease occurs at a cavity depth of 1.5 inches, but at the lower end of the bandwidth the insertion loss continues to increase as cavity depth decreases. This result should be expected since the cavity depth approaches a quarter wavelength for the upper limit of the bandwidth and greatly decreases from a quarter wavelength at the lower frequency as it decreases to 1.50 inches ($\lambda/4$ for 2000 MHz = 1.47 inches). The VSWR measurements for the same experiment indicate that as cavity depth decreases, the VSWR of the antenna increases from 500 to 1500 MHz but decreases from 1500 to 2000 MHz until a cavity depth of 1.5 inches is reached. This is illustrated in Fig. 3-5. This agrees with the insertion loss measurements because the ratio of power transferred should increase as the VSWR decreases and likewise decrease as the VSWR increases. This fact is also apparent in the results of the absolute gain measurements of the T-bar antenna shown in Fig. 3-6.

Therefore, the tradeoffs involved seem to balance out since the loss at the low end of the bandwidth is counterbalanced by an almost equal increase in performance on the high end. Furthermore, these variations are caused primarily by variations in the VSWR (which can be compensated with wide band matching) rather than efficiency losses. It is concluded that the cavity depth of the air filled T-bar antenna may be decreased to 1.5 inches with only a slight decrease in overall performance.

Dielectrically loading the T-bar fed slot with a low loss dielectric material should produce similar results to the air case with the air cavity size reduced approximately by $1/\sqrt{\epsilon_r}$. Experiments were conducted to investigate this expectation by varying the cavity depth and filling the distance between the T-bar and back wall with 1/16" thick sheets of polystyrene. Then the experiments were repeated with the area in front of the T-bar filled with polystyrene. For a shorter bandwidth the performance is improved with the addition of dielectric materials behind the T-bar but if a 4:1 bandwidth is required, the better of the two cases was found to be the air filled cavity.

At cavity depths of 1.5 and 1.25 inches the normalized far field patterns (H-plane) were recorded with and without dielectric loading behind the T-bar. The far field patterns are broadbeam until 1500 MHz where lobing occurs for the air filled cavity. This result should be expected since the aperture is 1.5 wavelengths long at 1500 MHz, and the TE_{30} mode is excited. With dielectric loading behind the T-bar, the antenna exhibits a less broad pattern and lobing occurs at a lower frequency (1300 MHz). The TE_{30} mode is excited at a lower frequency with the addition of dielectric, thus causing the lobing to occur at 1300 MHz.

The general shape of the patterns was unchanged with various cavity depths for the air case. However measured power levels decreased with cavity depth as predicted by the insertion loss measurements. Normalized patterns of the air filled case are shown in Fig. 3-7.

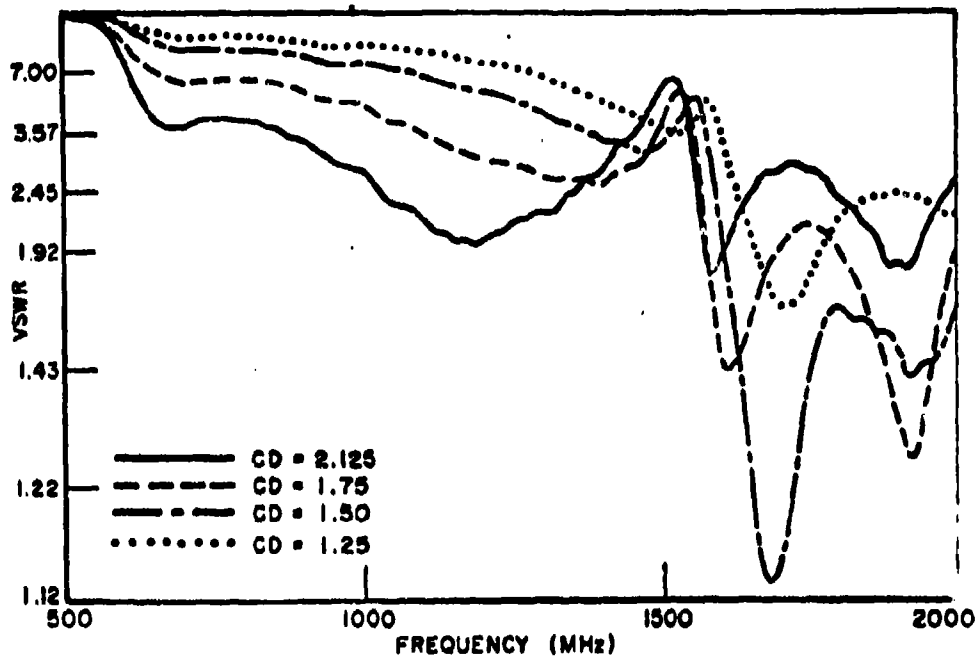

Fig. 3-5. VSWR measurements recorded as the cavity depth was varied.

It is desirable that the T-bar fed antenna exhibit a broad beam pattern over the entire specified bandwidth. To accomplish this goal, the antenna's electrical length must remain less than three-halves wavelength over the entire bandwidth or the higher order modes must be suppressed. Choosing the latter method to extend the pattern bandwidth, resistive tuning techniques were applied to the aperture. Resistive tuning stubs were constructed from narrow 20 ohm resistance cards to fit the width of the aperture. With a cavity depth of 1.5 inches and polystyrene dielectric behind the T-bar, the resistive tuning stubs' positions were varied in the aperture while measuring the insertion loss. Comparing the results to the dielectric case it was found that the insertion loss was increased over most of the bandwidth by approximately 5 dB, however it slightly decreased above 1700 MHz. Since resistance has been introduced to the aperture, the possibility of decreasing antenna efficiency exists.

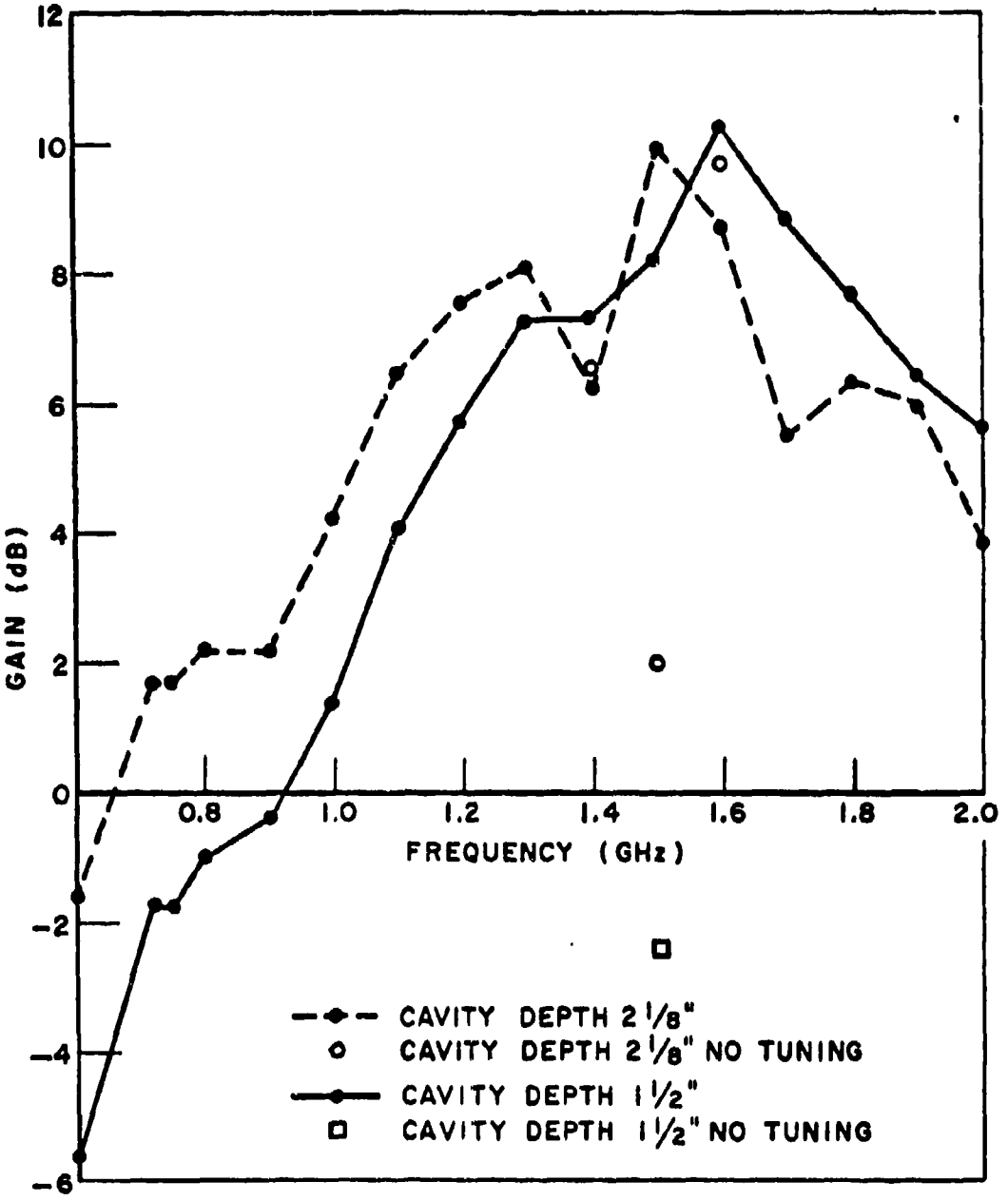

Fig. 3-6. Absolute gain of T-bar slot compared to isotropic.

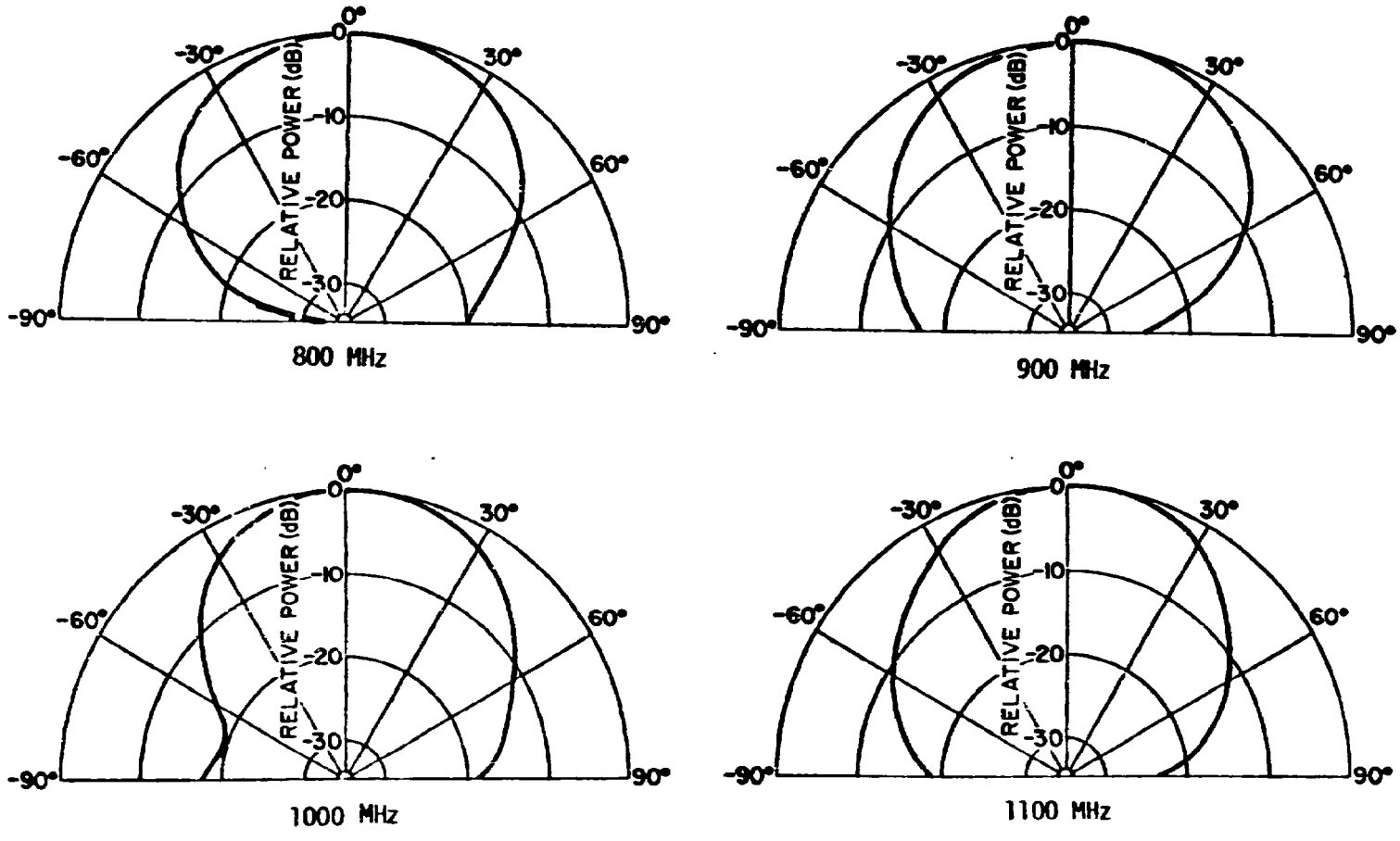

Fig. 3-7. Normalized far field patterns (H-plane) of the planar T-bar antenna. The air-filled cavity depth for these measured patterns is 1.5 inches.

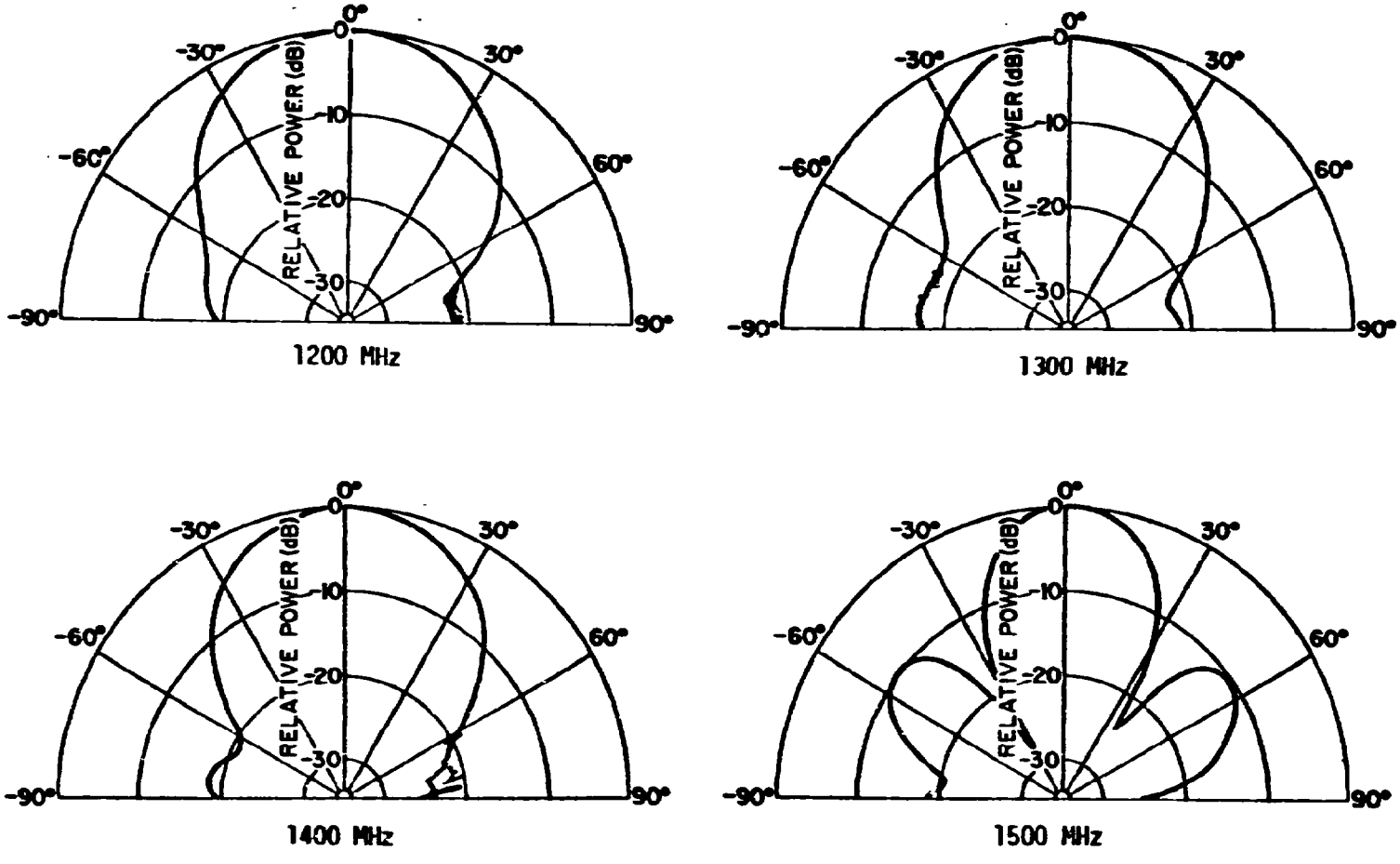

Fig. 3-7. (Continued).

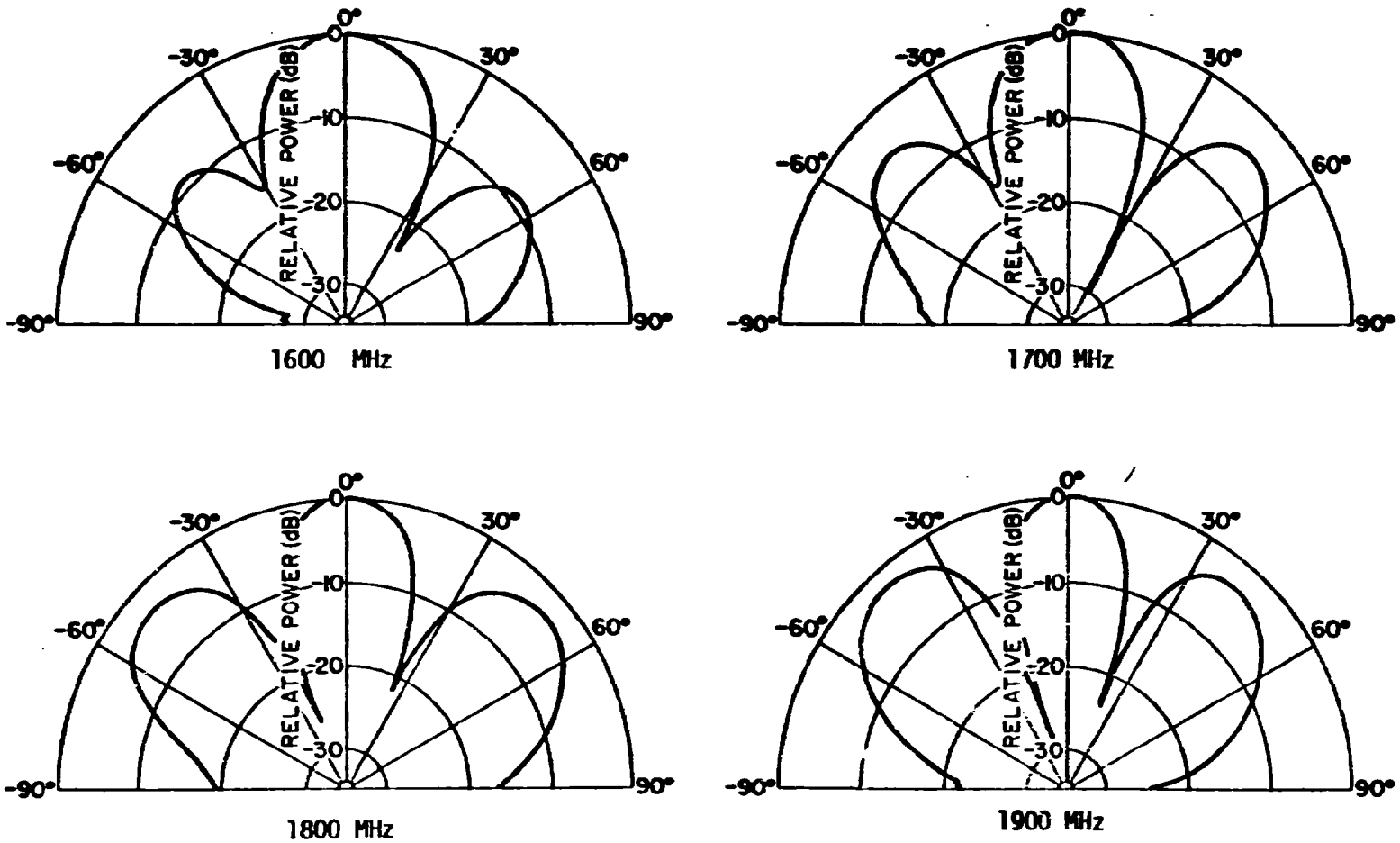

Fig. 3-7. (Continued).

With resistive tuning the VSWR was better across the entire bandwidth than either the air or dielectric loaded case and furthermore, the peak at 1500 MHz was suppressed. Therefore, the higher order modes have been tuned out at the expense of efficiency in the antenna as indicated by the insertion loss measurement. To further verify this conclusion, normalized far field patterns were recorded for the resistive tuned cavity with resistance cards located at 2.75 inches from each side wall of the cavity directly in front of the T-bar. The patterns showed that the TE_{30} mode was suppressed since the T-bar exhibited a 4:1 pattern bandwidth.

Since the cavity depth of 1.5 inches was still larger than desired, the tradeoffs between T-bar depth from the aperture and bandwidth performance was investigated. The T-bar depth from the aperture was reduced by a factor of 4 to only a depth of 3/16 inch, but the spacing between the T-bar and backwall remained the same so as to obtain similar performance to the previous 2.125 and 1.50 inch cavity depths. This results in cavity depths of 1.56 and 0.94 inches to replace each previous cavity depth respectively. Insertion loss studies were conducted to determine which cavity depths did produce similar results to previous measurements. The insertion loss measurements which compare most evenly with those of cavity depths 2.125 and 1.5 inches are 1.625 and 1.125 inches respectively. Allowing for experimental errors, the comparisons were considered quite close. Therefore, it was found that the cavity depth of the T-bar antenna can be reduced by decreasing the T-bar depth from the aperture plane while maintaining the same distance between the back wall and T-bar.

B. Conclusions Regarding the Planar Model

It is shown in Jasik that the T-bar fed slot antenna can be designed to exhibit a VSWR less than 2 over a frequency range of nearly 2:1 when the length to width ratio is approximately 3, and the T-bar to cavity shorting plate spacing is about $\lambda/4$ where λ is midfrequency in the 2:1 range. The results of this study indicate that if an increase in VSWR can be tolerated over the original 2:1 bandwidth, then the frequency bandwidth can be extended to a 4:1 range. To achieve this extension the design should be altered in the following fashion: (1) replace the circular cross section T-bar with a thin rectangular cross section T-bar, (2) the coax to T-bar connection must be a gradual transition, (3) cut a narrow slot centered within the T-bar whose length is $\lambda_{HF}/2$ (λ_{HF} is the wavelength of the upper endpoint of the frequency range), and (4) reduce the effect of the TE_{30} mode with tuning stubs located $\pm\lambda_{30}/2$ from the center of the aperture directly under the T-bar (λ_{30} is the wavelength of the frequency where the TE_{30} mode is excited). Furthermore, reducing the cavity depth to $\lambda_{HF}/4$ results in loss of performance on the low end but a nearly equal increase occurs on the high end of the bandwidth. Results also indicate that the cavity depth may be decreased by decreasing the T-bar depth from the aperture while maintaining the distance from T-bar to cavity shorting plate.

C. Cylindrical T-Bar Slot Antenna

Recall that the ultimate goal of this investigation is to design a circumferential T-bar fed slot antenna on a seven inch diameter cylindrical surface. Designing a cylindrical slot of the exact dimensions as the planar version resulted in a slot which spanned more than half the circumference of the cylinder as shown in Fig. 3-8.

Initially, the VSWR of the cylindrical antenna was investigated as the cavity depth was varied. The 1.5 inch cavity depth slot exhibits a VSWR less than 3.57 from 750 to 2000 MHz with the exception of a small region about 1300 MHz. As the cavity depth is decreased the VSWR increases, and in each case the aperture appears to be cutoff from 500 to 700 MHz. This cutoff is probably due to the cavity construction, i.e., the shorting plate of the cavity is not the same length as the aperture opening (pie slice shaped, see Fig. 3-8) causing a higher cutoff frequency for the antenna.

Attempting to improve the VSWR, polystyrene dielectric loading behind the T-bar was investigated. Results indicated that there is an improvement in the regions 600 to 750 MHz and 1250 to 1450 MHz with slight distortion between 1500 and 1600 MHz. This distortion resembles the peak in VSWR which the TE_{30} mode caused in the planar model. Therefore the cutoff frequency of the aperture has been extended at the expense of exciting the TE_{30} mode.

The normalized far field patterns (H-plane) of the air filled cavity shown in Fig. 3-9 exhibit a much broader pattern than the planar model with no lobing until 1800 MHz where the pattern completely splits into two lobes. As the cavity depth was varied, there was no distinct change in pattern shape, however relative power levels did change as predicted by VSWR results.

Insertion loss measurements (for the cylindrical air cavity) reveal that the slot within the T-bar does not have the same effect on the upper limit of the bandwidth as in the planar case. If the slot is removed from the T-bar, there is approximately a 3 dB increase in insertion loss from 1400 to 1800 MHz but a decrease of 2 dB from 1800 to 2000 MHz.

It is apparent from this study that the air filled cavity (1.5" deep) has a bandwidth of nearly 800 to 1700 MHz (2.1:1) in terms of VSWR, insertion loss, and nonlobing patterns. This could be extended to a lower frequency (500 MHz) if the corners of the backwall are corrected as shown in Fig. 3-10.

a) b) c)

Fig. 3-8. A T-bar slot antenna mounted transversely on a seven inch diameter circular cylinder.
a) front view
b) side view
c) top view with top cylinder removed.

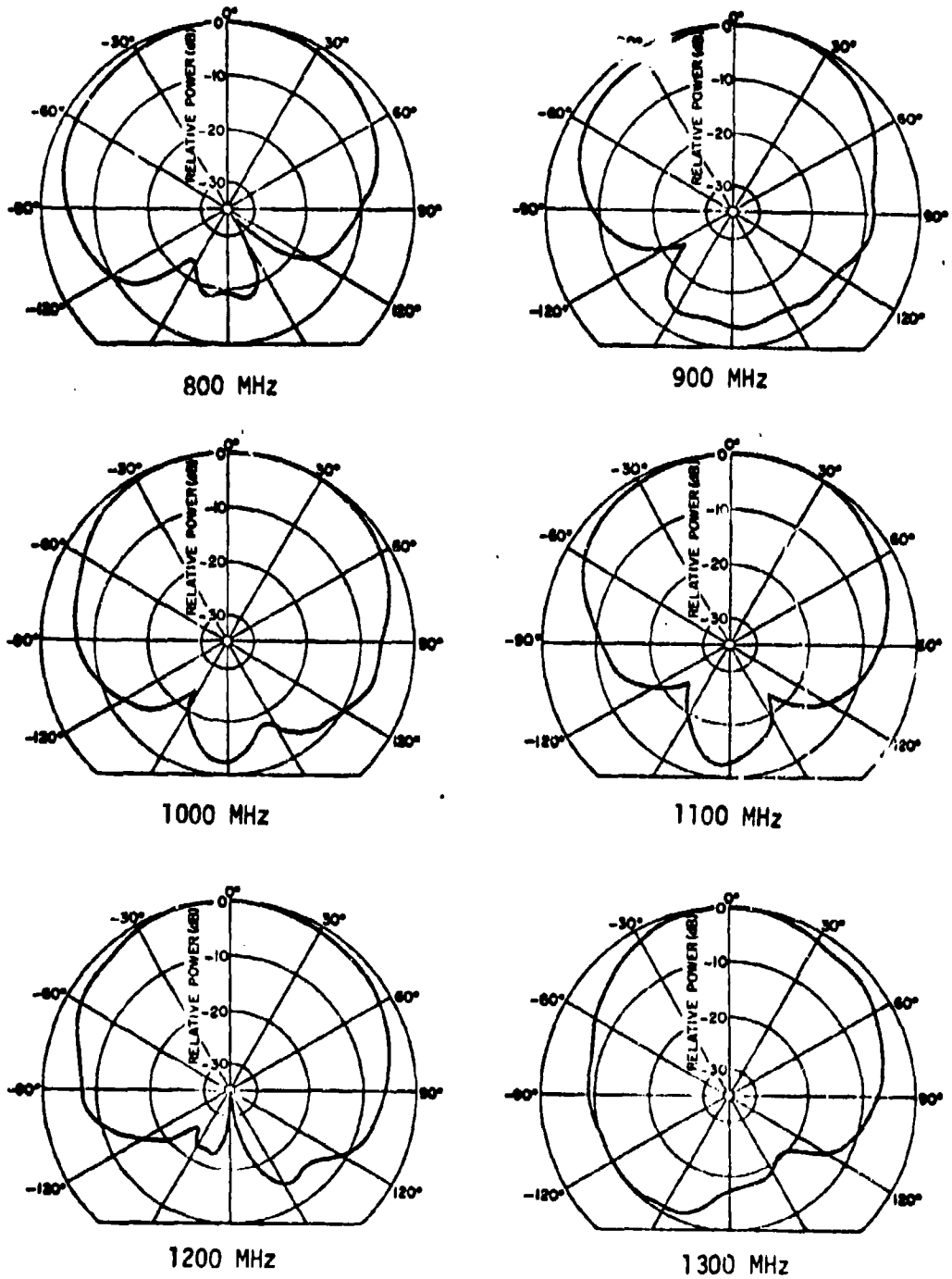

Fig. 3-9. Normalized far field (H-plane) patterns of the cylindrical T-bar slot antenna. The air-filled cavity depth is 1.5 inches.

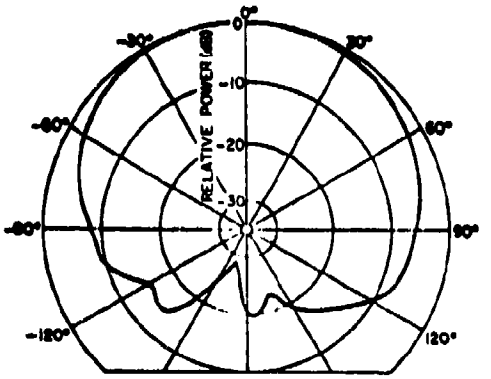

1400 MHz

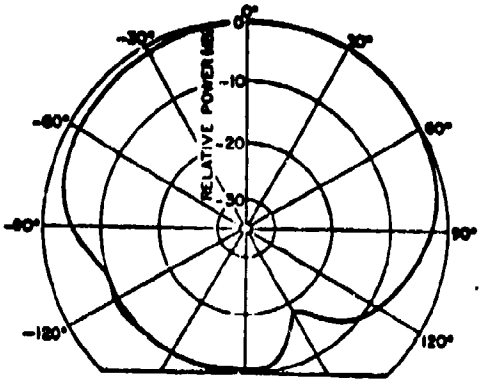

1500 MHz

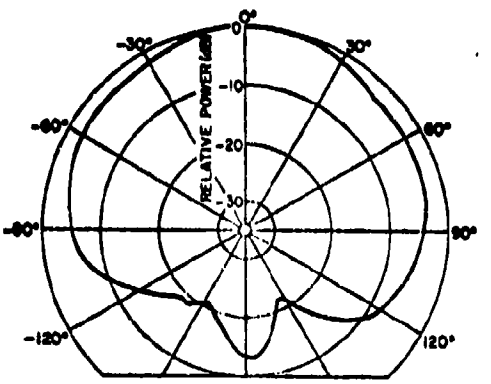

1600 MHz

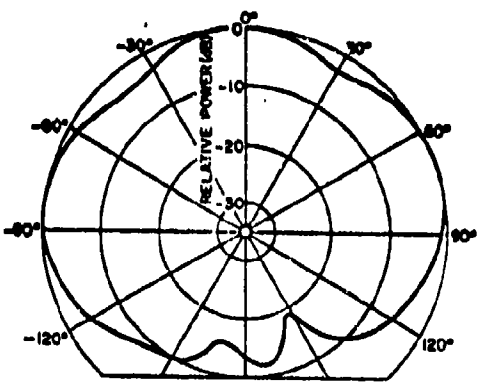

1700 MHz

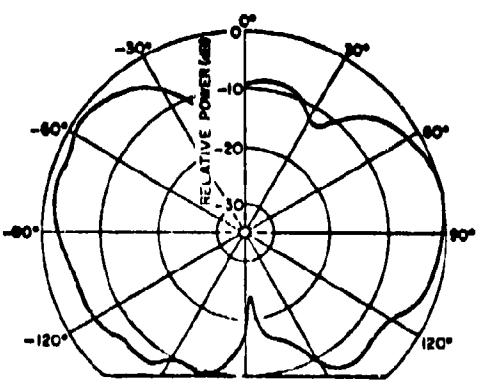

1800 MHz

Fig. 3-9. (Continued).

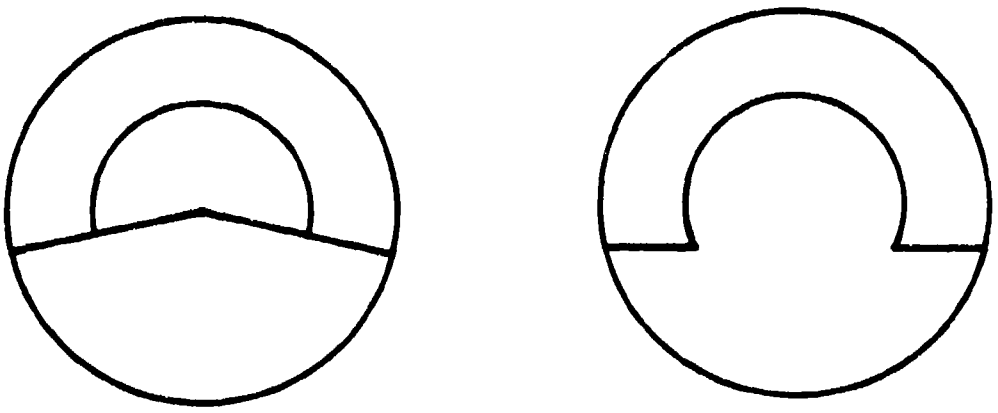

Fig. 3-10. a) Top view of present cylindrical T-bar antenna.
b) Top view of proposed improved cylindrical T-bar antenna.

When the cavity is dielectrically loaded behind the T-bar, the bandwidth is extended to 650 MHz but lobing occurs at 1600 MHz, thus the bandwidth is 650 to 1600 MHz (2.4:1) in terms of VSWR, insertion loss and no lobing patterns.

Resistive tuning of the cylindrical T-bar aperture was also considered. It was found that resistive tuning was not as effective for the cylindrical T-bar as for the planar T-bar. However, it does produce an acceptable pattern (i.e., no zero nulls) over an increased bandwidth (3.38) with a slight decrease in efficiency.

D. Conclusions Regarding the Cylindrical Model

It is apparent that the planar T-bar slot antenna can be configured to a cylindrical surface without degrading the performance of the antenna. In fact, the pattern performance is somewhat improved since the effect of the cylinder is to broaden the patterns and decrease the tendency of the antenna to form major side lobes.

IV. A LOSSY WIRE ARRAY

The problem addressed by the investigation discussed in this section is the development of a direction-finding antenna operating in the frequency range 500-2500 MHz. The antenna is required to fit within a vertical cylinder of about 7 inches diameter. It should be equally sensitive to vertically and horizontally polarized incident waves. In addition to these quantitative specficiations the following more general properties were considered desirable. The antenna radiation pattern should be simple so as to facilitate interpretation of the received signal voltages; this was taken to mean that the pattern should have a single lobe whose direction could be controlled. The efficiency of the antenna must not fall to an unusually low figure; the minimum tolerable figure was taken to be 10%, and the impedance was required to be well behaved over the frequency range.

The extent to which these objectives have been met is as follows. An antenna array has been devised which fits into the available space and provides a direction-finding facility from 500 to 4500 MHz. The major part of the investigation has been concerned with sensitivity to vertical polarization. However preliminary results suggest that a simple modification to the antenna geometry will provide the desired sensitivity to horizontal polarization also. The antenna has a single lobe in the horizontal plane. In the vertical planes, although secondary lobes appear, the sensitivity is maximum on the horizon over almost the entire frequency range. The efficiency of the antenna is greater than 10% over all, and greater than 20%, over 95% of the frequency range. The input impedance corresponds to a voltage standing wave ratio which is better than 2.5 at all frequencies when a transmission line of the proper characteristic impedance is employed. When connected for horizontal polarization the radiation pattern in the horizontal plane is more complex, but determination of the angle of arrival is still possible. The antenna is essentially a bent horizontal dipole and has considerable sensitivity to directions at high elevations above the horizon.

A. The Antenna Array

The antenna array is sketched in Fig. 4-1. It consists of six triangular elements arranged at angles of 60° in a circle. Only two are shown in Fig. 4-1a but all six are presented in Fig. 4-1b. Each element may be excited by a voltage generator or loaded with an impedance and thus be parasitic. The antenna in practice will be connected to transmission lines at the apices of the elements and these lines must be assumed to have some effect on the antenna performance. They are therefore represented by a central parasitic wire of the same conductivity as the rest of the array. Determination of antenna performance with and without this element present show that its influence is very slight.

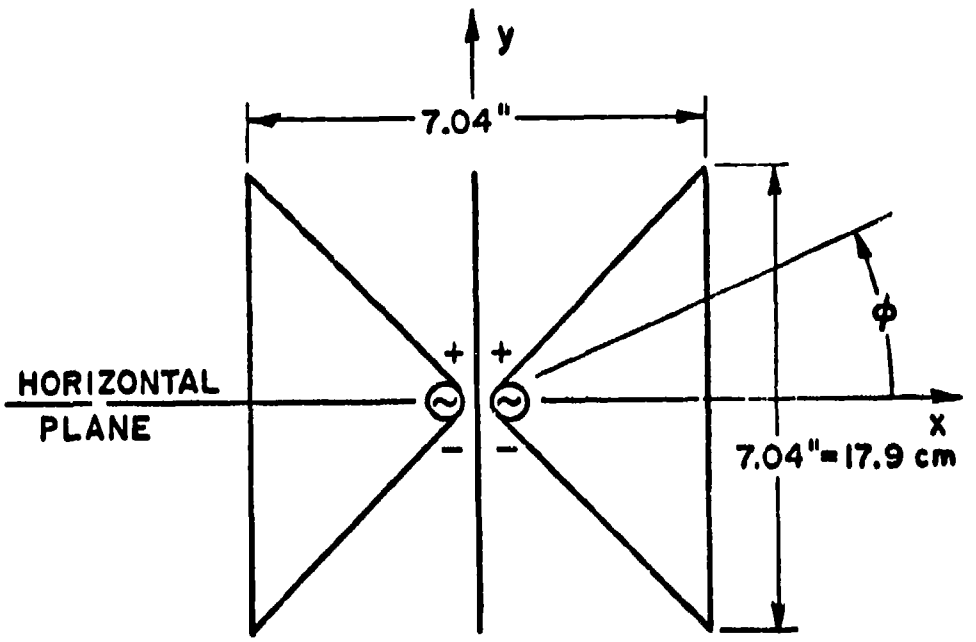

(a) SIDE VIEW

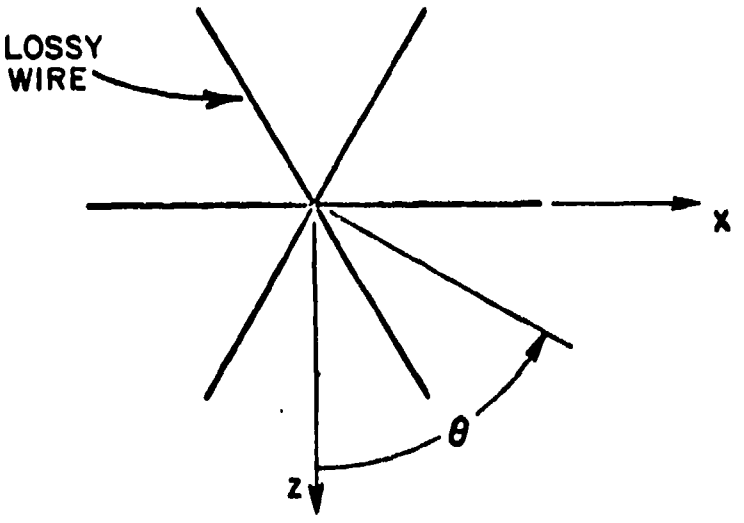

(b) TOP VIEW

Fig. 4-1. The array in its final configuration, showing dimensions and coordinates. The y axis is vertical.

The wires of which the elements are constructed have a diameter of 0.9 mm, and conductivity 1000 mho/m. These wire parameters are significant only when taken together; while the wire diameter remains a small fraction of a wavelength, increases in diameter and conductivity have similar effects. It was found in all the antenna configurations investigated that an increase in conductivity or diameter increased the radiation efficiency but caused an increase in the variation of the antenna impedance over the frequency range. The wire parameters quoted above were chosen so that the lowest value of efficiency would not fall below 10%, considered the lowest acceptable figure, while holding the impedance variation within tolerable limits.

Throughout this investigation the parasitic elements are loaded with impedances of 300 ohms resistive, which is close to the resistive part of the radiation impedance at the lowest frequencies considered. The effects of other, including reactive, impedances were investigated but no advantages were found.

The antenna described above is viewed as a transmitting antenna. It contains excited and parasitic elements. If the voltage generators (here assumed equal) are removed and their terminals connected to a common load, the voltage across that load as a function of angle of arrival of a plane wave is similar (except for a multiplying constant) to the radiation pattern of the antenna as a radiator. Because of this reciprocity we retain the term "excited" for the element(s) across whose terminals the received signal voltage is developed. The other elements we will continue to refer to as "parasitic".

The array was investigated in various excitation configurations over the range 500-4500 MHz. The lowest frequency was set by the diminishing efficiency; the highest frequency was set somewhat arbitrarily by the need for smaller segmentation of the elements at higher frequencies (the computer program requires that the antenna be divided into wire segments of length less than a quarter of wavelength) and the attendant greater computer storage and longer computation times. However it appears that side lobes become more prominant at the highest frequencies, and although interpretation of the received signal is still possible, less complex procedures would result from use of a new antenna designed for the higher frequency ranges.

B. Single Active Element

We consider first an arrangement in which one of the triangular elements is excited at its apex and all the others are loaded with a resistance of 300 ohms. Plots of relative electric field patterns appear in a previous technical report [1].

At 500 MHz the pattern has major and minor lobes in opposite directions. As the frequency increases the minor lobe grows and the major attenuates, the two having equal maxima at approximately 780 MHz. Above this frequency the major lobe lies in the direction opposite to that at 500 MHz. At 1000 MHz this change is fully developed. The half power beamwidth is 180°.

At yet higher frequencies the maximum gain generally increases and the beamwidth decreases. Further, lobes appear in both horizontal and vertical planes, but in the horizontal plane their maximma remain 6 dB below that of the major lobe, whose direction is constant, over the entire range of frequencies considered. In the vertical plane secondary lobes are stronger and at the highest frequencies their maxima may be larger than that of the lobe on the horizon. Even so the field remains strong on the horizon and over most of the frequency range takes its maximum value there.

Figure 4-2 is a plot of the impedance at the terminals, normalized with respect to 300 ohms. The corresponding voltage standing wave ratio is better than 2.5 over almost the entire frequency range of 500-4500 MHz. From the tendency of the curve one expects this to be true for a very much larger frequency range. Very large impedance bandwidths without intolerable loss of efficiency are the most striking results of the use of lossy wires.

Figure 4-3 is a plot of the radiation efficiency. This is greater than 10% for almost the entire range and usually greater than 20%. The lowest value is 6% at 500 MHz. Efficiency decreases rapidly below this frequency.

The performance of this antenna may be summed up as follows: The radiation pattern in the horizontal plane has a major lobe lying in a constant direction over the frequency range 1000-4500 MHz. The direction of the major lobe reverses in the interval 1000-500 MHz. In the vertical plane most of the radiated energy lies close to the horizon. The radiation resistance is relatively stable and the radiation efficiency is greater than 10% except at the extreme low end of the frequency range.

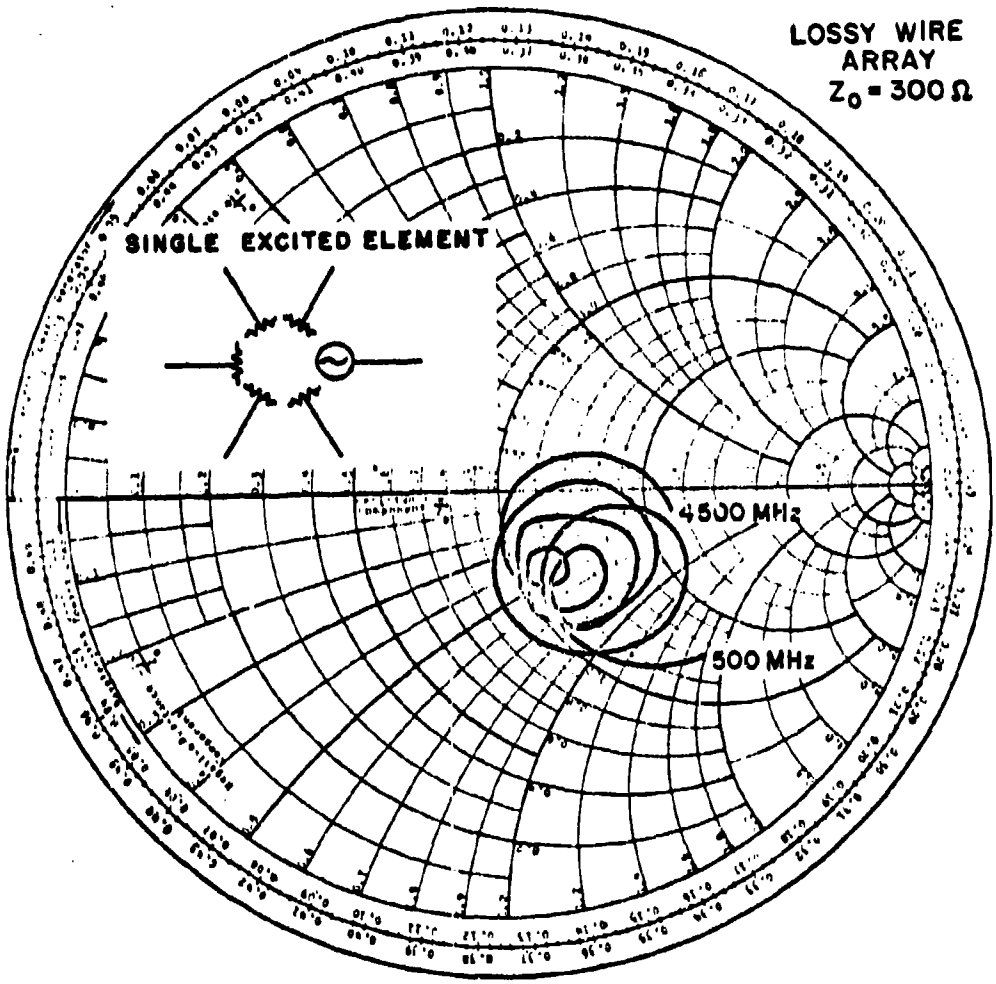

Fig. 4-2. Impedance of array with single excited element normalized with respect to 300 ohms

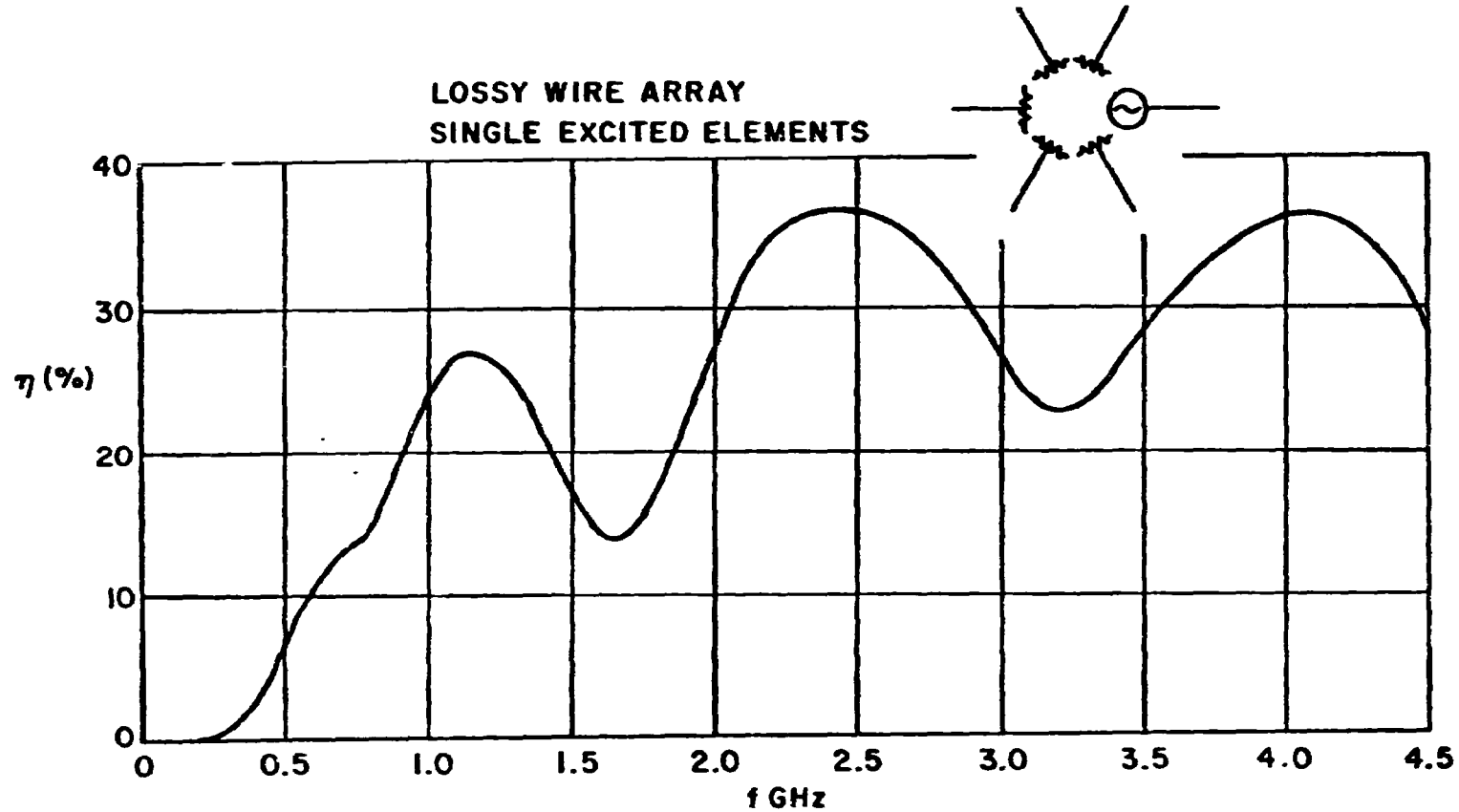

Fig. 4-3. Efficiency of array with single excited element.

For use of this device as a direction-finding antenna it is envisaged that the voltages on the terminals of each triangular half element would be sampled in turn, and compared. From these data the direction of the incoming signal may be determined. In many cases a close determination of the angle of arrival may be made by interpreting the relative magnitudes* on the basis of the known performance of the antenna. If the noise level permits, greater accuracy would result from processing ratios of voltages on pairs of terminals.

Shortcomings of this system are associated with

(i) large beamwidth, especially at low frequencies,

(ii) ambiguity due to multiple lobes; this is worse between 700 and 800 MHz where, in the horizontal plane, two approximately equal lobes lie in opposite directions, and

(iii) the efficiency at the extreme low frequency falls to only 6%, perhaps an unacceptably low figure.

C. Two Active Elements

To this point we have considered one element as the excited element of the array and the other five as parasitic. We now investigate the effect of exciting two elements with the same voltage while the remaining four are parasitic. The dual of this arrangement as a receiving antenna is an array in which the terminals of the active elements are connected to a common load whose impedance is half that loading the parasitic elements. As before each parasitic element is loaded with 300 ohms.

We consider first the case where the two active elements are adjacent - separated by an angle of 60°. The behavior of this array is qualitatively similar to the arrangement we have been describing, but it exhibits certain comparative improvements. Figure 4-4 illustrates horizontal plane radiation patterns corresponding to representative frequencies.

As with the single excited element, the major lobe in the present case reverses direction in the frequency range 500-1000 MHz with equal maxima in both directions occurring at approximately 780 MHz. Also as before these lobes have different shapes allowing the ambiguity to be resolved by the amplitude compaison techniques described in [1].

*Here the term "relative magnitudes" means which voltage is greatest, which second to greatest, which third, etc. We are concerned only with the question of whether one voltage is greater than another. Where we more specifically speak of the ratios of voltages, the word "ratio" will be used.

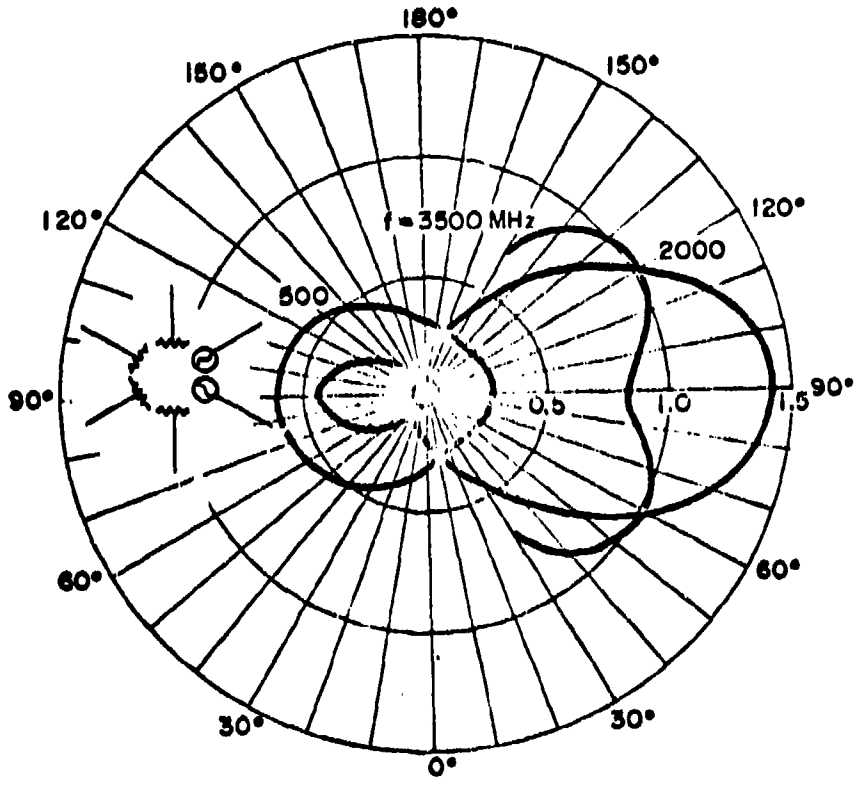

Fig. 4-4. Radiation patterns in horiz ntal plane with two excited elements at 60°. Three representative frequencies are illustrated.

The radiation pattern has a single major lobe for frequencies up to about 3000 MHz, above which the main lobe separates into two. Prior to separation the lobe broadens canceling the improvements noted earlier. At all frequencies the strengths of the received signals at the maximum of the main lobes are greater than those at the corresponding frequencies for the single active element case.

The fact that the antenna with a single excited element and the antenna with two excited elements have pattern maximum in directions which differ by 30° suggests that by exciting the two elements by voltages of equal phase but different magnitudes the maxima may be made to lie in any direction over a range of 60°. By exciting the elements in antiphase a null may be placed anywhere in this range (and also in certain regions outside the range). The corresponding process for the receiving antenna is the formation of linear combinations of the received voltages. We note that this is possible without the use of phase information although that would offer refinements to the technique.

Figure 4-5 is a plot of the impedance over the frequency range 500 to 3500 MHz normalized with respect to 150 ohms. As before the corresponding voltage standing wave ratio is less than 2.5 over almost the entire range.

Figure 4-6 is a plot of the efficiency of the antenna. At all frequencies the efficiency is greater than its value for the single excited element plotted in Fig. 4-3. Importantly, the lowest value of 6% in Fig. 4-3, occurring at 500 MHz, has been almost doubled to 11% in Fig. 4-6. The larger values of efficiency are of course related to the larger signal strengths referred to above.

D. Conclusion

An antenna array has evolved capable of direction-finding over the frequency range 500 MHz to 4500 MHz. The antenna has been studied in detail for the reception of vertically polarized waves, but it shows good prospects for successful operation with horizontal polarization. The impedance is stable, corresponding to a VSWR of less than 2.5 over the entire frequency range. The efficiency is greater than 10% at all frequencies.

The array consists of six triangular-loops arranged in a circle with their vertices towards the center. For vertically polarized incident waves each triangle has a resistive load at the vertex in series with the loop. The loads in pairs of loops may be connected together in different configurations. The voltages across the loads are sampled in turn, and are interpreted, on the basis of known radiation patterns, to determine the angle of arrival of the incident wave. For horizontally polarized waves the procedure is similar except that the loads are connected between the vertices of different triangles.

Work remaining to be done includes

(i) A more complete investigation of the horizontal polarization problem.

(ii) A more thorough investigation of the best way of interpreting the radiation patterns.

(iii) A study of the antenna for horizontal polarization. Present results are incomplete and suggest that the lowest operating frequency is about 1000 MHz.

(iv) An experimental study to confirm the computed results, and to determine the effect of the metallic cylinder which forms the supporting structure.

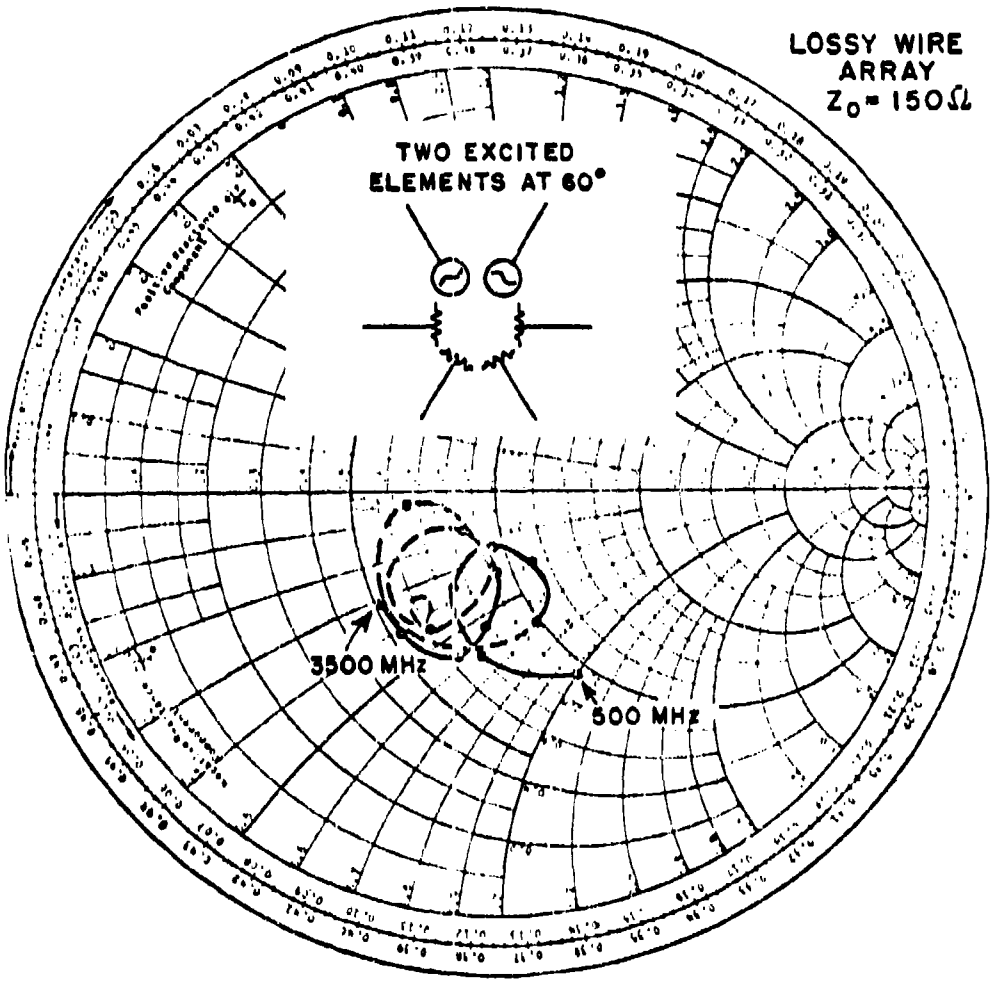

Fig. 4-5. Impedance of array with two excited elements at 60° normalized with respect to 150 ohms.

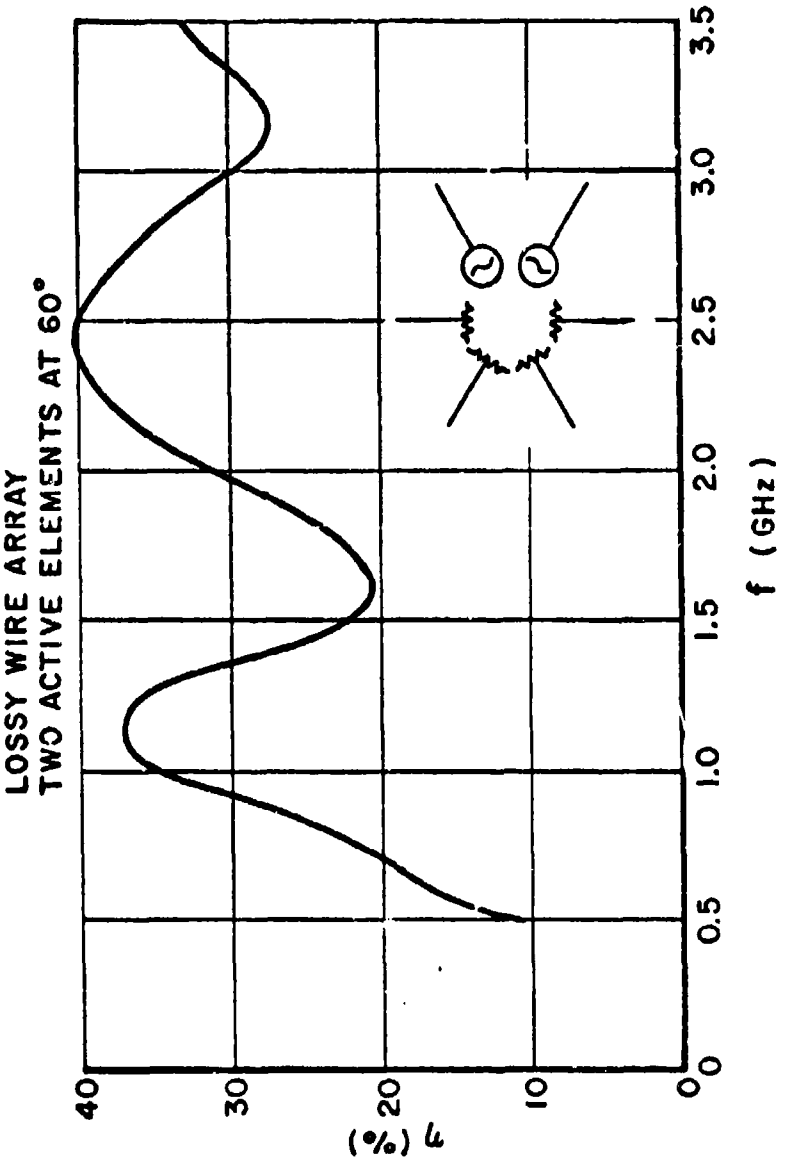

Fig. 4-6. Efficiency of array with two excited elements at 60°.

The problem addressed here has been that of the antenna itself. No effort has been made to find the best procedure for interpreting the received voltages, although a procedure has been suggested to demonstrate its possibility. The antenna has been investigated for its performance in free space; there will be modifications to the results presented here when it is mounted atop a conducting cylinder although it is anticipated that these modifications would not alter the conclusions drawn herein.

V. AN ALTERNATIVE LOW FREQUENCY ARRAY

In an attempt to develop an alternative design to the lossy wire array of the previous section, various bent monopole configurations were investigated. All these configurations fit within a 7" diameter cylinder and have a thin 1" diameter cylinder coaxial with the 7" cylinder as depicted in Fig. 5-1. Some of the wire configurations considered utilized the low conductivity wire of the previous section and some used lumped loading as an equally viable alternative.

The antenna configuration in Fig. 5-1 represents the most recent and also the best of the various configurations investigated. It utilizes highly conducting wire with a single lumped load at the junction of the monopole with the top loading wire. Since the monopole is inclined at an angle of 45° with the horizontal, it receives both horizontal (phi) and vertical (theta) polarizations.

A Smith Chart plot of the input impedance of this array is shown in Fig. 5-2.

Figures 5-3 a through f show the received voltages developed at the three ports for the vertical (theta) polarized case. It is apparent from the first of these figures (5-3a) that at the lowest frequency of interest, one would not be able to distinguish the direction of arrival of the incoming signal using only amplitude information. At the other frequencies, the amplitude variations are sufficiently great so as to permit direction of arrival determination.

Figures 5-4 a through f show the received voltages developed at the three ports for the horizontal (phi) polarized case. It is clear from the plots that there is more than ample amplitude variation at the ports for amplitude comparison purposes. However, examination of the plots reveals a 180° ambiguity in all cases. To resolve this ambiguity it would be necessary to utilize phase information.

The fact that the antenna responds to both polarizations may be a disadvantage however. For unless one knows apriori the polarization of the incoming waves (including the depolarization properties of the environment), the amplitudes at the receiving ports will be very complex functions of frequency, direction (and vertical angle) of arrival and the state of the environment. Allowing for this unpredictable complexity then, it is probably necessary that a polarization sensing element be incorporated into the antenna system or the design be changed such that this antenna system would respond to only the vertical polarization.

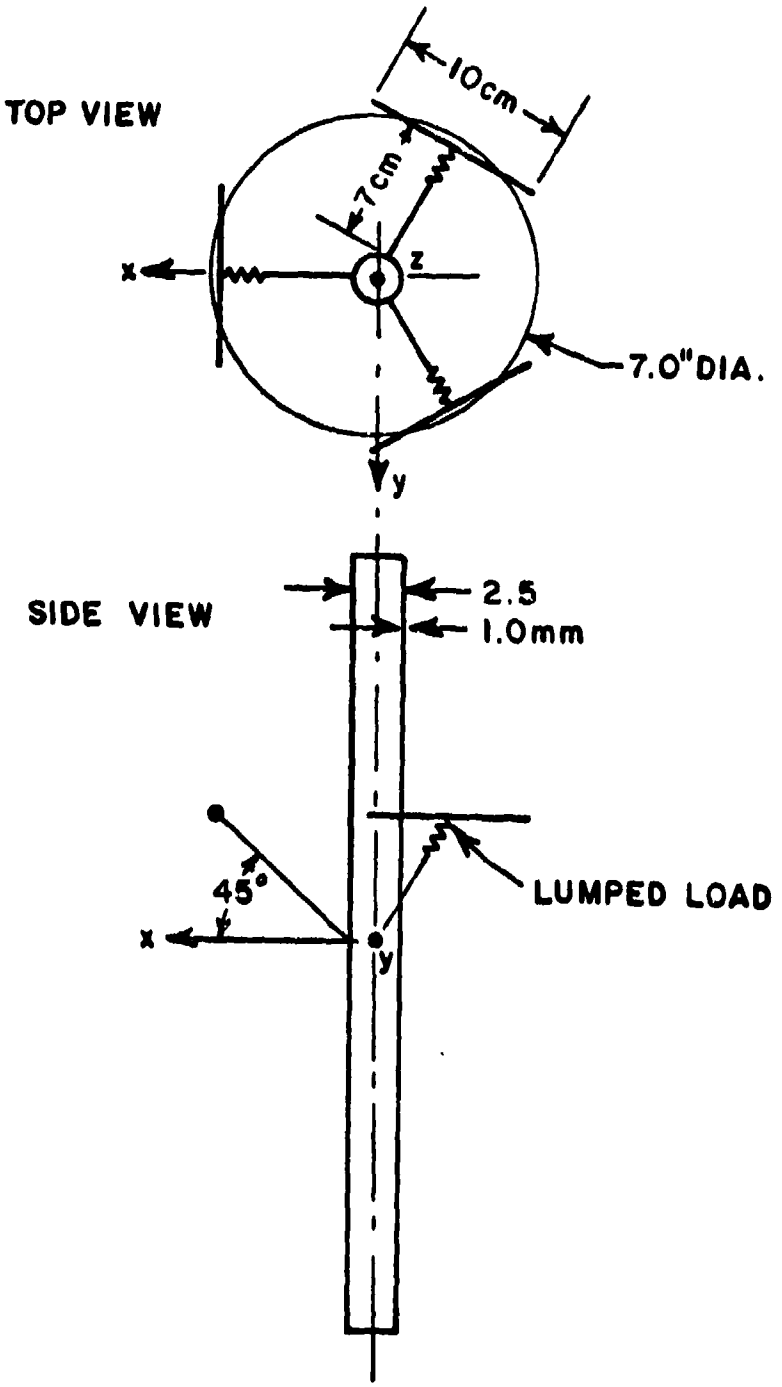

Fig. 5-1. Slant Tee monopole array with lumped loading on a one inch diameter inner cylinder.

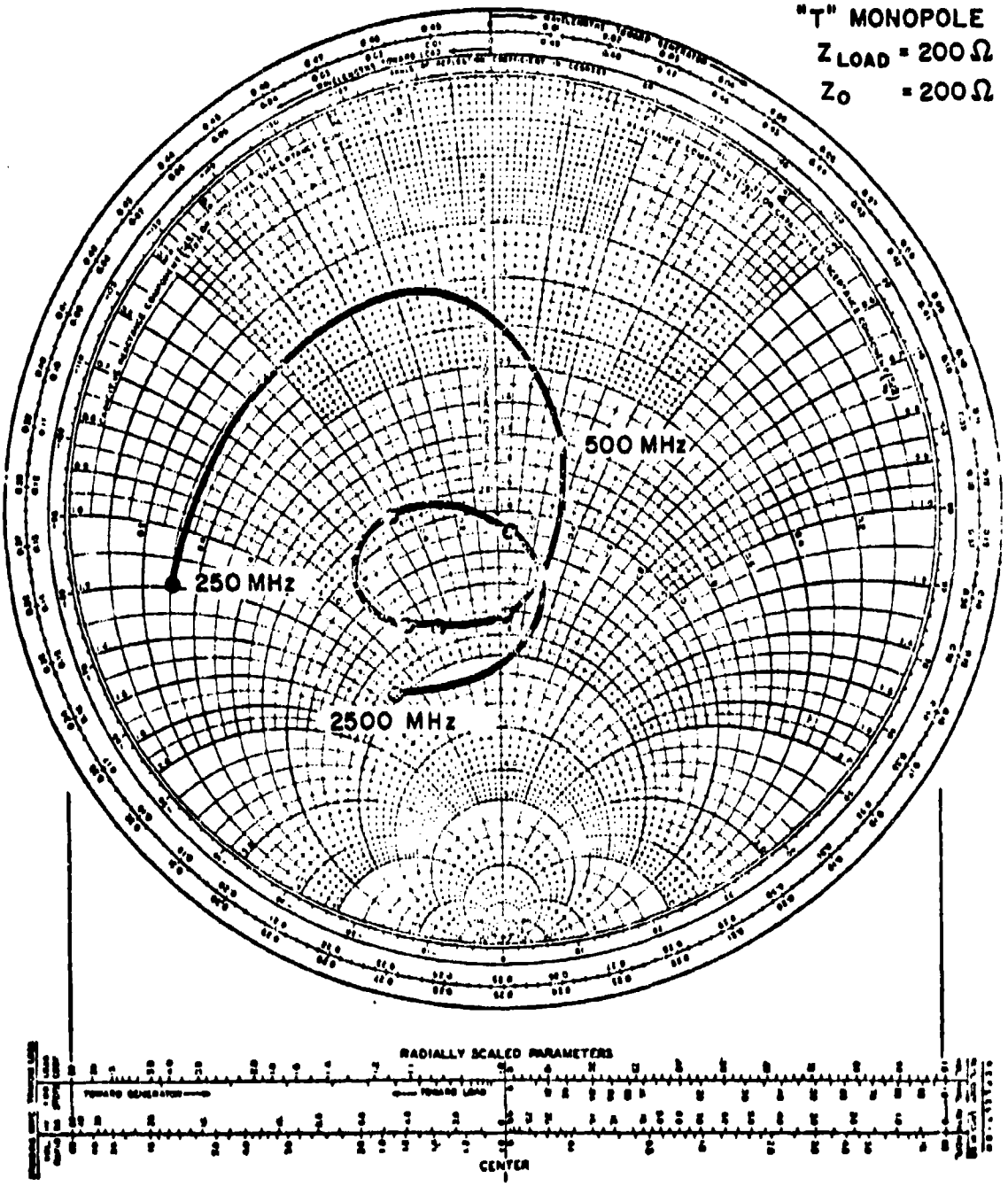

Fig. 5-2. Impedance of a loaded "T" monopole.

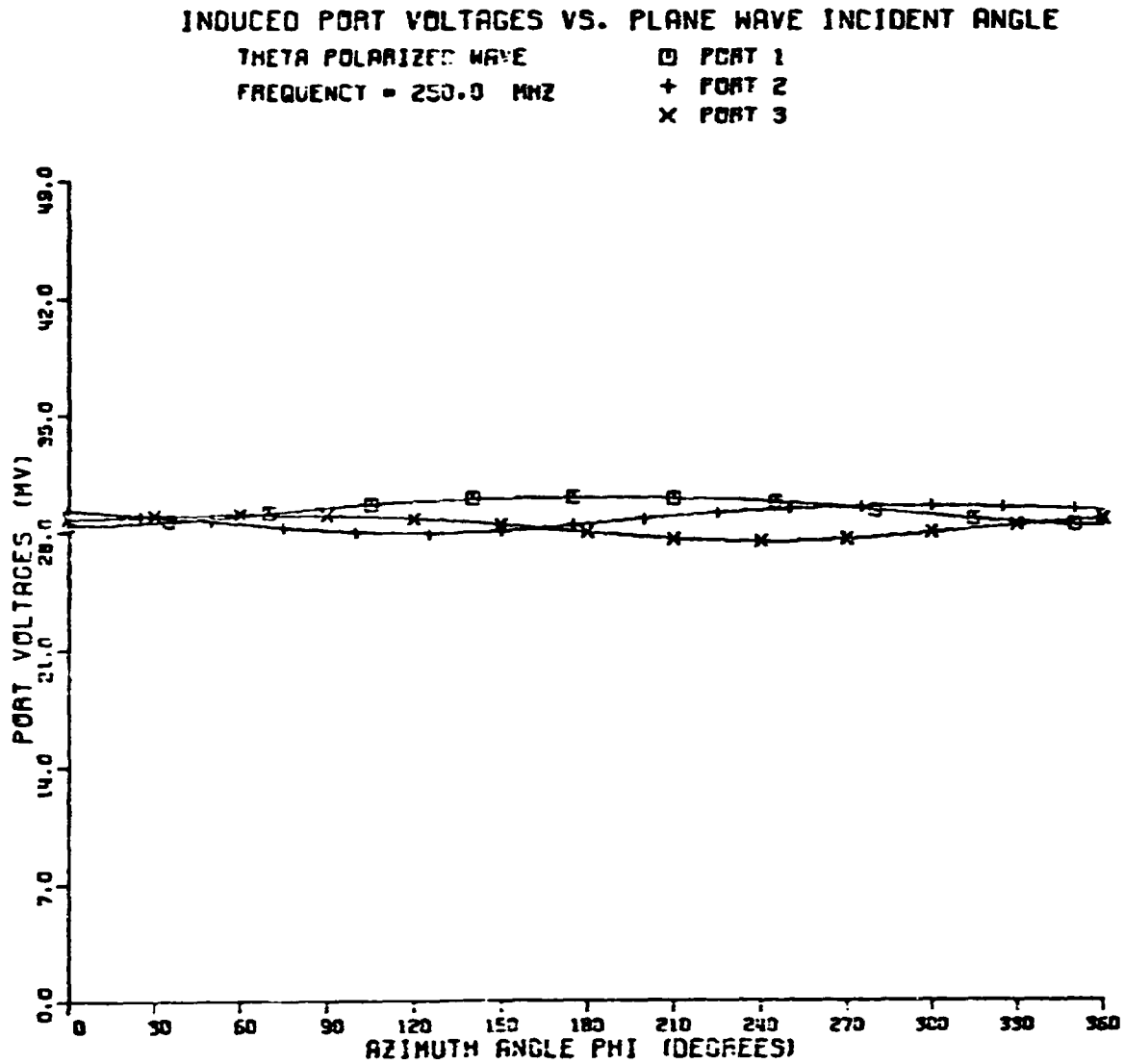

Fig. 5-3a. Received voltage for vertical polarization at 250 MHz.

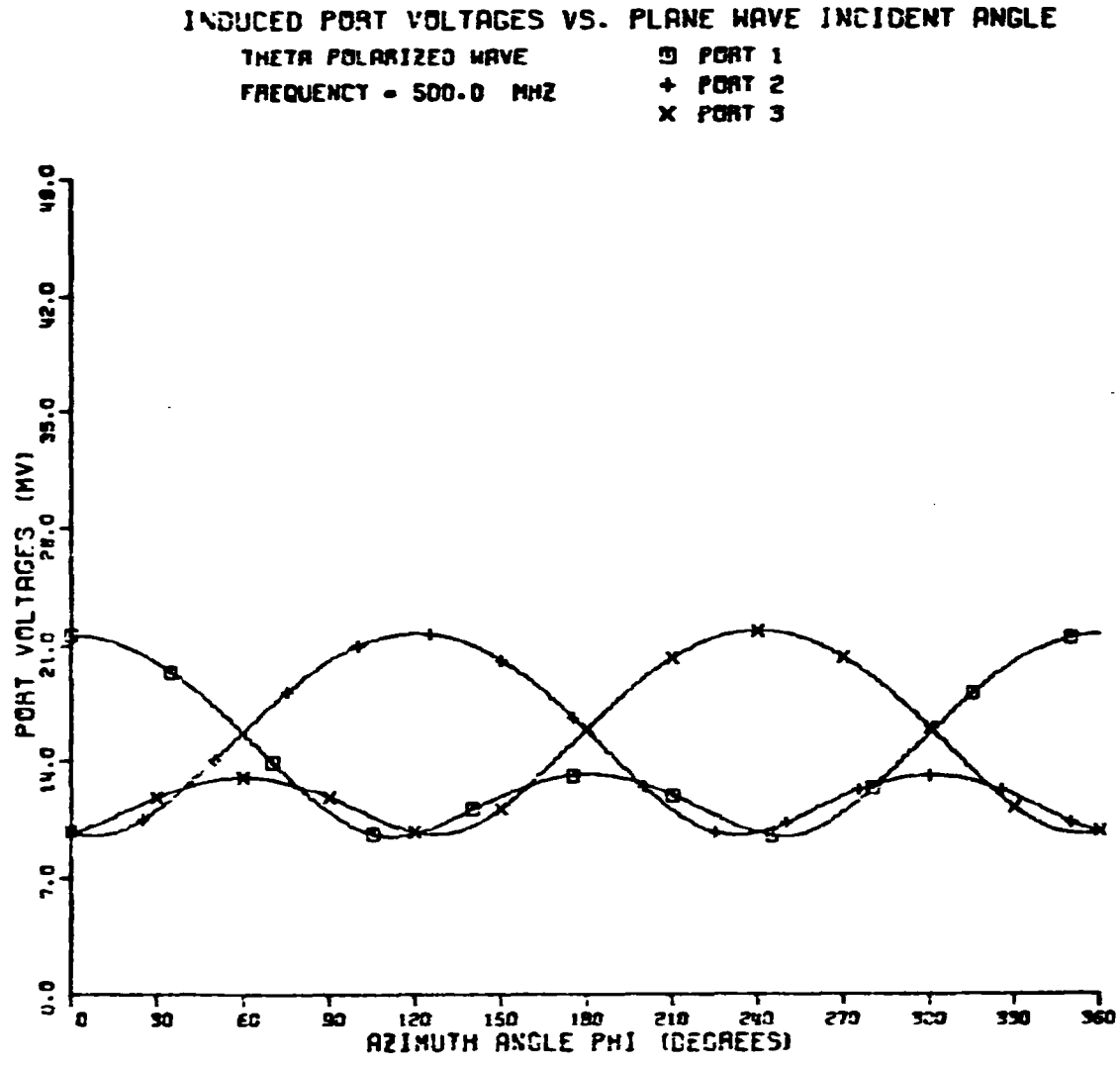

Fig. 5-3b. Received voltage for vertical polarization at 500 MHz.

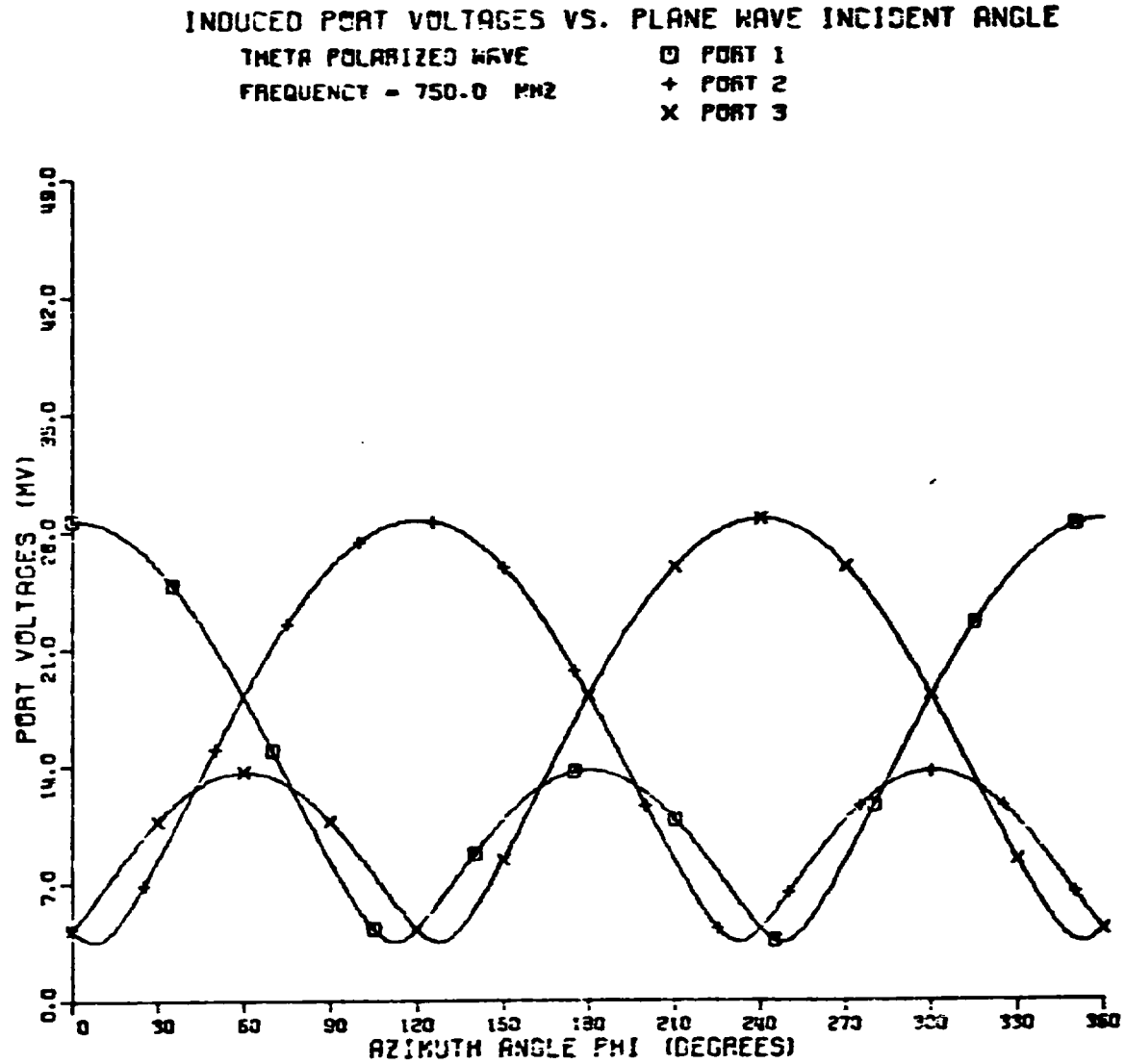

Fig. 5-3c. Received voltage for vertical polarization at 750 MHz.

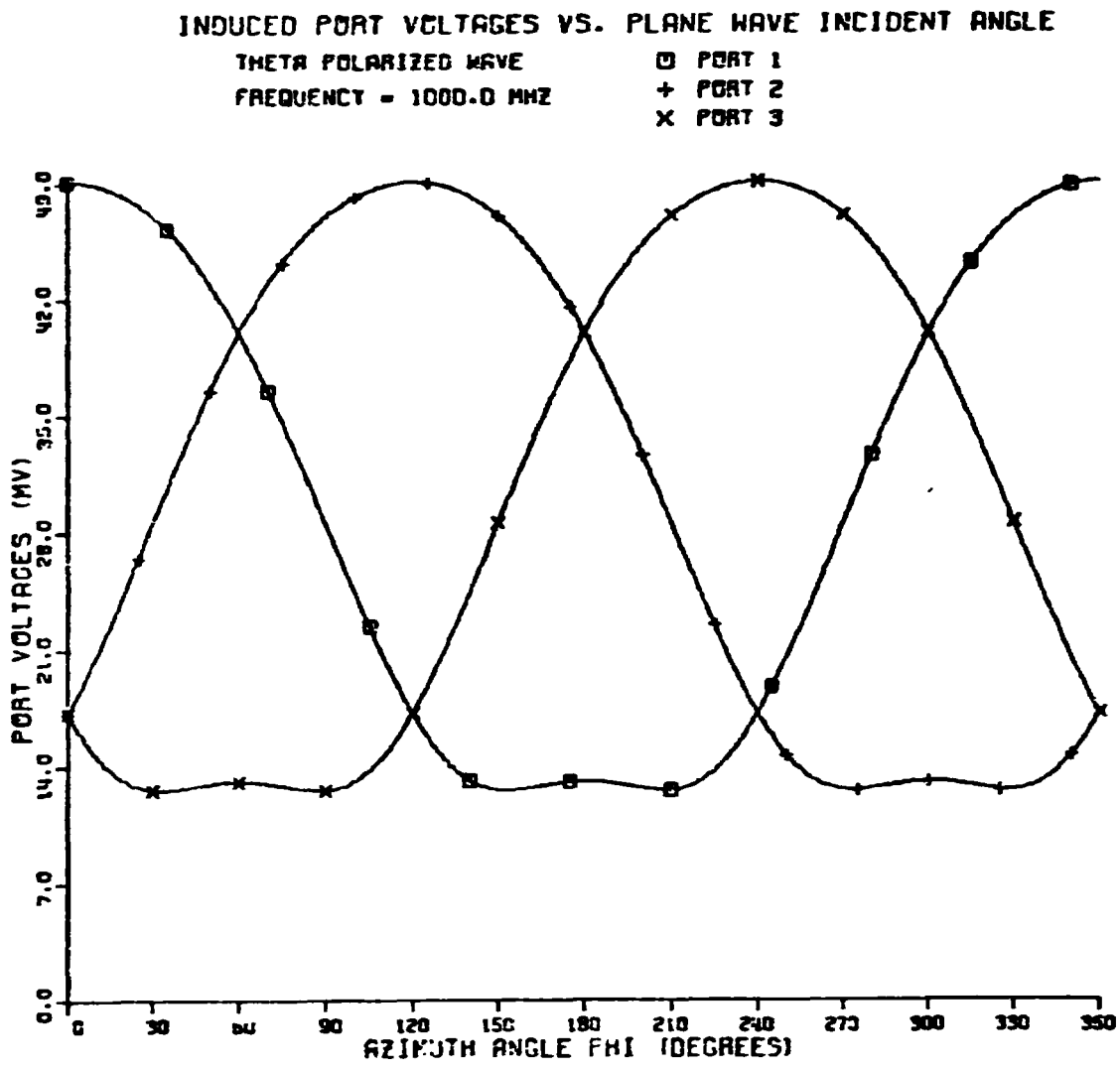

Fig. 5-3d. Received voltage for vertical polarization at 1000 MHz.

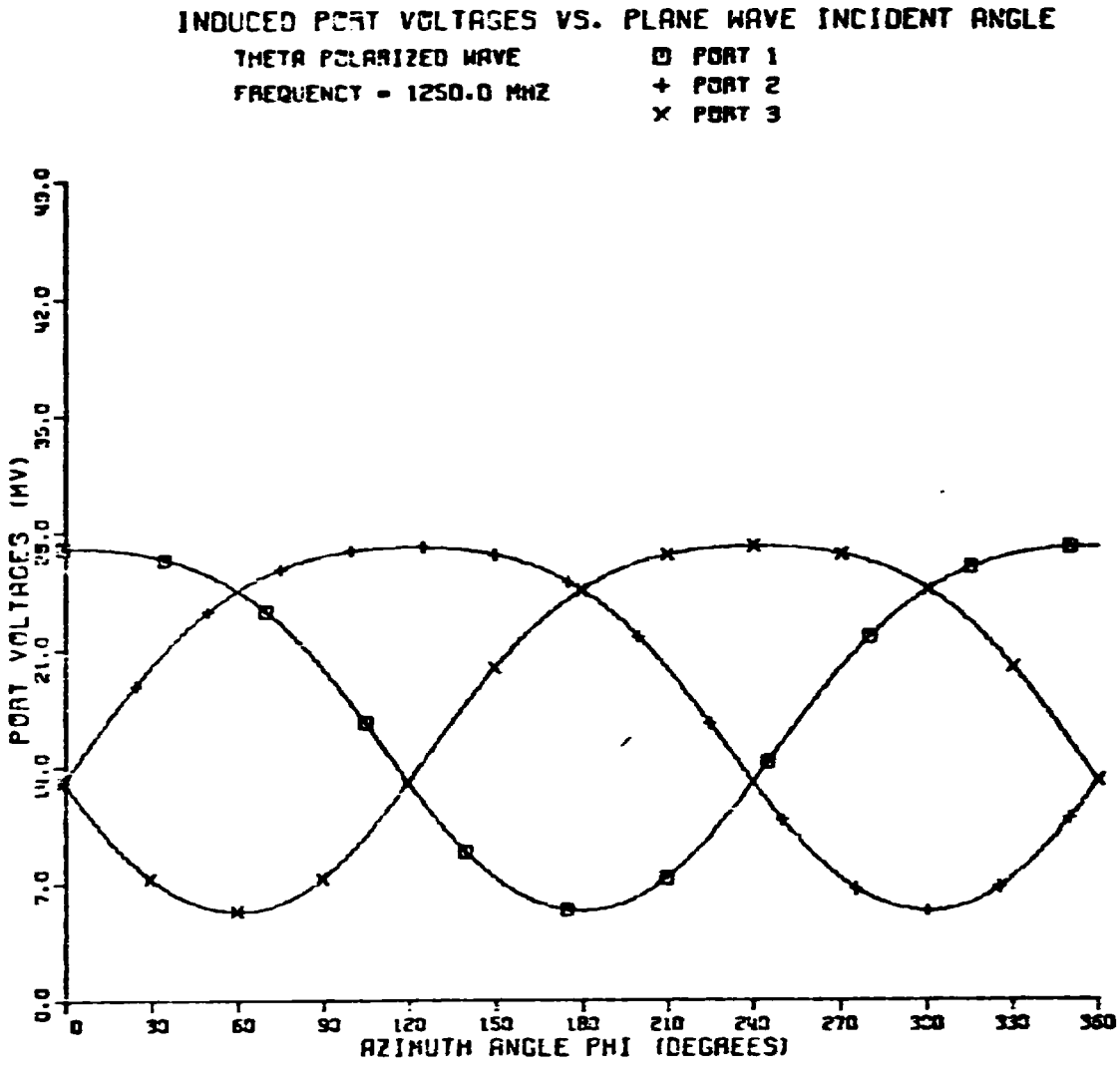

Fig. 5-3e. Received voltage for vertical polarization at 1250 MHz.

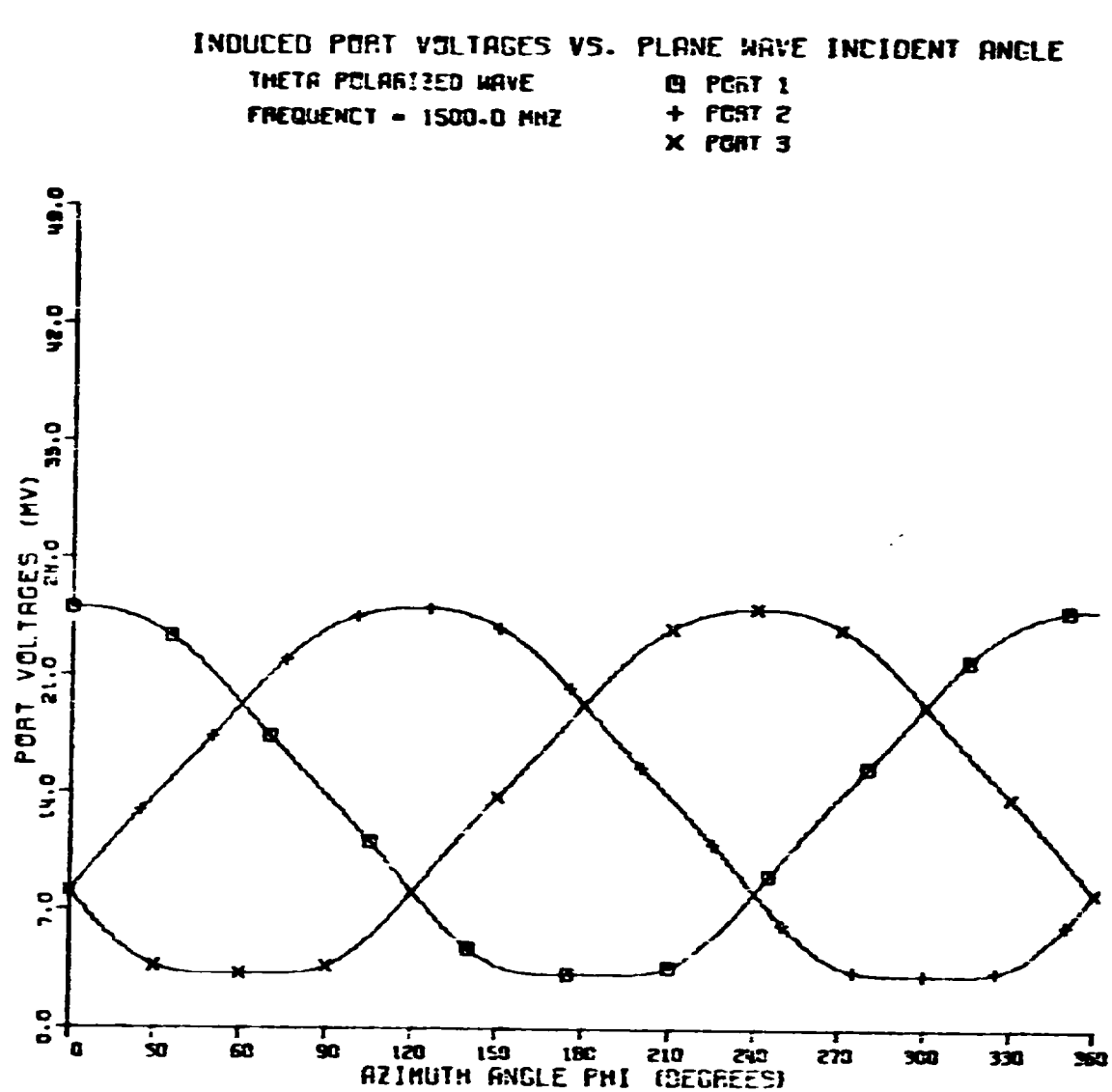

Fig. 5-3f. Received voltage for vertical polarization at 1500 MHz.

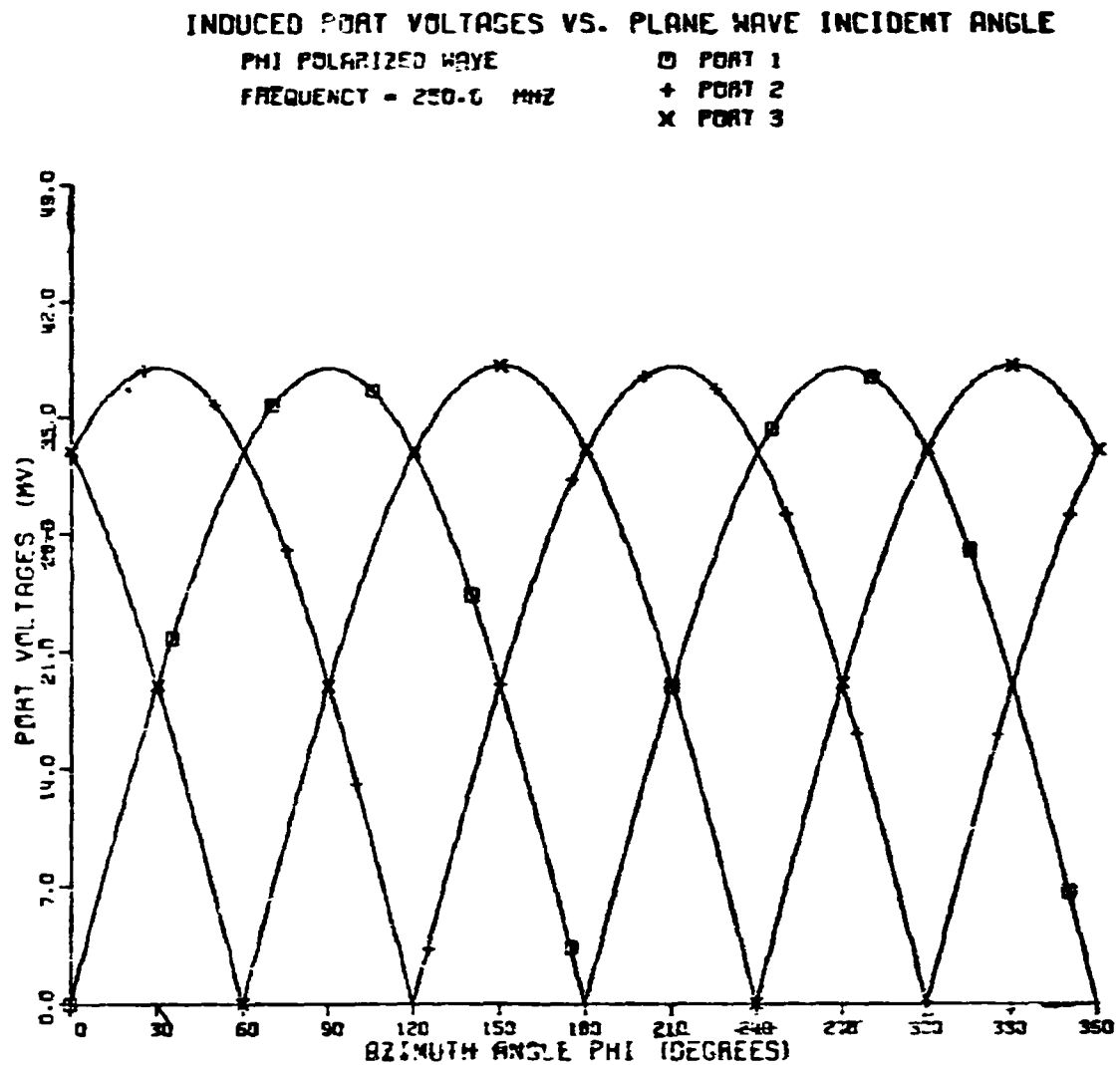

Fig. 5-4a. Received voltage for horizontal polarization at 250 MHz.

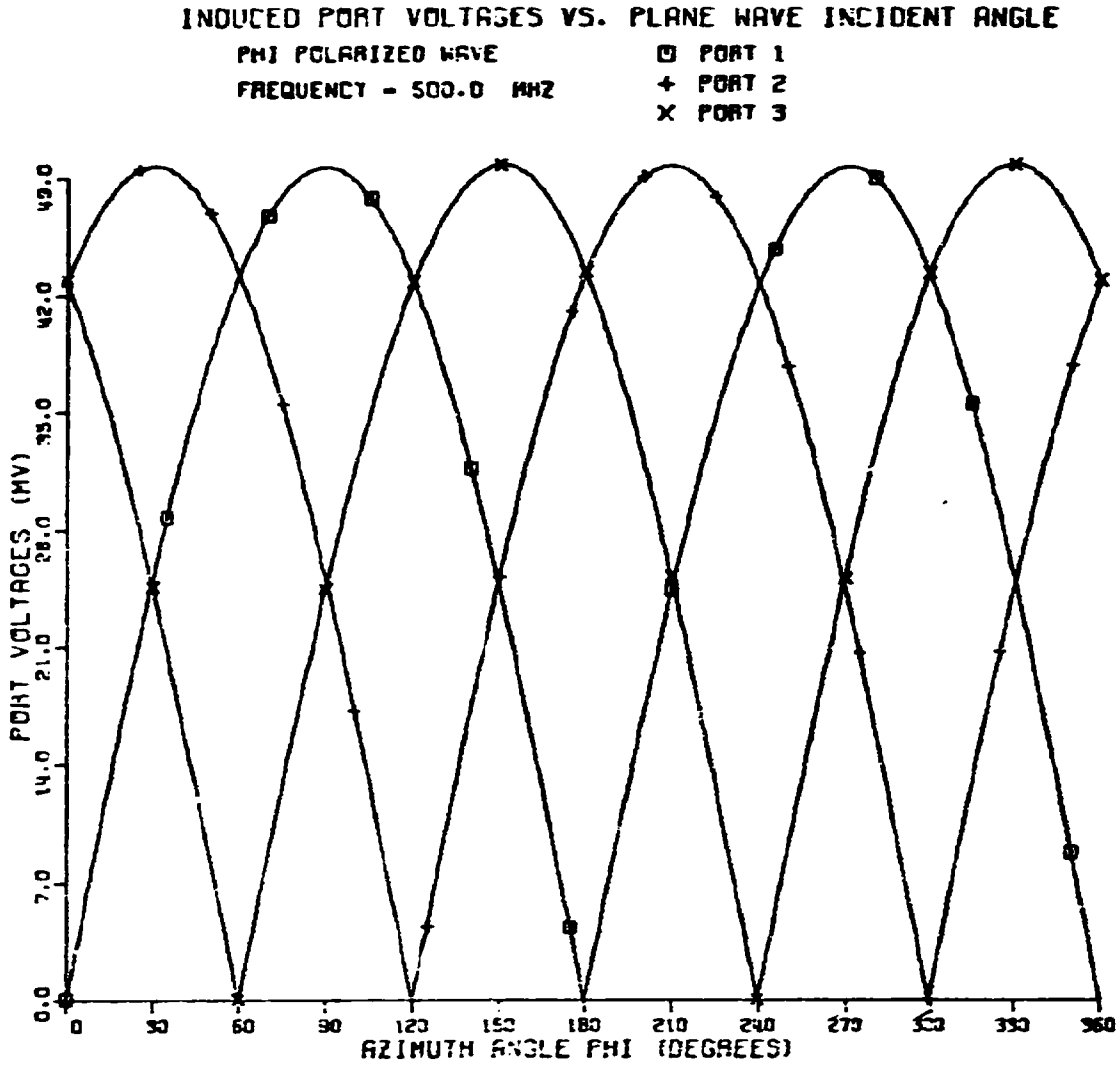

Fig. 5-4b. Received voltage for horizontal polarization at 500 MHz.

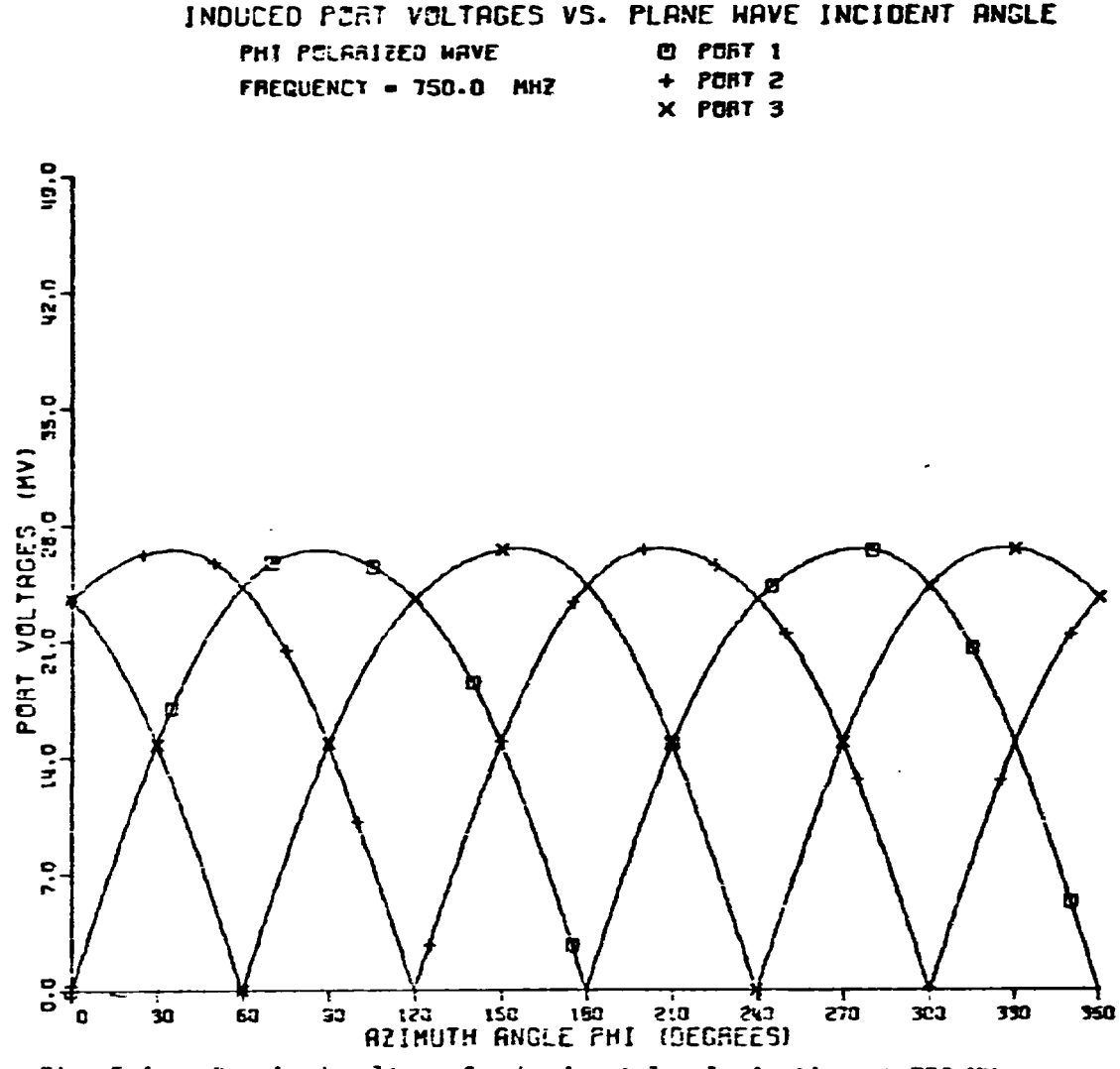

Fig. 5-4c. Received voltage for horizontal polarization at 750 MHz.

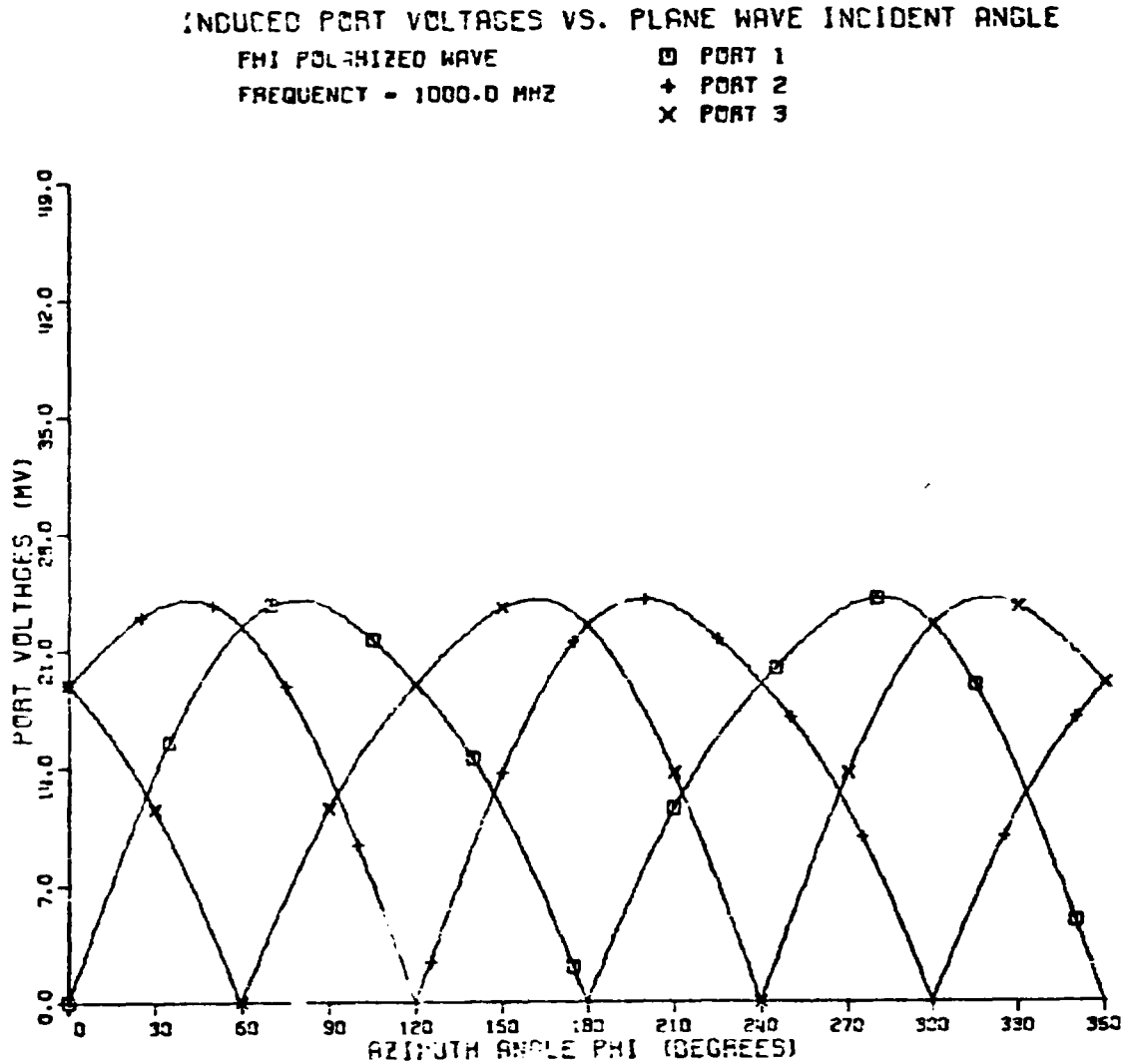

Fig. 5-4d. Received voltage for horizontal polarization at 1000 MHz.

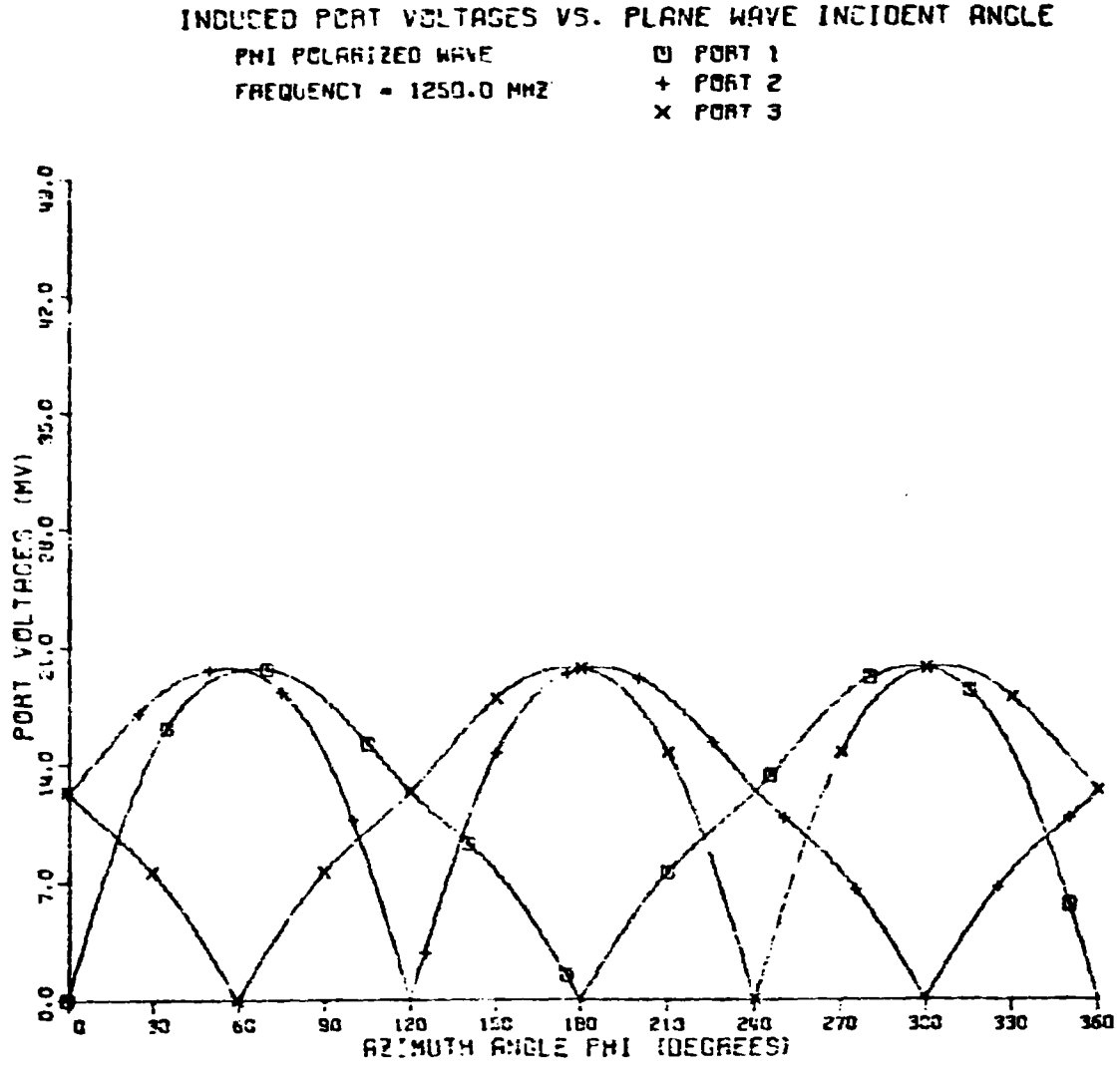

Fig 5-4e. Received voltage for horizontal polarization at 1250 MHz.

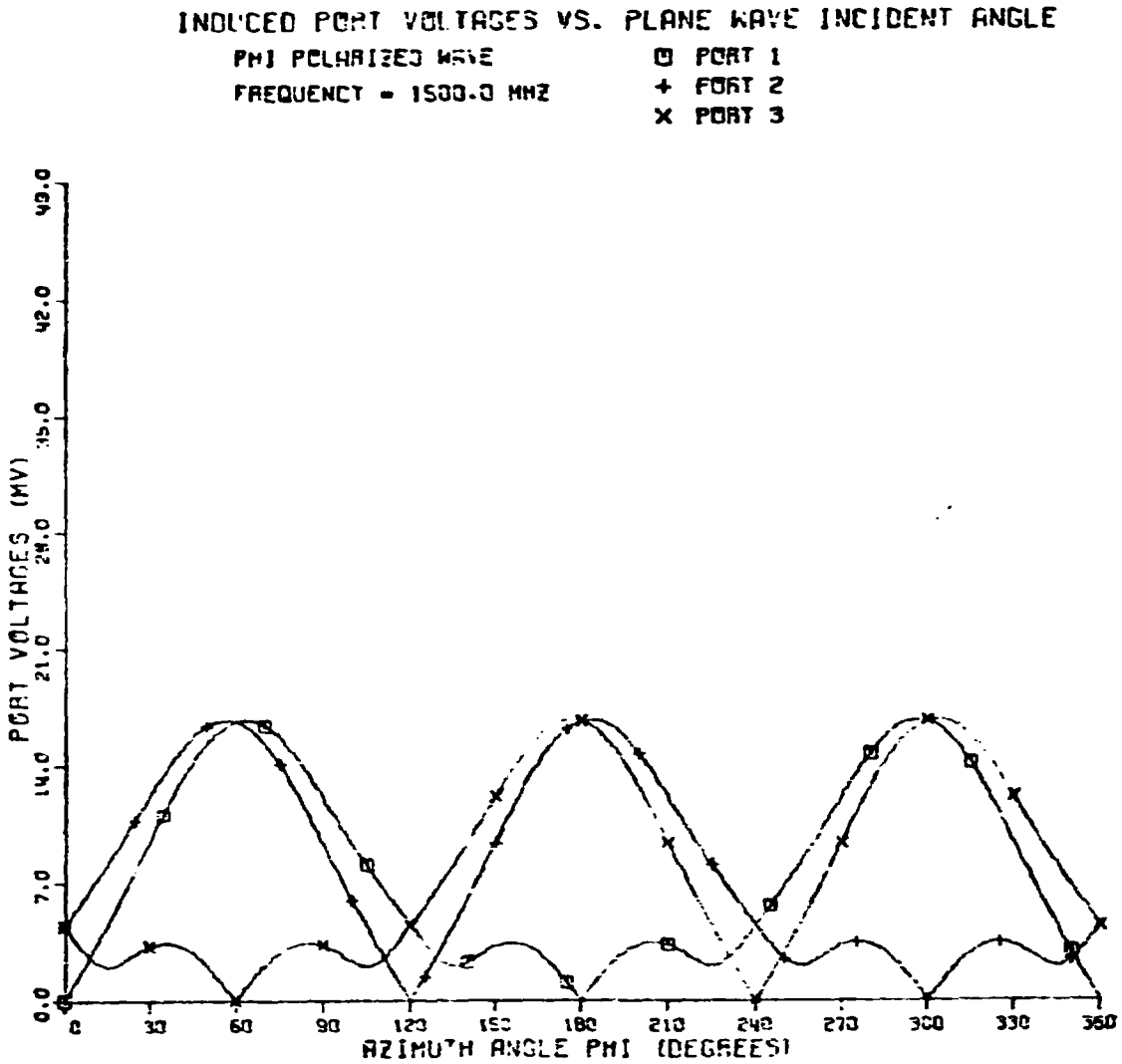

Fig. 5-4f. Received voltage for horizontal polarization at 1500 MHz.

VI. SUMMARY AND CONCLUSIONS

The theoretical investigation discussed in Section II of this final report and in Reference 2 has produced a comprehensive amount of data which enables one to see quite clearly the type of performance offered by various slot antennas on cylinders. Based upon these theoretical results, a prototype antenna system consisting of three 45° slot antennas spaced 120° apart around circumference of the 7" diameter cylinder has been designed and will be constructed during the following contract period. This antenna system will operate over at least a 2.7:1 bandwidth and be responsive to both polarizations. The antenna element chosen for use in the 3 element array was the compact version of the T-bar fed slot antenna developed during this research and development program. The compact T-bar fed slot antenna experimental development was discussed in Section III of this final report.

The results of the experimental investigation in Section III show that it is essentially impractical to use a slot antenna on the cylinder at the lowest frequencies of interest. Thus, as an alternative approach, the distributively loaded (i.e., lossy wire) array of Section IV was designed using modern computer modeling techniques. This array exhibits essentially a 9:1 bandwidth but its physical geometry dictates that it be mounted atop the cylinder. Further, while it can in principle be utilized in such a way that it will respond to both principle polarizations, it appears that there would be considerable difficulty in feeding the antenna under these conditions. To overcome these disadvantages, a simpler configuration was investigated in Section V. The configuration of Section V is basically a three monopole array utilizing lumped loading. It has a smaller bandwidth (i.e., 3:1) than the array of Section IV but would be considerably simpler to feed. However, it is simultaneously responsive to both polarizations and this may be a disadvantage rather than an advantage. For instance, even if the incoming signal is purely horizontal or purely vertical in its polarization, the depolarization properties of the environment will probably cause both polarizations to arrive at the antenna thereby complicating the nature of the received voltage. Since the degree of depolarization caused by the environment is unknown, the seriousness of the problem is impossible to ascertain.

In conclusion, the results of this research and development effort have led to a clear understanding of the properties of slot antennas on cylinders that are not large electrically. This knowledge has led to the design of a 3 element slot array for DF purposes. In addition, a suitable physically compact and electrically broadband slot antenna element has been developed for use in this array. While this array is not designed for the lowest frequencies of possible interest, several potentially promising wire element arrays have been devised and await experimental implementation.

Our recommendations for investigations to be done during a follow on program are given below.

1) Extend the GTD analysis of Section II to accomplish the following:

   a) Extend the cylinder calculations from cylinder sizes of ka = 3 down to ka = 1.

   b) Include probed aperture data from [3] into the GTD analysis so that the effects of larger slot sizes can be evaluated.

   c) Include the effects of a finitely conducting ground plane.

   d) Determine the radar cross section of the cylinder with a slot array on it.

2) Utilize the results of Section III to develop the following experimental hardware:

   a) Scale and construct a planar T-bar for the 1.5-4.0 GHz range.

   b) Using the results of (a), construct a 45° slot antenna on a 7" diameter cylinder and evaluate its performance.

   c) Using the results of (b), construct either a 3 or 4 element array of 45° slot antennas on the cylinder.

3) Extend the results of Sections IV and V to accomplish the following:

   a) Construct, test and evaluate the basic lossy wire element developed in Section IV.

   b) Investigate new designs, such as that of Section V, for for 250 to 1500 MHz frequency range considering both polarizations. These designs would originate via computer analysis and the most promising design(s) would be experimentally verified.

REFERENCES

1. J. Cashman and G. A. Thiele, "Direction Finding Array for Frequency Range 500-4500 MHz Using Array of Lossy Wire Triangular Loops," Report 3735-1, June 1974, The Ohio State University ElectroScience Laboratory, Department of Electrical Engineering; prepared under Contract N00140-74-C-6017 for Naval Regional Procurement Office.

2. P. H. Pathak, "Analysis of a Conformal Receiving Array of Slots in a Perfectly-Conducting Circular Cylinder by the Geometrical Theory of Diffraction," Report 3735-2, January 1975, The Ohio State University ElectroScience Laboratory, Department of Electrical Engineering; prepared under Contract N00140-74-C-6017 for Naval Regional Procurement Office.

3. M. R. Crews, "An Experimental Investigation of the T-Bar Fed Slot Antenna on Planar and Cylindrical Surfaces," Report 4111-1, March 1975, The Ohio State University ElectroScience Laboratory, Department of Electrical Engineering; prepared under Contract N000140-75-C-6116 for Naval Regional Procurement Office.

4. Jasik, Antenna Engineering Handbook, Sec. 8.9, McGraw Hill, New York 1961.